Novel Conjugated Polymers for Application in Optoelectronic Devices and Sensors

A Dissertation Submitted to the
Indian Institute of Technology Guwahati
as Partial Fulfillment for the Degree of

Doctor of Philosophy

Submitted by

Gunin Saikia

Department of Chemistry
Indian Institute of Technology Guwahati
Guwahati, India, 781 039

January, 2011

Novel Conjugated Polymers for Application in Optoelectronic Devices and Sensors

Submitted by

Gunin Saikia

Department of Chemistry

Indian Institute of Technology Guwahati

Guwahati-781039

January 2011

….DEDICATED TO MY FATHER,

LATE **BENUDHAR SAIKIA** AND

MOTHER, MRS. **JYOTI SAIKIA** ….

Statement

INDIAN INSTITUTE OF TECHNOLOGY GUWAHATI
Guwahati, Assam-781 039, India
Department of Chemistry

STATEMENT

I do hereby declare that the matter embedded in this thesis is the result of investigations carried out by me in the Department of Chemistry, Indian Institute of Technology Guwahati, Guwahati, Assam, India under the supervision of Dr. Parameswar Krishnan Iyer, Department of Chemistry, Indian Institute of Technology Guwahati, Guwahati, Assam, India.

In keeping with the general practice of reporting scientific observations, due acknowledgement has been made wherever the work described is based on the findings of other investigators.

11th January, 2011
Guwahati **(Gunin Saikia)**

Certificate

INDIAN INSTITUTE OF TECHNOLOGY GUWAHATI
Guwahati, Assam-781 039, India
Department of Chemistry

CERTIFICATE

This is to certify that the work contained in the thesis entitled **"Novel conjugated polymers for application in optoelectronic devices and sensors"** by Gunin Saikia, a Ph.D. student of the Department of Chemistry, Indian Institute of Technology Guwahati, for the award of degree of Doctor of Philosophy has been carried out under my supervision and this work has not been submitted elsewhere for a degree.

11th January, 2011
Guwahati

Dr. Parameswar Krishnan Iyer,
Supervisor
Department of Chemistry,
Indian Institute of Technology Guwahati,
Guwahati- 781039

ACKNOWLEDGMENT

Here I am reaching the finishing line, putting an end to my journey; a truly memorable and overwhelming journey towards my intellectual destination. I thank Almighty for guiding me throughout this voyage and now, as I look back in pride; I recollect numerous occasions and moments which make me proud to be a part of this world class centre of excellence. It has been my priviledge to be amidst some intellectual genius, who guided in my pursuit of knowledge. My heartfelt gratitude goes to all of them.

"A journey well begun is half done…" First and foremost, I would like to express my deepest sense of gratitude, to my supervisor Dr. Parameswar Krishnan Iyer for introducing me into this interdisciplinary and emerging area of research "molecular wires" and giving me the freedom to work and love the subject. I thank him for his guidance, encouragement, inspiration and freedom, which helped me to enhance my knowledge in this field and made my pursuit really exciting.

I would like to acknowledge my sincere gratitude to all my doctoral committee members, Dr. Anil K. Saikia, Dr. Pravat K. Giri and Dr. Biplab Mondal for their insightful advices and suggestions.

My special thanks go to Professor Mihir K. Chaudhuri for his constant inspiration and help and Professor Arun Chattopadhyay for extending his laboratory facilities. Next, I would like to take the opportunity to thank all the faculty members who had helped me in one way or another to finish this PhD work for and the entire initial help with learning chemistry. I am thankful to the Institute, Indian Institute of Technology Guwahati for providing me with the state of the art infrastructure and facilities for advanced research.

My sincere thanks are due to all other faculty members in the Department of Chemistry for their help and encouragement and the non-teaching staffs of the Department for their technical support. I thank The Head of Central Instruments Facility (CIF) for providing me Instrument facilities ie. FESEM, TEM, NMR, EPR, and Mass spectrometer. My sincere thanks to Chandan-da, Kula-da and kesho-da Central Instruments facility, IIT Guwahati for their help in all the characterizations required during my research work.

I am highly indebted to Dr. Robin K. Dutta and family, Tezpur University, Tezpur, who gave me constant help, his incisive suggestions and encouragement during my research time. My thank goes to Prof. P. K. Gogoi, Dibrugarh University, for his encouraging talks.

It is said our thoughts are shaped by the people we associate with, by the books we read and by the words we speak and by our daily surroundings. I want to thank few of my friends and colleagues who were there with me at those tiring and demanding times of highs and lows. I thank my group members Pranjol da, Bolin, Prasanta, Rana, Atul, Ratnawali, Sukanti, Muthuraj,

Meenakshi, and Radhakrishna for their timely help, support and for the wonderful time we shared during this period. I thank some of the trainees/ BTPs, Gourav, Bishnu, Maninder, Karthikkay, Nikhil, Prabin, Gouranga, Sumit, and Arghya for their help. I am also thankful to Dr. G. Das and his former group members, for their help and pleasant association with whom we shared the lab in the initial stage of my research.

I would like to take this opportunity to thank Prof. Monika Katiyar, Department of Materials and Metallurgical Engineering, Indian Institute of Technology Kanpur, Mr. Ranbir Singh, Samtel Centre for Display Technologies, Indian Institute of Technology Kanpur, for providing me the necessary laboratory and instrumental facilities during my visit to IIT Kanpur for the LED device fabrication.

I extend my sincerest thanks to my friends and seniors Ballav, Sahid, Sonit, Prasanta, Krishna, Jashmini, Biswa da, Saitanya, Siva, Manas, Harjyoti, Deepankar, Bhaskar, Dhruba, Rupam, Amardeep, Abhiguru, Biraj, Buljit da for their constant help, motivation, and enthusiastic company and all the wonderful time we spent in various events. I also thank Mousumi Gogoi for her encouragement and help.

I am thankful to all Research Scholars, friends, M.Sc. and B.Tech. students, IITG Club, all members of "Bohagar Duardolit" who made my stay here and there more enjoyable. I also thank all my Orkut and Facebook friends who shared their thoughts and views with me. I would also like to extend my gratitude to my old friends Diganta da, Mridulda, Diganta, Rabha, Hemashree ba and Bornali and DRL staff for their encouragement.

I wish to express my appreciation to Swapnali baidew/ Swarup Sir, Papori baidew, Manab da, Amarendra/ Lipika, and Madhurjya in the campus for the wonderful homely environment I had with them. The financial support from Department of Science and Technology (DST), New Delhi, Council of Scientific and Industrial Research (CSIR), New Delhi, Indian Institute of Technology Guwahati in the form of JRF and SRF is duly acknowledged.

I thank my father though, he is no more, but the remembrance is the main source of inspiration, encouragement and mental strength…

Finally, my Ph. D. endeavor could not be completed without the endless love, unending support, and blessings from my family, Grandmother, Mother and two younger brothers, Mamu & Rumu. They are the sole inspiration for each and every step that I achieve in my life.

11th January, 2011

Guwahati (Gunin Saikia)

CONTENTS

SYNOPSIS

The thesis entitled, "Novel conjugated polymers for application in optoelectronic devices and sensors" is divided into five chapters.

Chapter-1 Introduction:

The role of polymers in the electronics industry has been traditionally associated with insulating properties. Electroluminescence in organic semiconductors was first reported for anthracene single crystals in the 1960s. In the late 1970s MacDiarmid, Heeger and Shirakawa discovered that doped polyacetylene shows a high degree of conductivity. Due to this pioneering discovery and development of conducting polymers they were awarded the Nobel Prize in Chemistry in the year 2000.

In 1990, Friend et al (Cambridge) discovered that poly(p-phenylene vinylene) (PPV) can emit green light under an applied electric field when it is sandwiched between indium-tin oxide (ITO) and aluminum. Soon afterwards, red light emission by 2,5-dialkoxy substituted PPV as emissive layer was reported. This discovery of electroluminescence (EL) that is the emission of light when excited by flow of an electric current, in conjugated polymers has provided a new impetus to the development of light-emitting devices (LEDs) for display applications.

There are various types of π-conjugated polymers available in literature. As for example polyacetylenes (PA), poly-p-phenylenes (PPP), polythiophenes (PT), poly-p-phenylenevinylenes (PPV), polypyrroles (PP), polyfluorenes (PF), polyaniline(PANI) and poly-p-phenyleneethylenes (PPE). These types of electroluminescent conducting polymers and oligomers have applications in several areas of molecular electronics such as organic thin film transistors, light emitting diodes, lasers, photovoltaic cells and sensors.

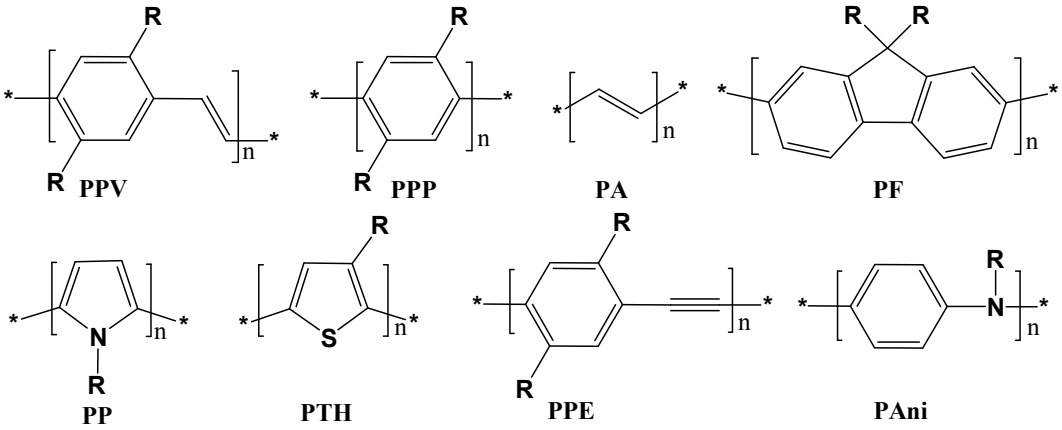

Figure: 1 Structure of various conjugated polymeric systems.

There has been considerable progress made with chemical modification of conjugated polymers to tune color of emission so that full-color displays can be fabricated. Blue emission is achieved in a few polymers, including the poly(fluorene)s, and poly-*p*-phenylenes. In general, blue-emitting materials suffer from the tendency to form aggregate states which show red-shifted emission, and it is generally found that this effect is enhanced for electroluminescence in comparison with photoluminescence. In producing a full-color display it is important to have pure red, green, and blue emissive polymers and the patterning of pixels onto an active-matrix array. The development of pure blue light emitting materials is still a challenge for scientists and engineers, for use in full-color organic EL displays. Organic EL display technology possesses various features including self-emission with superior visibility, suitability for slim products and high-speed response, and is attracting widespread attention as the next-generation flat panel display. Further improvements in the overall features, high EL quantum efficiency, and low power consumption in particular, are needed for realizing the full market potential, requiring the development of materials that achieve low driving voltage and high efficiency. Further research and development of materials and processes are needed to offer comprehensive solutions including key materials and technologies for organic EL display.

Electronic polymers have also emerged as one of the most important classes of transduction materials for sensor application due to their rapid transformation of a chemical signal into an easily measured electrical or optical event. Conjugated polymer based fluorescent chemosensors for physiologically relevant alkali, alkaline earth metal

ions, as well as heavy and transition metal ions have attracted considerable attention in recent years. Conjugated polymers, ionic as well as non ionic polymers were applied as sensors and have shown up to million-fold fluorescence amplification. Conjugated polymer based fluorescence sensors usually show high sensitivity because of their "molecular wire effect". Hence, designing polymers that possess functional groups capable of binding selectively to important analytes has remained a challenge. The recent literatures that have emphasized on the fundamental concepts and terminologies are well illustrated in this chapter.

Chapter 2 Synthesis and Characterization of Soluble Poly(p-phenylene) Derivatives for PLED Applications

In this chapter we are reporting the synthesis and characterization of poly(*p*-phenylene)(PPP) derivatives for blue light emitting PLED applications. Though PFO has shown great promise as a blue emitting material, it has a tendency to degrade on prolonged exposure to heat and atmospheric oxygen to generate undesired green emission bands. Development of alternative polymeric materials for blue light emission still needs more attention. We thus focused on developing PPP-based polymers as an alternative to PF. PPP derivatives with high molecular weights were synthesized (Scheme 1) and characterized by FT-IR, ^{1}H, ^{13}C NMR and GPC.

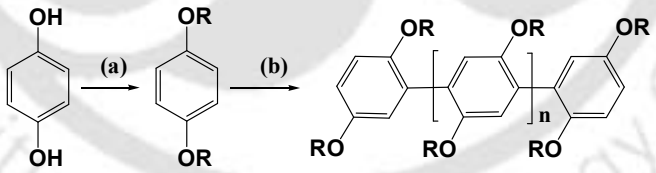

(a) KOH, DMSO, RT, 24 hrs (b) $FeCl_3$, $C_6H_5NO_2$, RT-36 hrs
R=C_6H_{13} or C_8H_{17} or $C_{11}H_{23}$

Scheme 1. General pathway for the synthesis of monomers and PPP polymers.

The decomposition temperatures of the polymers were above 300–400 ^{o}C. DSC analysis indicated their nature to be crystalline as all of them exhibited a melt temperature on controlled heating. The optical and electrochemical band gap was determined using UV-Vis spectroscopy and Cyclic Voltammetry techniques. Single-layer PLEDs fabricated with these polymers displayed high threshold voltages due to high potential barrier for

holes. I-V characteristic curve of this device in figure-2, showed high onset potential (12-14V).

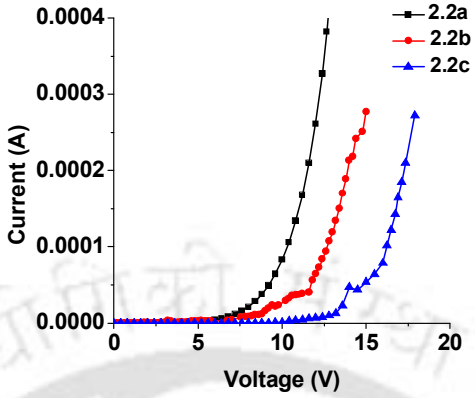

Figure 2 Current-Voltage (I-V) characteristics of three different derivatives of PPP, **2a, 2b** and **2c** based devices.

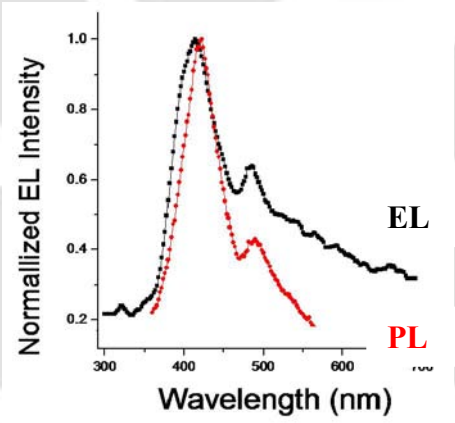

Figure 3 Normalized photoluminescence and electroluminescence spectra of one of the three PPP derivatives.

Their EL spectra reveal a small shift in blue peak and the emission from higher wavelength small shoulder peak is also observed. Figure 3 shows the comparison of EL and PL emission; all the devices show enhanced second peak at longer wavelength. It is not possible to make pure blue devices with these polymers in neat form. The reason for enhanced emission from this peak in EL is due to direct electronic excitation of these entities. Blending these polymers with a hole transporting material, in addition to improving the I-V characteristics, will reduce the interchain interaction and also improve the color purity of the device.

Chapter-3 Facile C−H Alkylation in Water; Enabling Defect-Free Materials for Optoelectronic Devices

This chapter discusses the development of environmentally friendly, high yielding and straightforward method for alkylation of unsubstituted fluorene derivatives that are precursors for preparing blue light emitting polymers. The role of various phase transfer catalysts in the synthesis of defect free dialkylated fluorene monomers in water for blue light emitting polymer is discussed. C-H alkylation of fluorene under aqueous conditions is achieved, and reported, wherein the formation of fluorenone (undesired side product) is inhibited, resulting in the exclusive formation of the desired dialkyl-substituted fluorene monomer. As a proof of concept, this method has also been successfully extended to perform N-alkylation of carbazole, diphenylamine, and N,N-dialkylation of aniline in high yields(Scheme 2).

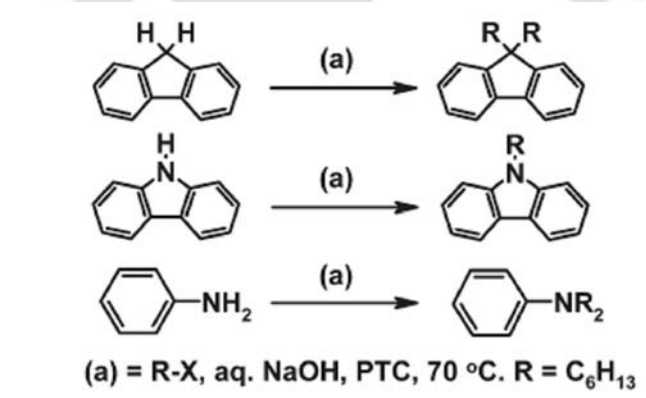

Scheme: 2

Furthermore, we observed that the PTC has a prominent role in facilitating the dialkylation reaction, in addition to other favorable conditions required to achieve the dialkylatedproducts. We have established a simple and economical methodology for the alkylation of fluorene (unsubstituted and substituted) and N-alkylation reactions in aqueous medium whose efficiency is much higher than that of currently applied methods.

Chapter-4 Synthesis, Characterization and Organic Light Emitting Device fabrication with Polyfluorene derivatives.

This chapter concerns with the synthesis, characterization as well as optical and electrochemical studies of polyfluorene derivatives. Polyfluorene (PF) [Scheme-

3(a,b&d)] with alkyl chains of varying lengths, alkyl chain having different substituents on the top of the chain[Scheme-3(a-d)] (Figure 5) have been synthesized and characterized by FTIR, ^{1}H NMR and ^{13}C NMR spectroscopy. Optical and electrochemical band gaps were determined using UV-Vis spectroscopy and cyclic voltammetry techniques. Thermal characteristics of all these polymers were determined by TGA. Molecular weights were determined by GPC using polystyrene as internal standard. Glass transition temperature of the synthesized copolymers has been investigated with the help of DSC. Scheme 3 shows the synthesis protocol followed to obtain the below monomers & polymers.

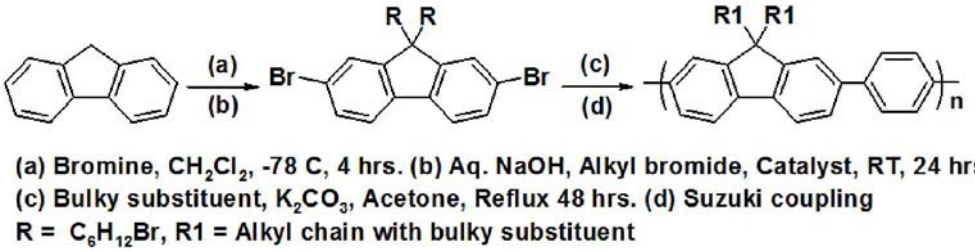

Scheme: 3 Synthetic protocol followed to obtain the below monomers & polymers.

Single layer devices were fabricated using these new materials. One representative I-V curve of a characteristic device of PF series is shown [Figure 4(a)] where turn on voltage of the device is high since there is an imbalance in charge injection and transportation due to large injection barriers and different charge carrier mobility. On introduction of BCP as electron transporting material (ETL) the threshold voltage decreases to a reasonable amount. We have not observed any EL at higher wavelength which confirmed that by modification of the synthetic root the monomers give us defect free polymeric materials for pure blue emission.

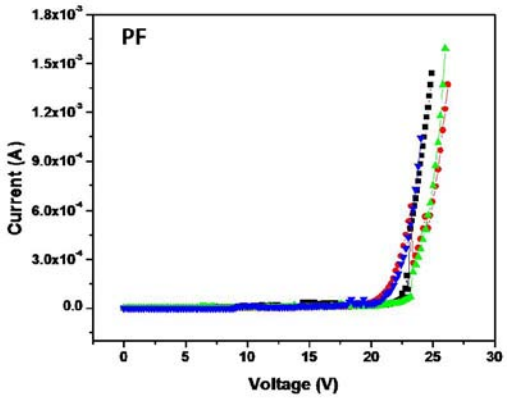

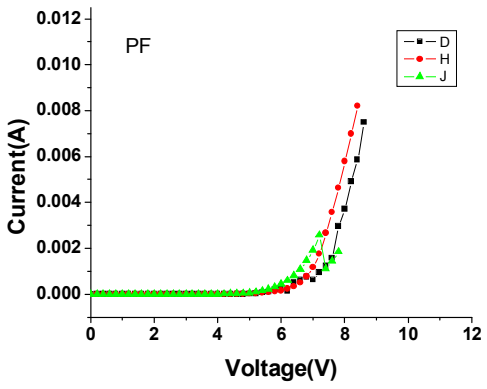

(a) **(b)**

Figure 4(a) and **(b)** I/V curve of Polyfluorene without ETL and with ETL, Octyl chain substituted.

When bulky groups are incorporated into the C-9 position of the fluorene units, it not only provides large steric hindrance and reduce inter-chain interaction but also enhances thermal stability and morphological features without substantially changing the electronic properties of the polymer backbone. Insertion of this type of groups not only increases the mobility of charge carriers in the polymer unit but also prevents the aggregation. These bulky aromatic systems are of considerable interest due to their presence as binding sites for metals in several biological systems, especially as mimics of histidine-imidazole system that can bind various metal ions specifically.

Chapter-5 Tuning the Optical Characteristics of Poly(p-phenylenevinylene) by in Situ Au Nanoparticle Generation

A composite of 1,4-dihexyloxy-poly(p-phenylenevinylene) (DHPPV) and gold nanoparticles (AuNPs) was prepared by an efficient and simple in-situ method. The formation of DHPPV/AuNP composites was confirmed through high-resolution transmission electron microscopy (TEM); UV/Vis absorption spectra showed a large blue shift in the polymer absorption peak, which was greater than 60 nm in solution, accompanied with a remarkable change in the intensity; whereas the photoluminescence (PL) spectra in solution state showed only marginal decrease in intensity in the presence of AuNPs. TEM analysis confirmed that AuNPs were embedded in the DHPPV matrix systematically, thus, presenting a simple tool to assemble hybrid nanowires comprising π–conjugated organic / polymeric systems and inorganic nanoparticles with likely applications in nanosized optoelectronic devices.

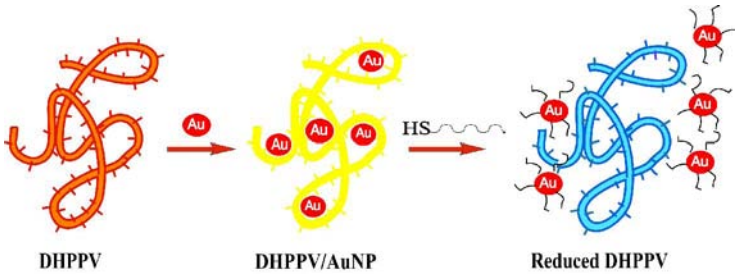

Figure 5. Graphical presentation of this work.

Poly (2,5-dihexyloxy)-1,4-phenylene vinylene) was synthesized by following previously established literature (Figure 6)

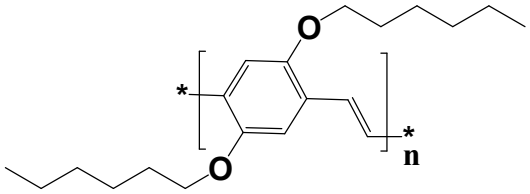

Figure 6. Structure of the DHPPV Polymer.

Chapter 6: Polyfluorene containing pendant benzimidazole as a non-invasive probe for the detection of Fe^{3+} and inorganic phosphates in saliva.

2-phenylbenzimidazole functionalized polyfluorene derivative, poly(9,9-bis(6'-benzimidazole)hexyl) fluorene-alt-1,4-phenylene (PBP) was synthesized (Scheme 4) by Suzuki coupling between 2,7-dibromo-9,9-bis(6-benzimidazolehexyl)-9H-fluorene and 1,4-phenylenediboronic acid characterized by FTIR, ^{1}H, ^{13}C NMR spectroscopic technique.

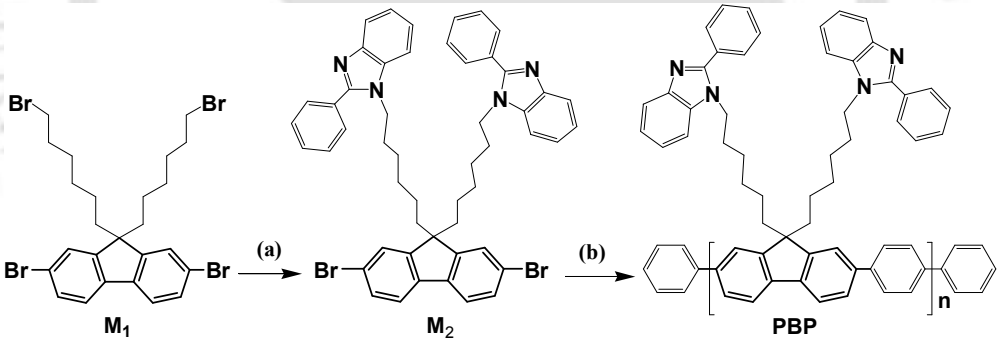

Where, (a)=2-Phenyl-1*H*-benzoimidazole and NaH in THF for 16 hrs at RT.
(b)=1,4-bisboronic acid, Pd(0) and K_2CO_3 in THF+water mixure at 80 ^{o}C for 36 hrs.

Scheme 4 Synthetic scheme of fluorene based benz-imidazole containing monomer and polymer.

The polyfluorene derivative containing phenylbenzimidazole as a pendent group on the side chains that shows high selectivity to detect salts of Fe^{3+} and PO_4^{3-} in aqueous based medium. The fluorescence of this polymer (PBP) was completely quenched by adding Fe^{3+} salts at very low concentration. Notably, it was observed that the fluorescence dequenching was ~106% of the PBP fluorescence. As this PBP-Fe^{3+} assay is selective towards inorganic phosphates we used it to detect phosphate levels in competitive

biological samples like untreated saliva with high accuracy. In conclusion, a polyfluorene derivative, poly(9,9-bis(6-2-Phenyl-benzoimidazole)hexyl) fluorene-alt-1,4-phenylene was synthesized and used for detection of biological targets like Fe^{3+} and phosphates in competitive biological environment and studied its ability to sense metal ions and anions by the fluorescence spectra.

Chapter 7 Poly-p-phenylene containing imidazole as a pendent group: A Cu^{2+}/Fluoride Ion dual sensor in aqueous condition.

In this chapter the development and application of poly-*p*-phenylene based conjugated polymers as chemo sensors is reported. 1, 4-Bis-(8-bromo-octyloxy) substituted poly-p-phenylene (PPP) was prepared by oxidative polymerization in inert atmosphere by using anhydrous ferric chloride in nitrobenzene at room temperature. Br group on the top of the alkyl chain was substituted by imidazole group. Characterization of all polymers was done by FT-IR, ^{1}H NMR, ^{13}C NMR spectroscopy and molecular weight was determined by GPC. The effect of various metal ions on the fluorescence emission spectra was studied. It was observed that fluorescence of the imidazole substituted PPP polymer was completely quenched by addition of Cu(II). It was also observed that on addition of fluoride ion to the PPP-Cu^{2+} solution the quenched intensity is again regained by more than 81%.

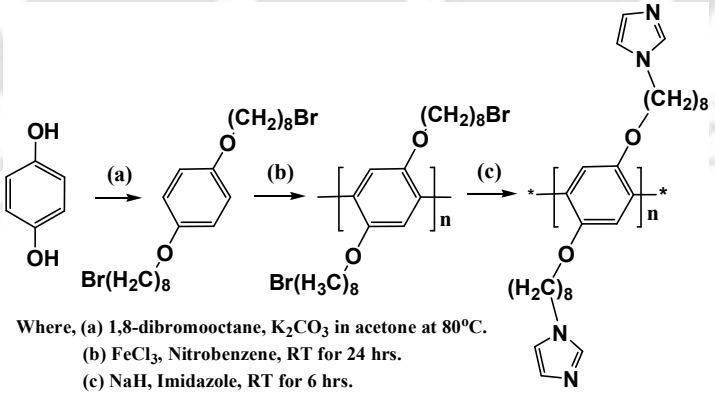

Scheme 5. General pathway for the synthesis of imidazole containing PPP polymers.

Manuscript related to this work is under preparation.

Chapter 1

Introduction

Chapter 1

1.1 Introduction

1.1.1 *The discovery of electroluminescent conjugated polymers*:

Organic and polymeric materials have been of interest recently for their potential applications in electronic devices such as organic light-emitting diodes (OLEDs)[1.1] and polymeric light-emitting diodes (PLEDs) for flat panel display (FPD)[1.2] and TFTs[1.3] applications. These PLED can be operated at low voltages with high external quantum efficiency with a balanced charge injection, have a wider viewing angle with improved color contrast, and can be made much thinner for lighter devices.[1.4] Conjugated polymers are unsaturated compounds having alternating single and double/triple bonds. Due to this extensive conjugation they behave as organic semiconductors in which the π-molecular orbitals are delocalized along the polymer back bone. The conjugated double bond creates an energy gap at the Fermi level, giving rise to a conduction band and a valence band, (Figure-1.1) and thus exhibiting semiconducting behavior.

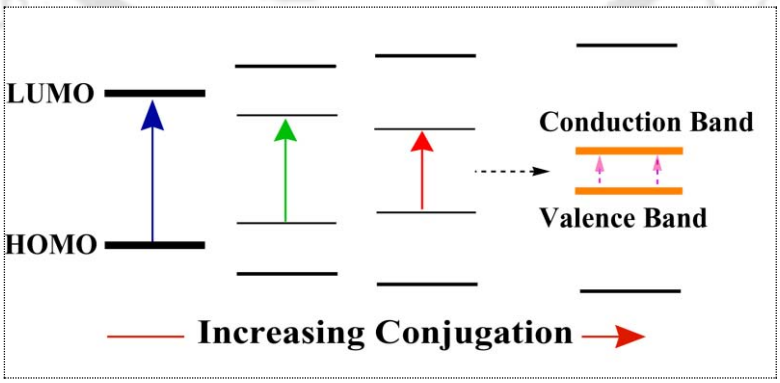

Figure 1.1 Extent of conjugation in conducting polymer

The role of polymers in the electronics industry has been traditionally associated with insulating properties. Before the discovery of the property of electroluminescence the conjugated organic molecule and conjugated polymers were thought to be insulating material. The electroluminescence (EL) of organic compounds was first demonstrated in 1953 by Bernanose[1.5] but was not significantly developed until MacDiarmid, Heeger and Shirakawa discovered that doped polyacetylene shows a high degree of conductivity like metals in the late 1970s and in 1987 when Tang et al[1.6] constructed a device by employing aluminum tris(8-hydroxyquinoline) as the luminescent material. In 1990 Friend et al constructed and reported the first example of a polymer-based OLED in which poly(*p*-phenylene-vinylene) (PPV) was used as the emissive layer.[1.2] Since this discovery, many conjugated polymers have been developed for use in LEDs including poly(1,4-phenylene) (PPP), poly(thiophene) (PT), and polyfluorene (PF).

The discovery of these synthetic metals has led to Nobel prize in chemistry in the year 2000[1.7] and has inspired chemists and physicists all over the world to pursue this area of research. In exploring new optoelectronic material and devices, a great deal of research effort is focused on reducing the dimensionality of the electronic structures in semiconductors. There are three categories that are usually considered for low dimensional semiconductor systems, which include; two dimensional (2D) quantum wells, one dimensional (1D) quantum wires, and zero dimensional (0D) quantum dots.[1.8] Conjugated polymeric systems often called as 1D semiconductors or quantum wires exhibit a wealth of quantum phenomena and have potential as emissive materials in future optoelectronic devices. Chemically synthesized semiconducting polymers are regarded as natural quantum wires. Unique optical and electronic properties of conjugated polymers are due to the electrons delocalized over the 1D polymer backbone, and make them

important materials for technological applications like light emitting diodes, nonlinear optical devices, and field effect transistors.[1.9]

There are various types of π-conjugated polymers studied extensively in literature (Figure 1.2.) As for example polyacetylenes (PA), Poly-*p*-phenylenes (PPP), polythiophenes (PT), poly-*p*-phenylenevinylenes (PPV), polypyrroles (PP), polyfluorenes (PF), polyaniline (PANI) and poly-*p*-phenyleneethylenes (PPE).

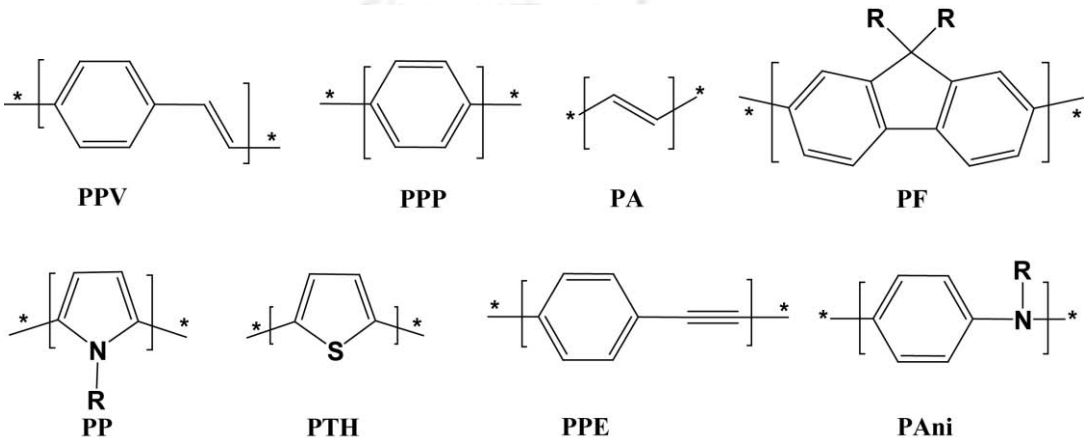

Figure 1.2 Structure of various π-conjugated polymeric systems.

Real blue emitting polymers are especially interesting and indispensable to realize the full color PLEDs. Organic EL display possesses various features including self-emission with superior visibility, suitability for slim products and high-speed response, and is attracting widespread attention as the next-generation flat panel display. High EL quantum efficiency, and low power consumption in particular is the main criteria to develop such materials, and need of the present society. Further research and development of materials and processes are required to offer comprehensive solutions including key materials and technologies for efficient organic EL display. Organic molecules or conjugated polymers have semiconducting properties like metals/synthetic metals, with improved characteristic features for making a light emitting device. This is the prime reason for attraction of conjugated polymers in modern materials chemistry and engineering. The features like light weight, transparency, semiconducting, thermally and mechanically stable like metals

leads to a tendency to realize conjugated polymers as substantially customizable substitutions for inorganic materials in optoelectronic applications. The work included in this thesis focuses on the synthesis of defect free conjugated polymers for application in blue emitting devices and as sensors.

1.1.2 *Various synthetic strategies used in synthesis of defect free conjugated polymers*:

This part describes how various synthetic strategies are efficiently used in the synthesis of defect free conjugated polymers with relevance to the work embodied in this thesis. The synthesis of well-defined/defect free conjugated polymers may lead to a significant improvement in the performance of electroactive polymers and as emissive layers in optoelectronic and photo voltaic devices. We are focusing on some of the most extensively studied synthetic roots of three different polymers, (PPP, PF, and PPV) and the most efficient methods are considered for our synthetic work.

1.1.2.1 Poly-p-phenylenes:

PPP is composed of phenylene rings as the backbone. Coupling of dihalo benzenes can be done by various literature reported methods such as Wurtz-Fittig[1.10] reaction of p-dibromobenzene, Ullmann reaction[1.11] of 1,4-diiodo-2,3,5,6-tetrafluoro benzene with activated copper at 250 ^{o}C, Grignard coupling of aryl bromides,[1.12] Suzuki Coupling[1.13] with Pd(0) catalyst and Yamamoto coupling with zero valent nickel. PPP can also be synthesized by direct oxidative coupling of benzene by copper chloride in presence of aluminum chloride, by electrochemical polymerization of benzene or by Diels Alder reaction. Iron chloride is a very good reagent for oxidative polymerization. As a catalyst, $FeCl_3$ is extremely cheap and easy to handle. No halogenated monomer is needed and the polymerization can be done on simple phenylene ring or alkoxy/alkyl substituted benzene derivatives. We have used $FeCl_3$ as catalyst in our reactions because of its easy

availability, low cost compared to other catalysts, and mild reaction conditions like room temperature stirring, no use of dry solvents, simple workup procedure and obtaining high molecular weight polymers which makes this procedure very handy and attractive.[1.14]

1.1.2.2 Polyfluorenes:

Polyfluorenes are well-known materials and applied extensively as emissive material for polymer light emitting diodes (PLEDs). A variety of synthetic methods such as Grignard, Stille, Yamamoto, Heck, and Suzuki couplings, etc. were utilized for the synthesis of polyfluorene derivatives that allowed significant advances in this area of research. For instance, Pei and Yang utilized Yamamoto coupling reactions of 2,7-dibromo- 9,9-disubstituted fluorenes to obtain high molecular weight polymers. Suzuki coupling reaction also led to the synthesis of well-defined polyfluorene with high degree of polymerization, along with highly conjugated and processible poly[2,7-(9,9-dialkylfluorene)]s.[1.15] Both Yamamoto and Suzuki polymerization have been used to synthesize a variety of 9,9- substituted polyfluorenes extensively.

1.1.2.3 Poly (phenylenevinylene):

Poly(*p*-phenylenevinylene) (PPV) was the first reported example of a polymer that could emit light upon passing electric current.[1.2] Synthesis of PPV was reported by Lenz and Handlovits in 1960 using Knovengel reaction,[1.16] McDonald and Campbell reported a method in the same year as Wittig reaction.[1.17] Rajaraman used McMurry condensation for the synthesis of PPV in 1980, using $TiCl_3$ as catalyst.[1.18] The most useful and successful reaction was reported by Gilch and Wheelwright and further investigated by Horhold and co-workers for the synthesis of high molecular weight PPVs.[1.19] Potassium tertiary butoxide was used for the synthesis of DHPPV in the work reported in this thesis because of its easy availability, efficient polymerization and mild reaction condition.

1.1.3 *Organic light emitting device*:

An organic light emitting diode (OLED), or polymer light emitting diode (PLED), is a light-emitting device (LED) where the active/emissive layer of the device is an electroluminescent polymer or organic molecule. The organic layer is located in between two electrodes, the anode and cathode. Conjugated polymeric materials are semiconducting in nature because of extensive π-electron delocalization. Basic polymer LEDs consisted of anode, cathode and a single organic/polymer layer, however, multilayer OLEDs consist of anode, cathode and 3-5 different layers to improve the electron or hole injection in a device (Figure 1.3).

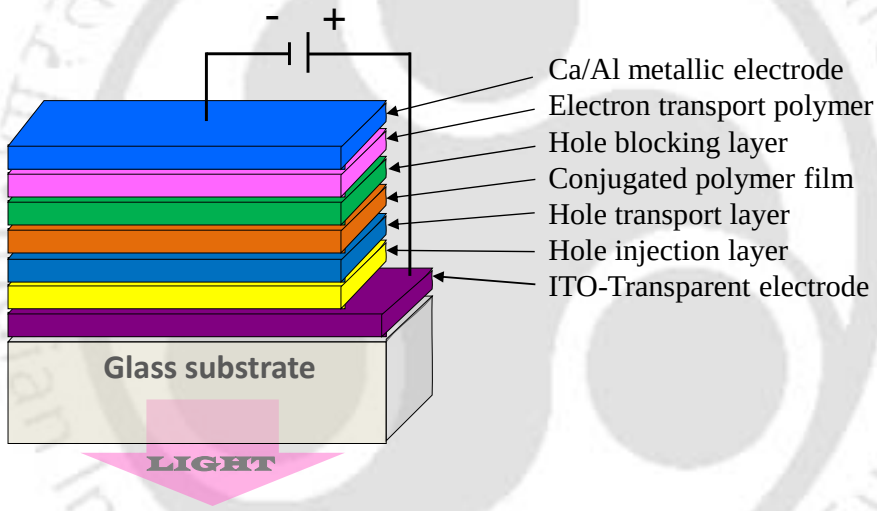

Figure 1.3 Multilayered structure of OLED

1.1.3.1 Advantages of OLED/PLED:

The different manufacturing process of OLEDs lends itself several advantages over flat-panel displays made with LCD technology.

1. Because of the processing advantages such as, spin casting, vapour deposition, inkjet printing, dip coating, spray coating and screen printing of the polymers and organic molecules on desired substrates fabrication cost of OLED is very low.[1.20]

2. Full colour display is possible because different conjugated polymers produce different colours in addition to several organic materials/dyes that show long range emission.
3. OLEDs are very much thinner in dimensions, so they are light weight, and easy to transport or hang on the walls as displays. Since they can be made on thin flexible plastic material large area flat panel display is also possible.[1.21]
4. OLEDs show higher luminous efficiency, higher flexibility, and also have faster response time than currently used display technologies. [Figure 1.4 (A)]
5. OLEDs show self-emission, have high brightness without using back light with high colour resolution in a very low operating voltage.
6. There is no viewing angle limitation in OLED and the viewing angle is too wide of upto 160 degrees. [Figure 1.4 (B)]

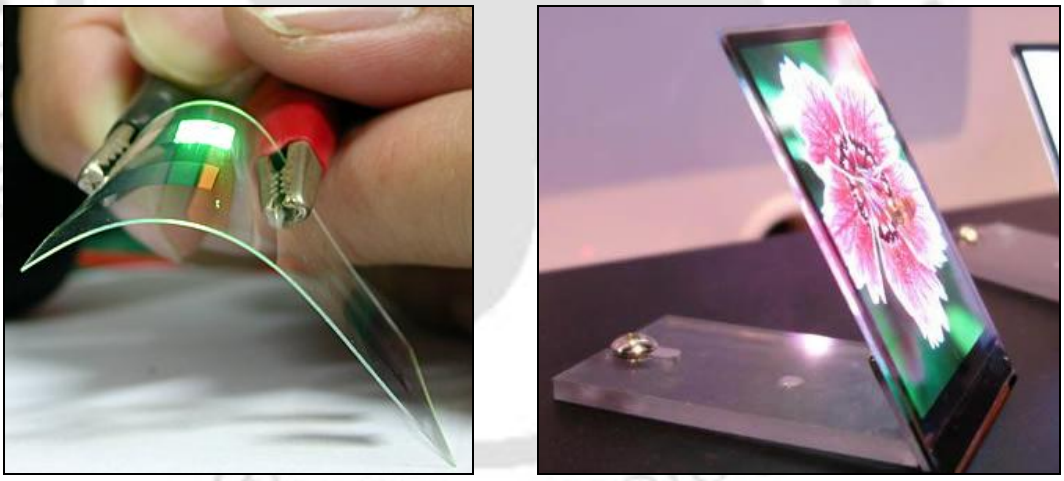

(A) **(B)**

Figure 1.4 (A) Flexible and transparent device **(B)** Thin OLED TV with wide viewing angle (photographs are taken from Google image search)

1.1.3.2 Disadvantages:

a. Though conjugated polymers are thermally stable they are still prone to degrade during device operation in the presence of trace amount of oxygen and water or due to the defects within the polymers.[1.22]

b. Usually ITO as an anode and Ca metal as cathode are used in OLED devices. The main disadvantage of using Ca is that with time it diffuses to the polymer active layer and forms insulating CaO in presence of trace oxygen and reduces the device efficiency. ITO also contains some free oxygen in it which may be responsible for the degradation of devices.[1.23] The lifetime of OLED device is ~100,000 hours with 2000 cd/m^2 brightness. This is less compared to inorganic LED devices.

1.1.3.3 Demand of OLED:

Other than OLEDs, Cathode ray tube (CRT), LCD's and Plasma displays have high market potential as display device. CRT's have great colour combination and fantastic sharpness but they are too heavy, occupy larger area, possess lousy focus and display shape worsens with increasing size. Liquid crystal displays (LCD) have some advantages such as great color saturation and high viewing angle over the Cathode ray tube (CRT). Plasma displays need powerful arrays of tiny neon lamps or fluorescent light for better brightness. They are very heavy because of the larger size; power consumption is more, and very much expensive. Among these three technologies, LCD's have highest market penetration. However, viewing angle limitation remains a serious issue in liquid crystal display; also the pictures are faded at high ambient light. Another disadvantage of LCD is dying up of the pixels in short duration and on continuous use. Compared to these display technologies OLEDs are much advantageous in many ways, like less power efficiency, low manufacturing cost, great color combination, ultra-thin devices, light weight and

flexibility, which would be some of the main reasons for the high demand of OLED in the coming years.

1.1.4 *Conjugated polymers as measuring probe in sensors*:

Recent investigations of conjugated polymers (CPs) with particular reference to optical and energy transfer phenomena and applications in fluorescence based sensing applications have opened up new dimensions in CP based sensor devices. Fluorescent conjugated polymers can interact with quenchers (biological and chemical analytes) in solution and in electronic devices like a very sensitive/selective molecular wire. Exploiting this idea and utilizing its photoluminescence and electroluminescence properties, scientists and engineers have been trying to understand more and more of the underlying science and develop sensitive, selective and rapid sensor devices.

The discipline of conjugated polymers continues to be a rich area of interest for fundamental studies in physics, chemistry and biology. We are able to design and perform synthesis of conjugated polymers from the molecular level and through a better understanding of structure – property relationships and can build increasingly complicated and difficult structures. The property of reversible electrochemistry of conjugated polymers led to many applications in transistors, sensors, re-chargeable batteries, solar cells, capacitors and even mechanical actuators. Selective detection of biologically important metal ions has tremendously gained importance because metal ions are involved in a variety of fundamental biological processes in living organisms. The mechanism of switching are, however, quite complex and the understanding of charge transport within and among molecules as well as associated ion and solvent exchange with surrounding media are growing up gradually. Through this understanding, we are able to tune the molecular structures and assemble devices from the nano to the macro level for improved performance.

The conjugated polymers as a link between the electronic world and the biological world have the potential to revolutionize bionics: to enable sensing of biological systems *in situ* but also to modify biological functions including directing new cell growth for the repair of organs. CPs can match the mechanical properties of biological tissue and can be chemically tuned to be biocompatible and potentially biodegradable. While much work still needs to be done in this area, the opportunity for controllable interactions with living tissue through a bio-conjugated polymer is close at hand.

In general, sensing anions in solution (aqueous or non-aqueous) requires a strong affinity for anions in water as well as the ability to convert anion recognition into a fluorescent or colorimetric signal. Conjugated polymer-based fluorescent (CPF) sensors in solution have attracted much attention because of the "molecular wire effect", represented in Figure 1.5, where interaction of quencher to one antenna of the entire chain can also cause major signal output. Thus CPs, using this effect, greatly enhance the sensitivity of the polymer-based sensors.[1.24]

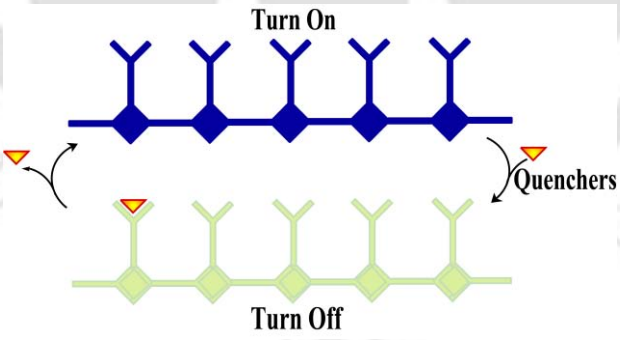

Figure 1.5 Molecular wire effect of conjugated polymers.

Compared with the recognition of metal ions, it is much more challenging to selectively recognize anions in an aqueous system due to the strong hydration effects of anions. Anions like fluoride displays a high hydration enthalpy ($\Delta H°$)-504 kJ/mol), and its

recognition by abiotic hosts is a definite challenge. As a result, a great deal of effort has been devoted to the design of molecular receptors that selectively sense the anion.[1.25]

In most cases, the binding sites of the sensors capable of hydrogen bonding with the anions make a change in optical properties. In particular the sensor word attributed to a device detects, records, and/or measures a physical / chemical property and may ultimately responds to this property. It consists of two main parts, a measuring probe (recognition element, antenna) and a transducer (meter). Our focus is on the antenna part. There are so many artificial antennas available in literature. The more surface area of the antenna, the more effective the sensor. They may be anionic, cationic or can be neutral conjugated polymeric systems. Figure 1.6

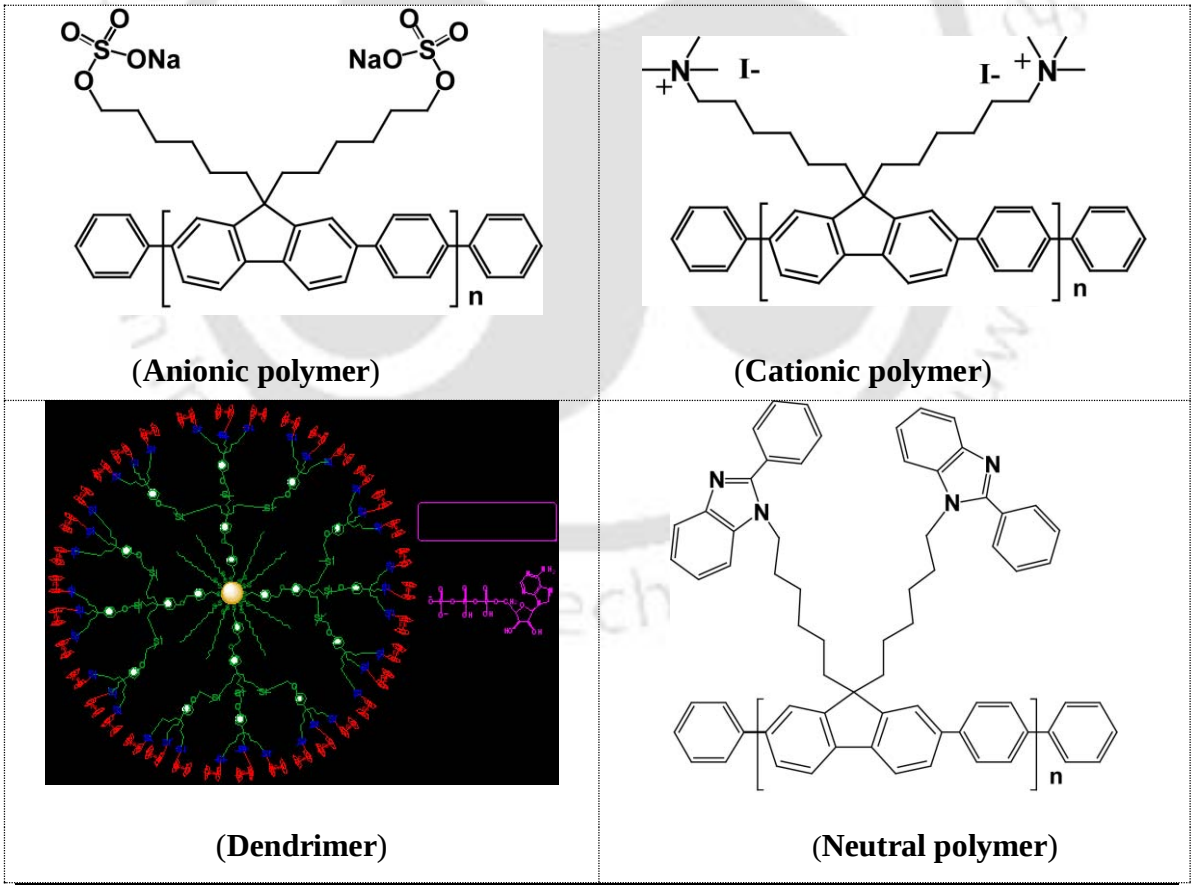

Figure 1.6 Structure of some artificial antenna.

As for example…

(A) Conjugated Polymers

(B) Dendrimers

(C) Nanoparticles,

(D) Composites

(E) Chromophore-Embedded Nanobeads

(F) Quantum Dots

1.1.5 *Objectives*:

a. Synthesis of CPs such as PF employing the already reported literature routes usually gives defective material that is difficult to purify. Also use of expensive catalysts and harsh reaction conditions in making these materials affects the overall economy of the reaction and needs extraordinary precautions and specialized conditions for obtaining defect free product. This encouraged us to investigate a simpler route for the synthesis of monomers and polymers that would be economical, environmentally friendly, and high yielding in contrast to the existing methods. We have established a green alkylation route for fluorene using PTC in water that could be extended to several other important intermediates and precursors, e.g., dialkylation of substituted and partially substituted fluorene, N-alkylation of carbazole and diphenylamine, and N,N-dialkylation of aniline, all of which are vital as charge-transporting and luminescent materials for optoelectronic devices and sensors.

b. Pendent alkyl chains and bulky groups can be introduced by substituting the backbone with solubilizing saturated chains. The processing parameters are thus enhanced, improving their thermal, optical, and morphological properties.

c. As a consequences of changes in the pendent group, the stereo chemistry of the polymer changes and there by establishing a better possibility to understand structure-property relationship not only in solution state but also in solid films or inside a device.

d. Fabricating LED's for pure colour emission is a challenge for the scientists and engineers because of the degradation of polymers inside the device or due to the presence of defects within the polymer. Optical and electrical properties of conjugated polymers are greatly dependent on the purity and presence of defect in the materials present. So design and synthesis of the polymers is important and crucial step so as to avoid the impurity and minimization of defects.

e. The conjugated polymers on doping could conduct electricity leading to the exploration of this type of materials for several diversified applications such as organic light-emitting diodes, field effect transistors, photovoltaic cells, and sensors.[1.7] Tuning of the HOMO-LUMO band gap can be performed by varying the polymer backbone and functional groups, by physical doping/blending with inorganic metals, nanoparticles (NPs), or organic dyes with the polymer and casting them onto substrates as thin films. [1.26-1.27] Alternatively, fabricating a multilayer device with these materials has also shown improvements in device performance. This has helped to enhance the carrier injection, lower the turn-on voltage, and improve brightness, leading to overall improvement of organic device efficiency. Herein, we report in situ synthesis of Au nanoparticles (AuNPs) in the presence of a PPV derivative, DHPPV, dissolved in chloroform solution has a remarkable effect on the optical properties of the polymer.[1.28]

f. Recognition of different biologically important metal cations and anions has been in constant attention in recent years. Polyfluorenes are highly florescent in nature and the fluorescence can be quenched completely if it can bind with some quenchers. In the reverse way if the quencher can be displaced from the polymer the fluorescence can be regained. The present work focused on the design and synthesis of novel conjugated polyfluorene with receptors capable of recognizing metal ions and anions utilizing its fluorescent property. We have utilized PFs with benzimidazolyl pendant group towards the non-invasive detection of metal cations and anions of biological importance, such as Fe(III), and inorganic phosphate from saliva.

g. By the interaction with the specific metal cations and biologically important anions in the presence of competitive solvent environment their potential application in chemical, biological and environmental sensing has been demonstrated. Poly-p-phenylene is another important conjugated polymer which has not been utilized for sensor applications. We present here an imidazole substituted poly-p-phenylene derivative which shows high selectivity and sensitivity for binding biologically important Cu(II) and environmentally significant fluoride anion in aqueous medium.

1.2 Conclusion:

Various CPs have been studied extensively for their properties like photoluminescent, electroluminescent and semiconductivity. Utilizing these properties, CPs have been used as a emissive material in organic light emitting diodes, active layer in solar cells and as chemical or biological sensors. Significant progress has been made in understanding the fundamental working processes involved in generating efficient and reliable bright light across the entire visible spectrum. Polyfluorene-based materials have been investigated

extensively because of many attractive properties they possess. Additional experimental results are needed to discern the nature of the unwanted green emission that often appears during device operation. Also quantum efficiencies need to be significantly improved. A more complete understanding of the primary factors that govern device performance and lifetime will aid in these discoveries. Significant progress is required before OLEDs can be created for use in a broad range of consumer applications in a cost-effective manner. However, limited commercial applications are already being developed as OLED displays have been used in digital cameras, cell phones and car stereos. The possibility of creating flexible, ultra-thin displays with high information content remains a novelty but may be realized in the future.

Involvement of conjugated polymers as sensor has rendered the investigations of their synthesis, structural and property relationship studies not only intriguing but also relevant to the understanding of their biochemical activities. Hence, synthesis and structural delineation of conjugated polymers aiming at the introduction of an active site and its interaction with the chemical and biological species is an active area of current research.

1.3 Future Applications of Conjugated Polymers:

1.3.1 *Solar cells*:

Conversion of solar energy into electrical power is a renewable, clean and cheapest form of energy and have experienced tremendous progress in performance of conjugated polymers the last decade.[1.29] The photoactive blend layer is sandwiched between an indium tin oxide (ITO) positive electrode (anode) and a metallic negative electrode (cathode). In a typical polymeric cell a low band gap conjugated polymer donor and a soluble molecular acceptor are used.[1.30] Typical acceptors are soluble fullerene derivatives such as [6,6]-phenyl-C61-butyric acid methyl ester ($PC_{61}BM$). As a

component in the active layer, a conjugated polymer donor serves as the main absorber to solar photon flux, as well as the hole transporting phase.[1.31] Therefore, wide optical absorption to match the solar spectrum and large hole (bulk) mobility are basic requirements to design an ideal polymer donor. Furthermore, it completely depends upon the band gap of the active material, smaller the band gap more efficient will be the solar cell.

1.3.2. *Rechargeable batteries*:

During the last decade, an impressive development of novel battery-powered autonomous devices has been observed. Rechargeable batteries have been fabricated using doped conductive polymers as the cathode and various metals such as aluminum, copper and zinc as the anode. The development of a thin (<1 mm), lightweight (<10 g) and flexible photovoltaic (PV) solar battery is possible by coupling on top of each other or side-by-side a thin film solar cell[1.30] and a lithium-polymer battery.[1.32] Such a device, able to create electricity and store it, offers energy autonomy without cost in terms of space, weight or flexibility.[1.33]

1.3.3 *Electro chromic devices*:

An electrochromic (EC) smart window is one in which the light transmission properties can be changed in a controlled and reversible manner when an electric current flows through the device. Conducting polymers represent an attractive class of electrochromic materials owing to their facile switching properties and controllable optical properties.[1.34] For example; the use of spectrally selective low-E coating on window glass has made a major impact in energy savings. But this is a passive technology.

1.3.4 *Optic fiber*:

Utilizing nonlinear optical property of conjugated polymers can be used in fiber optic industry and information technology for processing data and information in real time.

1.3.5 *Bioimaging*:

The use of conjugated polymers is not confined to device applications. As the polymers exhibit extremely high fluorescence brightness under UV excitation, they can be used in fluorescence based imaging applications. Conjugated polymers are being used to make fluorescent nanoparticles and their properties are comparable to the best known alternatives, such as quantum dots or dye-doped silica, and as they are relatively benign they appear to be promising for uses in biological fluorescence imaging studies where nanoparticle toxicity may be of concern.

1.4 References:

1.1 Friend, R. H.; Gymer, R. W.; Holmes, A. B.; Burroughes, J. H.; Mark, R. N.; Taliani, C.; Bradley, D. D. C.; Dos Santos, D. A.; Breads, J. L.; Logdlund, M.; Salaneck, W. R. *Nature* **1999**, *397*, 121.

1.2 Burroughs, J. H.; Bradley, D. D. C.; Brown, A. R.; Marks, R. N.; Mackay, K.; Friend, R. H.; Burns, P. L.; Holmes, A. B. *Nature* **1990**, *347*, 539.

1.3 (a) Bao, Z. *Adv. Mater*. **2000**, *12*, 227.

(b) Siringhaus, H.; Tessler, N.; Friend, R. H. *Science* **1998**, *280*, 1741.

1.4 Mitschke, U.; Bauerle, P. *J. Mater. Chem*. **2000**, *10*, 1471.

1.5 Bernanose, A. J. *Chem. Phys*. **1955**, *52*, 396.

1.6 Tang, C. W.; Van-Slyke, S. A. *Appl. Phys. Lett*. **1987**, *51*, 913.

1.7 Chaing, C. K.; Fincher, C. R.; Park, Y. W.; Heeger, A. J.; Shirakawa, H.; Louis, E. J.; Gau, S. C.; MacDiarmid, A. G. *Phys. Rev. Lett*. **1977**, *39*, 1098.

1.8 Ogawa, T.; Kanemitsu, Y. Optical properties of low dimenetional materials, *World Scientific*, Singapore, 1995.

1.9 Wise, D. L.; Wnex, G. E.; Trantolo, D. J.; Cooper, T. M.; Gresser, J. D.; Photonic Polymer Systems, *Marcel Dekker, Inc*., New York. **1998**.

1.10 Goldsmith, G. *Montash* **1886**, *7*, 40.

1.11 Hellman, M.; Bilbo, A. J.; Pummer, W. J. *J. Am. Chem. Soc*. **1955**, *77*, 3650.

1.12 Yamamoto, T.; Hayashi, Y.; Yamamoto, A. *Bull. Chem. Soc. Jpn*. **1978**, *51*, 2091.

1.13 Suzuki, A. *Acc. Chem. Res*. **1982**, *15*, 178.

1.14 (a) Saikia, G.; Singh, R.; Sarmah, P. J.; Akhtar, Md W.; Sinha, J.; Katiyar, M.; Iyer, P. K. *Macromol. Chem. Phys*. **2009**, *210*, 2153–2159.

(b) Jinyun, Z.; Caimao, Z.; Song, W.; Lei, Z.; Xi, Y.; Rui, Z.; Jingui, Q. *Polymer* **2002**, *43*, 1761.

(c) van Breemen, A. J. J. M.; Herwig, P. T.; Chlon, C. H. T.; Sweelssen, J.; Schoo, H. F. M.; Benito, E. M.; de Leeuw, D. M.; Tanase, C.; Wildeman, J.; Blom, P. W. M. *Adv. Funct. Mater*. **2005**, *15*, 872.

1.15 (a) Miyaura, N.; Yanagi, T.; Suzuki, A. *Synth. Commun.* **1981**, *11*, 513.

(b) Inbasekaran, M.; Wu, W.; Woo, E.P. *US Patent 5,777,070*, **1998**. 19.

1.16 Lenz, R. W., Handlovits, C. E. *J. Org. Chem*. **1960**, *25*, 813.

1.17 McDonald, R. N.; Campbell, T. W. *J. Am. Chem. Soc*., **1960**, *82*, 4669.

1.18 Rajaraman, L.; Balasubramanion, M.; Nanjan, M. J. *Current. Sci*. **1980**, *49*, 101.

1.19 (a) Gilch, H. G.; Wheelwright, W. L. *J. Polym. Sci. A, Polym. Chem*. **1966**, *4*, 1337.

(b) Horhold, H.-H.; OzegoWski, J.-H.; Bergmann, R. *J. Prakt. Chem*. **1977**, *319*, 622.

1.20 Pardo, D. A.; Jabbour, G. E.; Peyghambarian, N. *Adv. Mater*. **2000**, *12*, 1249.

1.21 Gustafsson, G.; Cao, Y.; Treacy, G. M.; Klavetter, F.; Colaneri, N.; Heeger, A. J. *Nature* **1992**, *357***,** 477.

1.22 Sugiyama, K.; Ishii, H.; Ouchi, Y.; Seki, K. *J. Appl. Phys*. **1987**, *297*, 2000.

1.23 Gong, X.; Iyer, P. K.; Moses, D.; Xiao, S. S.; Bazan, G. C.; Heeger, A. J. *Adv. Funct. Mater*. **2003**, *4*, 325.

1.24 (a) Thomas, S. W.; Joly, G. D.; Swager, T. M. *Chem. Rev*. **2007**, *107*, 1339.

(b) de Silva, A. P.; Gunaratne, H. Q. N.; Gunnlaugsson, T.; Huxley, A. J. M.; McCoy, C. P.; Rademacher, J. T.; Rice, T. E. *Chem. Rev.* **1997**, *97*, 1515.

(c) Beer, P. D.; Gale, P. A. *Angew. Chem.* **2001**, *113*, 502.

1.25 (a) Gale, P. A.; Garcia-Garrido, S. E.; Garric, J. *Chem. Soc. Rev.* **2008**, *37*, 151.

(b) Sessler, J. L.; Gale, P. A.; Cho, W.-S. *Anion Receptor Chemistry*; Royal Society of Chemistry: Cambridge, U.K., 2006.

(c) Martinez- Manez, R.; Sancenon, F. *Chem. Rev.* **2003**, *103*, 4419.

(d) Choi, K.; Hamilton, A. D. *Coord. Chem. Rev.* **2003**, *240*, 101.

(e) Bondy, C. R.; Loeb, S. J. *Coord. Chem. Rev.* **2003**, *240*, 77.

1.26 Shim, H. K.; Jang, M. S.; Ahn, T.; Hwang, D. H.; Zyung, T. *Macromolecules* **1999**, *32*, 3279.

1.27 (a)Huynh, W. U.; Dittmer, J. J.; Alivisatos, P. *Science* **2002**, *295*, 2425.

(b) Wu, C.; Szymanski, C.; McNeill, J. *Langmuir* **2006**, *22*, 2956.

1.28 (a) Chen, X. C.; Green, P. F. *Langmuir* **2010**, *26*, 3659. Cury, L. A.; Ladeira, L. O.; Righi, A. *Synth. Met.* **2003**, *139*, 283.

(b) Szymanski, C.; Wu, C.; Hooper, J.; Salazar, M. A.; Perdomo, A.; Dukes, A.; McNeill, J. *J. Phys. Chem. B* **2005**, *109*, 8543.

1.29 Kim, J. Y.; Lee, K.; Coates, N. E.; Moses, D.; Nguyen, T.-Q.; Dante, M.; Heeger, A. J. *Science* **2007**, *317*, 222.

1.30 Brabec, C. J.; Sariciftci, N. S.; Hummelen, J. C. *Adv. Funct. Mater*. **2001**, *11*, 15.

1.31 Li, Y.; Zou, Y. *Adv. Mater*. **2008**, *20*, 2952.

1.32 Ilic, D.; Birke, P.; Holl, K.; Wohrle, T.; Haug, P.; Birke-Salam, F. *J. Power Sources* **2004**, *129*, 34.

1.33 Dennler, G.; Bereznev, S.; Fichou, D.; Holl, K.; Ilic, D.; Koeppe, R.; Krebs, M.; Labouret, A.; Lungenschmied, C.; Marchenko, A.; Meissner, D.; Mellikov, E.; Meot, J.; Meyer, A.; Meyer, T.; Neugebauer, H.; Opik, A.; Sariciftci, N. S.; Taillemite, S.; Wohrle, T. *Solar Energy* **2007**, *81*, 947.

1.34 (a) Alkan, S.; Cutler, C. A.; Reynolds, J. R. *Adv. Func. Mater.* **2003**, *13*, 331.

(b) Argun, A. A.; Cirpan, A.; Reynolds, J. R. *Adv. Mater.* **2003**, *15*, 1341.

(c) Cirpan, A.; Argun, A. A.; Grenier, C. R. G.; Reeves, B. D.; Reynolds, J. R. *J. Mater. Chem.* **2003**, *13*, 2422.

(d) Heuer, H. W.; Wehrman, R.; Kirchmeyer, S. *Adv. Funct. Mater.* **2002**, *12*, 89.

Chapter 2

Synthesis and Characterization of Soluble Poly(p-phenylene) Derivatives for PLED Applications

Chapter – 2

Synthesis and Characterization of Soluble Poly(p-phenylene) Derivatives for PLED Applications

Abstract:

PPP derivatives with high molecular weights were synthesized and characterized by FT-IR, ^{1}H NMR, ^{13}C NMR and C, H, N analysis. The decomposition temperatures of **2.2a**–**2.2c** were above 350 $^{\circ}$C. DSC analysis indicated their crystalline nature as all of them exhibited a melt temperature on controlled heating. Optical and electrochemical band gaps were determined using UV-vis spectroscopy and CV. Single-layer PLEDs fabricated with **2.2a**–**2.2c** displayed high threshold voltages due to high potential barrier for holes. Their EL spectra revealed a small shift in blue peak and the emission from higher wavelength shoulder peak is enhanced.

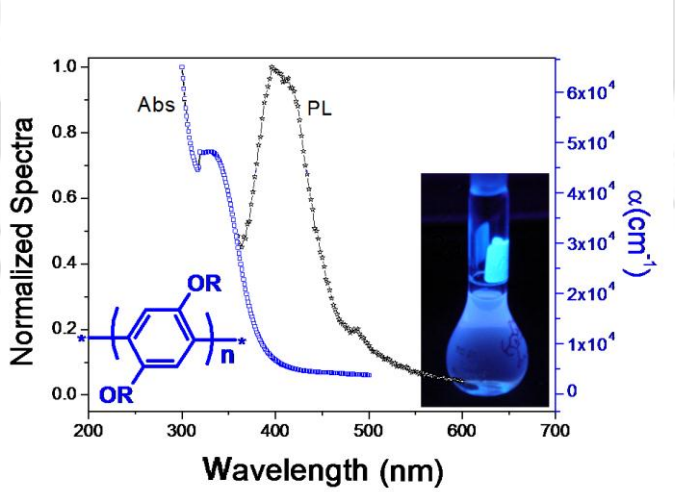

2.1 Introduction:

The discovery of electroluminescence (EL) in conjugated polymers has provided a new thrust to the development of light-emitting devices (LEDs) for display applications.[2.1] Wide range of conjugated polymer systems that include poly(p-phenylene) (PPP), polyfluorene (PFO), poly(p-phenylenevinylene) (PPV), polyacetylene (PA) have been investigated as active materials for polymer light emitting diodes (PLEDs).[2.2] Pursuing efficient and stable blue LEDs based on conjugated polymers still remains a major challenge. Although PFO has shown great promise as a blue emitting material, it has a tendency to degrade on prolonged exposure to heat and atmospheric oxygen to generate undesired green emission bands.[2.3–2.5] While efforts are on to commercialize organic / polymer light-emitting diodes (OLED)/(PLED) for various display applications, fundamental issues like development of alternative polymeric materials for pure blue light emission still need more attention. We thus focused on developing PPP-based polymers as an alternative to traditionally reported blue light emitting materials. Unsubstituted PPP is intractable and insoluble material. By substituting the backbone with solubilizing saturated chains, the processing parameters are enhanced; the energy levels can be tuned besides improving their thermal, optical, and morphological properties. Substitution of electron releasing long chain alkyl groups (e.g., CH_3, C_4H_9, C_6H_{13}) onto the phenyl ring increases the highest occupied molecular orbital (HOMO)/ lowest unoccupied molecular orbital (LUMO) band gap.[2.6] Additionally there are no reports of major stability issues in the structure of PPP like fluorenone formation associated with PFO and interchain aggregation that result in blue, green or even green emission with prolonged time. The synthesis of PPP and its derivatives have been achieved employing several expensive catalytic methods that employ nickel and palladium-based catalysts in anhydrous solvent systems.[2.7–2.10] All these methods need either excessive heating or strict inert atmospheric

conditions or extremely dry solvents and in several cases even a combination of many of the above, making the overall reaction time consuming, difficult to handle catalysts and expensive. Oxidative polymerization, which utilizes $FeCl_3$ as a catalyst, is extremely cheap and easy to handle. No halogenated monomer is needed and the polymerization can be done on benzene ring or alkoxy/alkyl substituted benzene derivatives. These advantages, coupled with mild reaction condition like room temperature stirring, no use of dry solvents, simple workup procedure and obtaining high molecular weight polymers makes this procedure very handy and attractive.

The use of PPP in different applications has been limited by the insolubility of pure PPP in common organic solvents, which, when chemically synthesized, usually is obtained in powder form. Thus, films of PPP and its derivatives have mainly been obtained by vacuum evaporation of pure oligomers. For PPP to be utilized in devices and other optoelectronic applications it should have a high relative molecular mass, homogeneous structure, and good molecular packing. In the present work, we have synthesized and characterized high molecular weight dialkyl-substituted PPP derivatives by oxidative polymerization using anhydrous $FeCl_3$ as a catalyst.[2.11] The polymers obtained by this method are found to be easily soluble in common organic solvents (e.g. $CHCl_3$, tetrahydrofuran, xylene, and toluene) and displayed blue luminescence in optical studies. The thermal properties were studied by performing thermo-gravimetric analysis (TGA) and differential scanning calorimetry (DSC). PLED devices were fabricated using these polymers as emissive materials.

2.2 Experimental Section:

2.2.1 *Reagents and Materials*:

Alkyl halides were purchased from Sigma Aldrich. All other chemicals were purchased from Merck, India and Ranbaxy, India and were used as received unless mentioned.

2.2.2 *General Procedure for the Synthesis of 1,4-Dialkoxybenzenes*:

A general method adopted for the synthesis of oligomers and polymers is outlined in Scheme 2.1:

Synthesis of 1,4-dialkoxybenzene (**2.1a**–**2.1b**) was carried out using a previously established procedure from the literature.[2.11–2.13] In a 250 mL round-bottomed flask, KOH (10.39 g, 185 mmol) and dry dimethyl sulfoxide, 48 mL) was stirred under N_2 atmosphere for 3h at room temperature. To the mixture was added hydroquinone (2.04 g, 18.52 mmol) and 1-bromoundecane (17.43 g, 74.1 mmol) and stirred for additional 25 h. The brown solution thus obtained was poured into water (400 mL). The aqueous layer was extracted with hexane (400 mL) and the organic layer was separated, washed with water, dried over anhydrous Na_2SO_4, and concentrated to obtain yellow-brown liquid. Excess 1-bromoundecane was distilled off under reduced pressure and the crude, on further purification by silica gel column chromatography (ethyl acetate/hexane, 0.5:9.5), yielded 1,4-diundecyloxybenzene (**2.1c**) as white solid flakes.

2.1c: 4.61 g, Yield: 80%; ^{1}H NMR (400 MHz, $CDCl_3$): δ_{ppm}, 6.79(s, 4H), 3.88(m, 4H), 1.73(m, 4H), 1.42(m, 4H), 0.87(m, 4H). ^{13}C NMR (100 MHz, $CDCl_3$): $\delta_{ppm,}$ 14.25, 22.80, 26.17, 29.45, 29.52, 29.70, 32.01, 68.67, 115.29, 153.02. FT-IR (KBr) = 2923, 1239, 1030, 827, 773, 726 cm^{-1}. m.p., 81 $^{\circ}$C. GC-MS: m/z, (M^{+1}) 418.

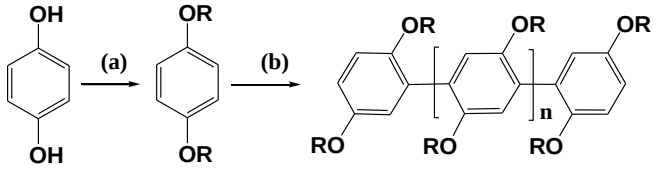

(a) KOH, DMSO, RT, 24 hrs (b) $FeCl_3$, $C_6H_5NO_2$, RT-36 hrs
R=C_6H_{13} or C_8H_{17} or $C_{11}H_{23}$

Scheme-2.1

2.2.3 *General Procedure for the Preparation of Polymers 2.2a–2.2c*:

Polymers, poly(1,4-hexyloxybenzene) (**2.2a)** and poly(1,4-octyloxybenzene) (**2.2b)** were prepared by methods reported earlier.[2.11–2.14] The synthesis of poly(1,4-diundecyloxybenzene) (**2.2c**) proceeded as follows. In a 100 mL three-necked round-bottom flask equipped with a nitrogen inlet, anhydrous ferric chloride (0.38 g, 2.26 mmol) was dissolved in 13 mL of nitrobenzene. **2.1c** (0.25 g, 0.59 mmol) dissolved in 12.5 mL nitrobenzene was added to the flask using a syringe. The reaction mixture was stirred at room temperature for 36 h, followed by precipitation from ethanol. Precipitates were stirred for 1h, centrifuged and washed repeatedly with ethanol and 10 mL 5% aq. EDTA solution to ensure the complete removal of monomers and trace amount of excess catalyst present there. The resulting polymer **2.2c** was dried under reduced pressure to obtain 0.18g as light brown powder.

2.2c: Yield: 72%, ^{1}H NMR (400 MHz, $CDCl_3$): δ_{ppm}, 7.05, 3.89, 1.65, 1.26, 0.89. ^{13}C NMR (75.5 MHz, $CDCl_3$): δ_{ppm}, 14.22, 22.81, 26.29, 29.50, 29.80, 32.04, 69.65, 117.32, 149.96. *Elemental analysis calculated for* ***2c***: C, 80.71; H, 11.61; *found*: C, 80.87; H, 12.10.

2.2.4 *Fabrication of Electroluminescent Devices*:

For device fabrication, cleaned indium tin oxide (ITO) coated glass substrates were first treated by oxygen plasma. Poly(3,4-ethylenedioxythiophene): poly(styrene sulfonate) (PEDOT:PSS) was coated on these substrates at 1000 rpm followed by vacuum drying at

120 °C for 1 h. Then the solution of polymer, 18 mg/mL concentration in toluene, was spin coated on the substrates at 1000 rpm followed by vacuum drying at 100 °C for 1 h. Subsequently Ca (215 Å) and Al (1250 Å) were deposited by vapour deposition to form the cathode. Figure 2.1 shows the schematic architecture of the fabricated devices.

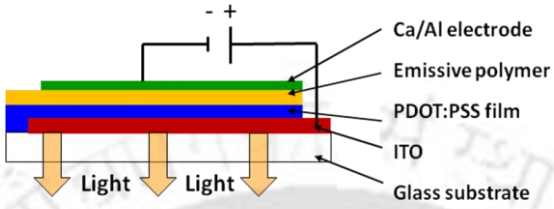

Figure 2.1 Schematic structure of the device fabricated

2.3 Results and Discussion:

2.3.1 *Synthesis of Monomers and Polymers*:

The 1,4-dialkoxy substituted benzenes were synthesized following the procedure reported by Weder and Wrighton.[2.15] Hydroquinone was reacted with *n*-bromoalkanes at room temperature in presence of KOH in dry DMSO to provide the required alkylated products in 75–80% yields (Scheme 2.1). The formation of the product was monitored by the disappearance of band at 3261cm^{-1} for O-H stretching and appearance of bands at 2931–2864 cm^{-1} and 1032 cm^{-1} for *o*-alkoxy-substituted moieties in the FT-IR spectrum.

The dialkyl-substituted derivatives (**2.1a**–**2.1c**) were characterized by gas chromatography-mass spectrometry (GC-MS), Fourier-transform infrared (FT-IR) spectroscopy, ^{1}H NMR, and ^{13}C NMR spectroscopy. The disappearance of the hydroxyl proton signal at δ_{ppm}, 4.5 in the ^{1}H NMR spectrum and a new peak at δ_{ppm}, 4 for O-CH_2 protons indicated the formation of 1,4-dialkoxy benzenes. The peak at δ_{ppm}, 70 for O-CH_2 carbon in ^{13}C NMR further supported the O-alkylation. In GC-MS the molecular ion peaks were obtained at 278, 334, and 418 for 1,4-dihexyloxy benzene (**2.1a**), 1,4-

dioctyloxy benzene (**2.1b**), and 1,4-diundecyloxy benzene (**2.1c**), respectively confirming the formation of desired products. As per previously established procedure,[2.11] the oxidative polymerizations of monomers (**2.1a**–**2.1c**) were then carried out using 4 equiv. of anhydrous $FeCl_3$ in nitrobenzene followed by precipitation from ethanol. The mixture was stirred for 1 h, centrifuged and washed repeatedly with ethanol. The resulting polymer was dried under reduced pressure to give a light brown powder of high yield. Polymers **2.2a**–**2.2c** was characterized by FT-IR spectroscopy, ^{1}H NMR, ^{13}C NMR, and gel permeation chromatography (GPC). The ^{1}H NMR showed the absence of signal at δ_{ppm} 6.8 for the phenyl proton of the monomer and appearance of broad signal at δ_{ppm} 7.1 for aromatic protons of the polymer. In ^{13}C NMR a new signal at δ_{ppm} 127 was obtained for the phenyl substituted aromatic carbon. The polymers were found to be readily soluble in a range of solvents, e.g., chloroform, dichloromethane, THF, xylene, toluene, chlorobenzene, etc. GPC analysis showed a number-average molecular weight of the polymer **2.2a** to be Mw, 37360 $gmol^{-1}$ [polydispersity index (PDI), 1.34].[2.11] Polymer **2.2b** Mw, 35220 $gmol^{-1}$ (PDI, 1.89) and polymer **2.2c** Mw, 3673 $gmol^{-1}$ (PDI, 1.10). The molecular weight of **2.2c** was always less compared to **2.2a** and **2.2b** due to the presence of longer chains on the monomer units. Due to the presence of these long alkyl chains there would be difficulty in adjacent monomer units to come closer to each other restricting formation of polymer with higher molecular weights leading to premature termination of the growing chains.

2.3.2 *Thermal Properties of the Polymers*:

The thermal stability of the polymers were studied by TGA performed under N_2 atmosphere at a heating rate of 10 $^{\circ}$C min^{-1}. Polymer **2.2a** was found to be thermally stable up to 430 $^{\circ}$C, **2.2b** was found to be stable up to 400 $^{\circ}$C whereas **2.2c** having lower molecular weight as compared to **2.2a** and **2.2b** was stable up to 300 $^{\circ}$C. (Figure 2.2)

These data are marked improvement on the thermal stability of the PPP polymers reported in literature where structurally similar polymers were stable only up to 190–250 °C.[2.16] This is due to higher molecular weight and defect free structures generated by carefully executed synthesis. **2.2c** that has lower molecular weight compared to **2.2a** and **2.2b** further justifies this molecular weight dependence thermal stability concept. The DSC studies of the polymers were carried out under nitrogen atmosphere at 10 °C min^{-1}. In its second heating cycle an exothermic peak was observed at 41 °C (Figure 2.3). The exothermic peak was the second order transition of the polymers (**2.2a-2.2c**). On further heating, another endothermic peak due to crystallization was observed at 71 °C for **2.2a**. PPP polymers have a flexible geometry and two adjacent phenyl rings are twisted. Additionally the bonds in the backbone are not necessarily single, but co-linear and have partial double bond character, making the backbone stiff and difficult to rotate. Planarity of these polymers may be contributing to easy crystallization and lower glass transition value similar to earlier reports on rigid oligomeric systems.[2.16]

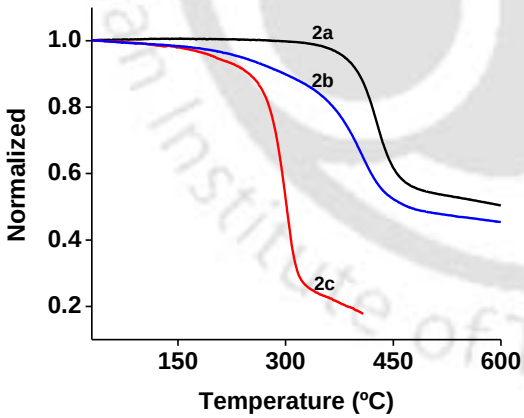

Figure 2.2 TGA plots of **2a-2c** performed at a heating rate of 10 °C /min

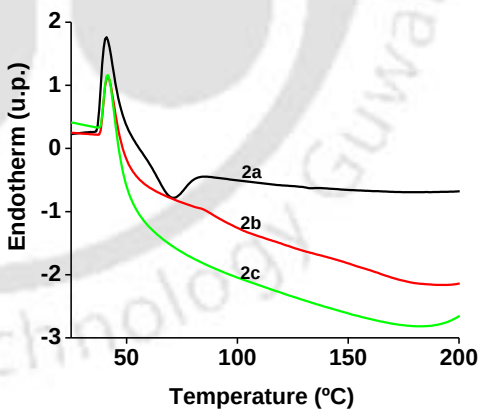

Figure 2.3 DSC plots of the polymers **2a-2c** performed at a heating rate of 10 °C /min

2.3.3 *Optical Properties in Solution*:

The optical properties of **2.2a**–**2.2c** were studied using UV-vis and fluorescence spectroscopy. UV-vis absorption maxima of alkyl-substituted polymers have been observed in the range of 329–334 nm (Figure 2.4). There is an insignificant change in the absorption position of the three derivatives, indicating that increasing the substituent length have no direct effect on the UV-vis absorption position.

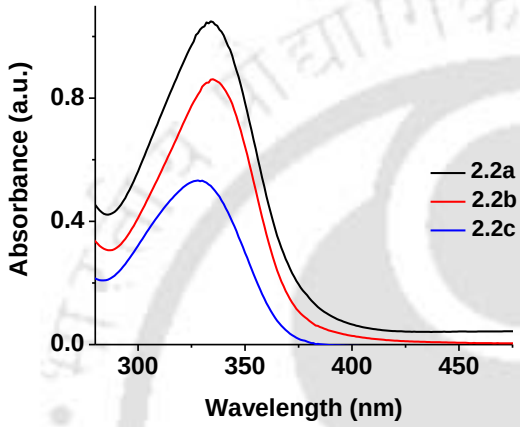

Figure 2.4 Absorbance spectra of **2.2a-2.2c** in chloroform

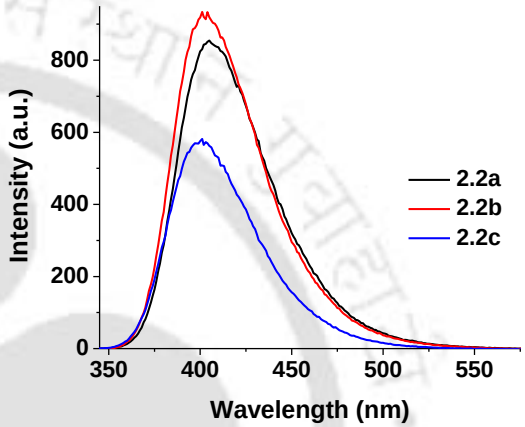

Figure 2.5 Fluorescence spectra of **2.2a-2.2c** in chloroform

The polymers exhibited a strong emission in dilute solution because of their rigid backbone structure with the maxima observed in the range from 401 to 406 nm (Figure 2.4). This new series of PPP polymers consistently exhibited shorter wavelengths emission compared to similar polymers reported in the literature.[2.17–2.20]

2.3.4 *Optical Properties of Thin Films*:

The UV-vis and photoluminescent maxima of **2.2a**–**2.2c** films were measured on glass slide. Minor 4–6nm bathochromic shift was observed for all the polymers in the solid state compared to their solution (Figures 2.6 and 2.7) (Table 2.1). Polymer **2.2b** when compared to **2.2a** and **2.2c** shows a red shift in absorption (16 nm) and PL (18 nm)

spectra. This is consistent with the result that the second peak at 488 nm in PL spectrum is also dominant for **2.2b** as compared to the other two materials.

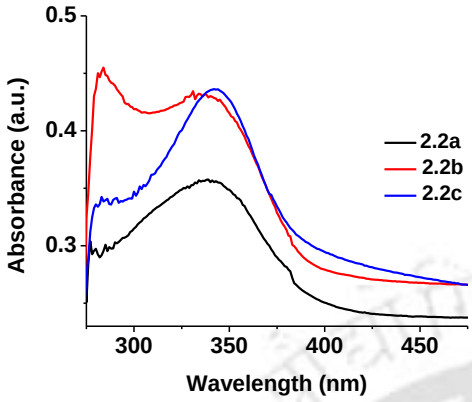

Figure 2.6 Absorbance spectra of **2.2a-2.2c** thin film on glass substrate.

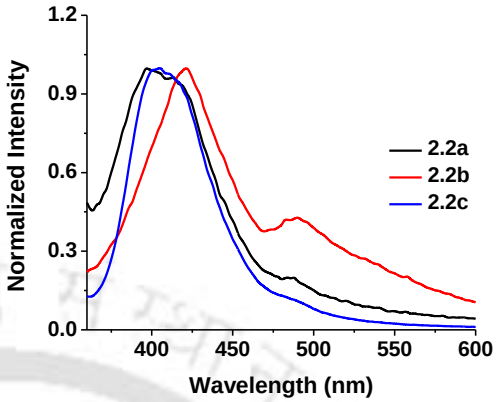

Figure 2.7 Fluorescence spectra of **2.2a-2.2c** thin film on glass substrate.

This is due to strong interchain interaction in the film form in addition to aggregates responsible for the higher wavelength absorption. Photoluminescence quantum efficiency (PLQE) values for these polymers were in the range of 0.3–0.6% (Table 2.1). There seems to be considerable quenching due to interchain interactions and aggregate formation. This is similar to earlier reports of photon per electron efficiency in solid state.[2.17–2.20]

Table 2.1 Comparison of absorption and PL emission from thin films of **2a-2c**.

Polymer	Absorption peak (nm)	PL peak (nm)	PLQE
2a	330	400 and 487	0.3%
2b	346	419 and 488	0.6%
2c	330	401 and 487	0.4%

The tendency of these polymers to crystallize may be another reason for the quenching of emission. PL of PPP series shows better color purity compared to typical PFO, and peak emission is also at lower wavelength. Also, there does not seem to be any problem related to atmospheric degradation that could lead to presence of significant emission at longer wavelength.

2.3.5 *Electrochemical Studies*:

The redox behaviours as well as the HOMO and LUMO energy levels of the polymers were investigated by cyclic voltammetry (CV) (Figure 2.8) using 0.01 M ferrocene in acetonitrile as reference (Table 2.2).[2.21] In the present work, tetrabutylammonium perchlorate (TBAP) was used as a supporting electrolyte. Acetonitrile was used as the solvent. Pt wire was used as the working electrode.[2.22] The onset potential (E^{ox} and E^{red}) can be used to estimate the HOMO and LUMO values of the conjugated polymer. According to the equation reported by Li et al. and de Lieu et al., $E_{LUMO} = [E^{red} + 4.39\ eV]$ and $E_{HOMO} = [E^{ox} + 4.39\ eV]$, the LUMO and HOMO energy of the polymer were determined and compared with that of the UV-vis data, calculated according to the equation $E = 1240/\lambda_{max}$.[2.23] Band gap of polymers from the UV-vis data of solid film were 3.46 eV, 3.48 eV, and 3.63 eV, respectively for **2.2a**, **2.2b**, and **2.2c**. These data indicate that energy gaps calculated from the electrochemical potentials and those of optical energy gaps are in agreement and the polymers were electrochemically stable as exhibited by their ability to withstand several electrochemical cycles in the solid state.

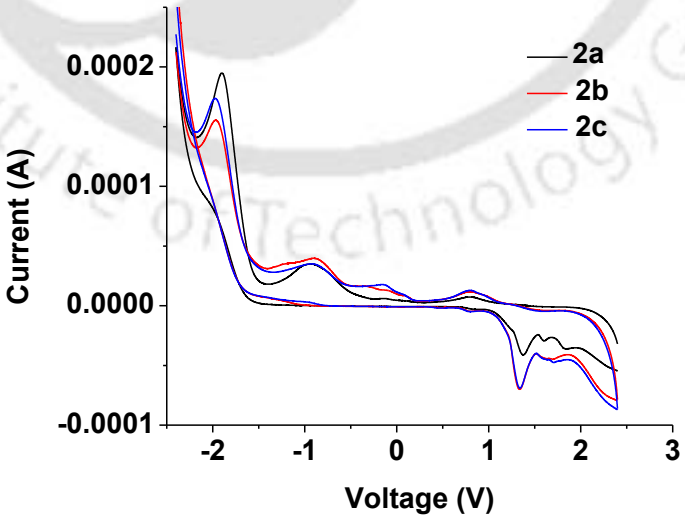

Figure 2.8 Cyclic voltammogram of the polymers **2a**-**2c**.

Table 2.2 Calculation of band gap from CV study

Polymer	2.2a	2.2b	2.2c
HOMO	6.18	6.04	6.08
LUMO	3.14	2.93	2.89
Band gap/eV	3.04	3.11	3.19

2.3.6 *Electroluminescent Properties*:

We have made single layer light emitting devices using these polymers. Figure 2.9(a) shows the current-voltage characteristics of the devices. Table 2.3 shows the threshold voltage (E_{th}) of devices to be $8X10^5$, $2.3X10^6$, and $2.5X10^6$ Vcm^{-1} for **2.2a**, **2.2b**, and **2.2c**, respectively. According to the HOMO and LUMO of the material (**2.2a**, **2.2b**, and **2.2c**) as shown in Figure 2.9(b), the injection barrier for holes is much higher than the thermal excitation energy of the holes, which leads to the higher threshold voltage. High threshold voltages can also indicate poor hole transport through these devices.

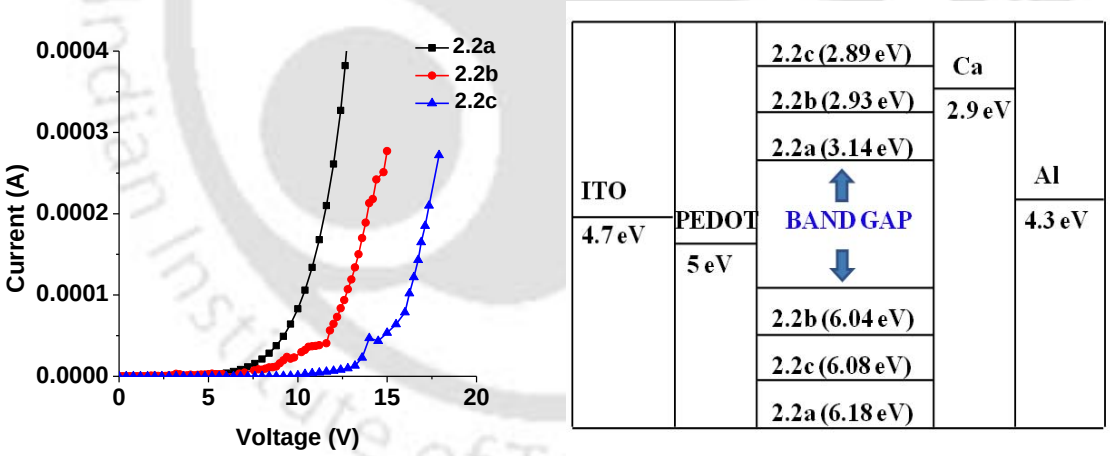

Figure 2.9 (a) Current-Voltage (I-V) characteristics (b) Energy band diagram of **2.2a**-**2.2c** based OLED devices.

This is in agreement to an earlier report by Yang et al., who blended these polymers with a hole transporting material to reduce the turn-on voltage.[2.24] To improve turn-on voltage

inclusion of hole injection and/or electron and hole transport materials in the device is required.

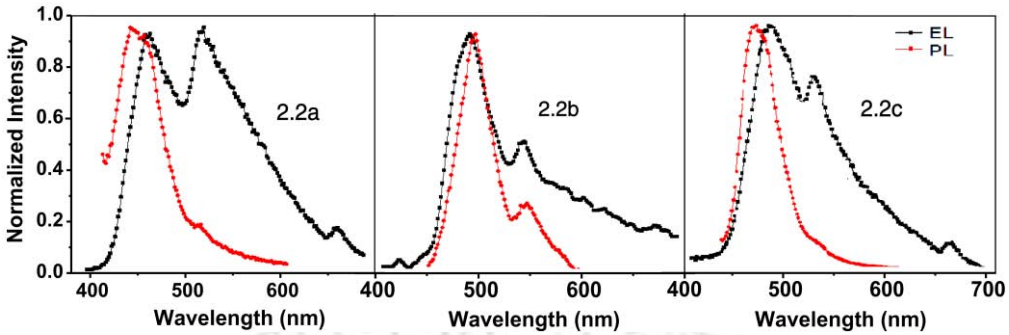

Figure 2.10 Normalized photo and electro-luminescence spectra of the polymers **2.2a-2.2c**.

Figure 2.10 shows the comparison of EL and PL emission for **2.2a**–**2.2c** (tabulated in Table 2.3). All the devices show enhanced second peak at longer wavelength. It is not feasible to make pure blue devices with these polymers in neat form. The longer wavelength peak is also present in PL of thin films, assigned to interchain interactions and aggregate formation.

Table 2.3 EL characteristics for **2.2a-2.2c.**

Polymers	PL peak of thin film (nm)	EL peak (nm)	E_{th} of the devices (V/cm)
2.2a	400 and 487	420 and 488	8×10^5
2.2b	419 and 488	414 and 485	1.6×10^6
2.2c	401 and 487	422 and 486	2.5×10^6

The reason for enhanced emission from this peak in EL is due to direct electronic excitation of these entities. Blending these polymers with a hole transporting material, in addition to improvement of the I-V characteristics, will reduce the interchain interaction and also improve the color purity of the device.

2.4 Conclusion:

A series of PPP-based polymer derivatives have been developed that have high molecular weight and show improved thermal stability compared to earlier literature reports. Polymerization reactions are carried out at mild conditions like room temperature stirring and normal atmospheric pressure with a very cheap catalyst, which can be easily removed from the product. The introduction of alkoxy side chains not only improves solubility of polymers in organic solvents but also affect the optical properties including UV-vis absorption peaks, band gaps (from 3.05 to 3.20) and photoluminescent peaks. Increase in carbon chain length also plays a role in controlling the steric factor in both solid and solution state. The blue spectrum in fluorescence experiments is ~400 nm with less color purity. Due to crystallization, neat films show quenching of PL emission. PLEDs made with neat polymers exhibit high turn-on voltages and enhanced emission in the higher wavelength. Further improvement in the devices may be possible by blending these materials with hole injection and hole/electron transport materials.

2.5 References:

2.1. Burroughes, J. H.; Bradley, D. D. C.; Brown, A. R.; Marks, R. N.; Mackay, K.; Friend, R. H.; Burns, P. L.; Holmes, A. B. *Nature* **1990**, *347*, 539.

2.2. Wise, D. L.; Wnek, G. E.; Trantolo, D. J.; Cooper, T. M.; Gresser, J. D. Photonic Polymer Systems, Marcel Dekker, New York, 1998.

2.3. List, E. J. W.; Guentner, R.; Scanducci de Freitas, P.; Scherf, U. *Adv. Mater*. **2002**, *14*, 374.

2.4. Gong, X.; Iyer, P. K.; Moses, D.; Bazan, G. C.; Heeger, A. J.; Xiao, S. S. *Adv. Funct. Mater*. **2003**, *13*, 325.

2.5. Romaner, L.; Pogantsch, A.; Scandiucci de Freitas, P.; Scherf, U.; Gaal, M.; Zojer, E.; List, E. J. W. *Adv. Funct. Mater*. **2003**, *13*, 597.

2.6. Shim, H. K.; Jang, M. S.; Ahn, T.; Hwang, D. H.; Zyung, T. *Macromolecules* **1999**, *32*, 3279.

2.7. Tamao, K.; Kodama, S.; Nakajima, I.; Kumada, M. *Tetrahedron* **1982**, *38*, 3347.

2.8. Yamamoto, T.; Hayasi, Y.; Yamamoto, A.; *Bull. Chem. Soc. Jpn.***1978**, *51*, 2091.

2.9. Colon, I.; Kelsey, D. R. *J. Org. Chem*. **1986**, *51*, 2627.

2.10. McCarthy, T. F.; Witteler, H.; Pakula, T.; Wegner, G. *Macromolecules* **1995**, *28*, 8350.

2.11. Paul, G. S.; Sarmah, P. J.; Iyer, P. K.; Agarwal, P. *Macromol. Chem. Phys.* **2008**, *209*, 417.

2.12. Jinyun, Z.; Caimao, Z.; Song, W.; Lei, Z.; Xi, Y.; Rui, Z.; Jingui, Q. *Polymer* **2002**, *43*, 1761.

2.13. van Breemen, A. J. J. M.; Herwig, P. T.; Chlon, C. H. T.; Sweelssen, J.; Schoo, H. F. M.; Benito, E. M.; de Leeuw, D. M.; Tanase, C. J.; Wildeman, P. W.; Blom, M. *Adv. Funct. Mater*. **2005**, *15*, 872.

2.14. de Halleux, V. M.; Geerts, Y. H. *React. Funct. Polym.* **2000**, *43*, 145.

2.15. Weder, C.; Wrighton, M. S. *Macromolecules* **1996**, *29*, 5157.

2.16. Shirota, Y. *J. Mater. Chem.* **2000**, *10*, 1.

2.17. Remmers, M.; Neher, D.; Gruner, J.; Friend, R. H.; Gelink, G. H.; Warman, J. M.; Quattrocchi, C.; do Santos, D. A.; Bredas, J. *Macromolecules* **1996**, *29*, 7432.

2.18. Tasch, S.; Niko, A.; Leising, G.; Scherf, U. *Appl. Phys. Lett.* **1996**, *68*, 1090.

2.19. Gruner, J.; Wittman, H. F.; Hamer, P. J.; Friend, R. H.; Huber, J.; Scherf, U.; Mullen, K.; Moratti, S. C.; Holmes, A. B. *Synth. Met.* **1994**, *67*, 181.

2.20. Leising, G.; Tasch, S.; Meghdadi, F.; Laurence, A.; Froyer, G.; Scherf, U. *Synth. Met.* **1996**, *81*, 185.

2.21. Huang, W.; Ding, A.-L.; Pei, J.; Lai, Y. H. *J. Mater. Chem.* **2001**, *11*, 3082.

2.22. Kaifer, A.; Kaifer, M. G. *Supramolecular Electrochemistry* Wiley-VCH, Weinheim, 1999.

2.23. Sotzing, G. A.; Seshadri, V. *Chem. Mater*. **2004**, *16*, 5644.

2.24. Yang, Y.; Pei, Q.; Heeger, A. J. *J. Appl. Phys*. **1996**, *79*, 934.

Chapter 3

Facile C–H Alkylation in Water: Enabling Defect-free Materials for Optoelectronic Devices

Chapter – 3

Facile C−H Alkylation in Water: Enabling Defect-free Materials for Optoelectronic Devices

Abstract:

A facile method for the alkylation of fluorene achieved via direct C−H alkylation under aqueous conditions is reported, wherein the formation of fluorenone is inhibited, resulting in the exclusive formation of the desired dialkyl-substituted fluorene monomer. As a proof of concept, this method has also been successfully extended to perform N-alkylation of carbazole, diphenylamine, and N,N-dialkylation of aniline in high yields (figure 3.1).

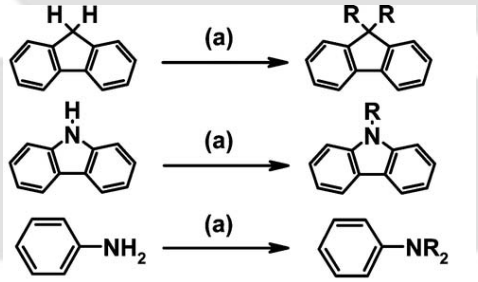

(a) = R-X, aq. NaOH, PTC, 70 °C. R = C_6H_{13}

3.1 Introduction:

Polydialkylfluorenes possess excellent photophysical, thermal, and processing properties, which have made them one of the most promising materials presently being used to fabricate blue-light emitting diodes (LEDs) and biosensor applications.[3.1, 3.2] The presence of a rigidly planar biphenyl unit with a methylene bridge allows functionalization at the 9-position resulting in high solubility and processability in the resulting polymers. However, several studies have demonstrated that poly(9,9-dialkylfluorene) degrades to give a longer wavelength emission band in the presence of oxygen over time which is more intense in electroluminescence (EL) than in photoluminescence (PL).[3.3] Numerous papers attribute this band to the formation of emissive fluorenone units in the polymer backbone that intensifies with increasing fluorenone concentration.[3.4] Thus, under all circumstances, the 9-position hydrogens in fluorene are the sole culprits that undergo oxidation to form fluorenone units when subjected to high thermal conditions during device fabrication or photo-degradation when exposed to light. Hence, finding an appropriate and facile method for the preparation of "defect free" alkyl-substituted fluorene monomers not only remains a challenge but would also be a striking achievement to produce stabilized blue light emitting devices.

A common practice associated with C9 alkylation reactions of fluorene reported so far utilizes high-boiling solvents such as DMSO, DMF, HMPA, etc. as the reaction medium.[3.5–3.10] Yields obtained by these methods were in the range of 63−80 %. DMSO, a solvent used very often, has several drawbacks, most prominently it's environmentally adverse impact and secondly the tedious reaction workup for the separation of DMSO from the final product. Few other alkylation methods reported in the literature have utilized a combination of different solvents with metal catalysts, phase-transfer catalysts (PTCs), very strong bases, multiple synthetic steps, and extreme reaction conditions,[3.7–

[3.10] yet the art of making defect-free dialkylated fluorene has not been achieved. Employing the above routes affects the overall economy of the reaction and needs extraordinary precautions and specialized conditions for obtaining defect-free dialkylated product. This encouraged us to investigate a simpler route for the dialkylation of fluorene that would be economical, environmental friendly, and high yielding in contrast to the existing methods. The reactivity of the C−H bond present at the 9-position of "unsubstituted fluorene" is extremely poor compared to the fluorene molecule having electron-withdrawing halogen substituents at the 2,7-positions or only at the 2-position. Hence, activation of the C−H bond in "unsubstituted fluorene" is predominantly challenging owing to which this compound has been avoided or overlooked for alkylation reactions. In this chapter, we demonstrate that alkylation of "unsubstituted fluorene" can be performed by means of an uncomplicated and facile route, allowing insertion of a wide variety of alkyl chains on the 9-position of fluorene in exceptional yields. Importantly, we establish that this alkylation route could be extended to several other important intermediates and precursors for, e.g., dialkylation of substituted and partially substituted fluorene, N-alkylation of carbazole and diphenylamine, and N,N-dialkylation of aniline, all of which are vital as charge-transporting and luminescent materials for optoelectronic devices and sensors. While working on this challenge, we emphasized on the use of reagents and reaction conditions that are economical, safe, and lead to high-yielding products.

Initial attempts to perform dialkylation on "unsubstituted fluorene" in the presence of excess haloalkane (up to 20 times), aq NaOH, and tetrabutylammonium iodide (TBAI) in DMSO and/or water at elevated temperatures yielded fluorenone as the sole product, which made us realize that the art of making dialkylated fluorene is not so straightforward as perceived and one of the prime reasons for "unsubstituted fluorene" to be overlooked.

Several repetitions of the reaction under varying conditions confirmed that the foremost problem in these reactions is trace amounts of oxygen, which was found to be so reactive that in the presence of base, fluorenone was formed as the exclusive product even at temperatures of 35−50°C. Fluorenone formation can be easily visualized by the distinct yellow colour of the isolated product and from the 1720 cm^{-1} ketone peak in the IR data. This trace oxygen has either been ignored or considered to be very trivial while performing the fluorene dialkylation reactions; nonetheless, it is the most perilous condition in obtaining defect-free dialkylated fluorene to be used as intermediates and precursors for numerous applications in foreseeable future. After several failed attempts, modifications were made in the reaction (Scheme-3.1) so as to obtain the desired dialkylated product in 85−98 % yields. (Table-3.1) To the best of our knowledge, there are no literature reports wherein difunctionalization of alkanes, more specifically "unsubstituted fluorene", has been successfully performed with a series of haloalkanes in the absence of metal catalysts, organic solvents, inert gases, and high pressure/temperature to obtain desired dialkylation products in high yields as reported here.

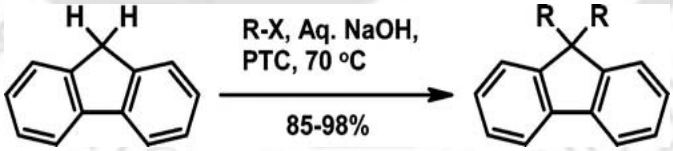

Scheme 3.1: General synthetic scheme for synthesis of unsubstituted 9,9-Dialkylfluorene

3.2 Results and Discussion:

Fluorene was reacted with a range of alkyl halides that include chloro-, bromo-, and iodo-terminated hydrocarbons (Scheme-3.1) at moderate temperature of 70 °C in the presence of 50% aq NaOH and TBAI to obtain the desired dialkylated products in high yields

(Table-3.1). Before the addition of alkyl halide into the reaction mixture, the complete removal of oxygen via repeated freeze−thaw degassing cycles of 15 min each (alternatively warming to room temperature) was performed to remove undesired oxygen gas. Bromoalkanes, due to their economy and better reactivity, have been extensively used for alkylation of fluorene. We have chosen six different types of bromoalkanes that include long-chain, branched-chain, and dibromo-substituted-chain derivatives.

Table 3.1 Yields Obtained for Alkylation of Fluorene with Ten Different Alkyl Halides in Aqueous NaOH, TBAI as PTC at 70 °C

Entry no.	RX (alkyl halide)	Time (h)	Yield (%)
3.1a	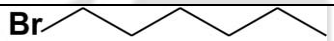	4	96
3.1b		4	98
3.1c	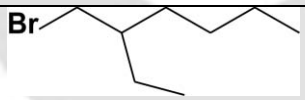	4	88
3.1d		6	88
3.1e	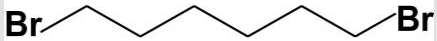	6	95
3.1f		6	90
3.1g	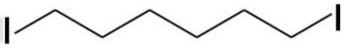	5	90
3.1h		5	88
3.1i	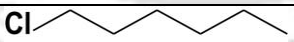	7	85
3.1j		7	87

Exceptionally high yields of up to 98 % (entry **3.1b**) have been obtained on reacting fluorene with 1-bromooctane. Similarly, highly dialkylated fluorene yields were also obtained by the reaction of fluorene with 1-bromohexane (96 %), 1-bromoundecane (88 %), 2-ethylhexyl bromide (88 %), 1,6-dibromohexane (95 %), and 1,8-dibromooctane (90

%) (entries **3.1a**, **3.1c**–**f**). Reaction of fluorene with 1,6-diiodohexane (90 %) and 1,8-iodooctane (88 %) (entries **1g**,**h**) also gave highly dialkylated product yields, whereas less reactive chloroalkanes, i.e., 1-chlorohexane and 1-chlorooctane, when treated with fluorene gave decent yields of 85 % and 87 % (entries **3.1i**,**j**) within 7 h under the same conditions, proving the versatility of this reaction for a wide variety of substrates having diverse structure and less reactivity. Since the reaction is performed in aqueous medium the separation of the desired dialkylated product was also very straightforward. All the dialkylated products obtained were well characterized by FT-IR, ^{1}H NMR, ^{13}C NMR, and mass spectroscopy and confirmed to be free from fluorenone.

Table 3.2 Comparative Reactivity Study of Fluorene Dialkylation by 1-Bromohexane in the Presence of Various PTCs in Water at 70 °C

Entry no.	phase-transfer catalyst (PTC)	time (h)	yield (%)
3.2a	tetrabutylammonium iodide(TBAI)	4	96
3.2b	tetrabutylammonium bromide(TBAB)	8	90
3.2c	tetrabutylammonium chloride(TBAC)	8	60
3.2d	tetrabutylammonium fluoride (TBAF)	12	50
3.2e	tetraethylammonium iodide (TEAI)	8	90
3.2f	tetraethylammonium bromide (TEAB)	10	85
3.2g	tetraethylammonium chloride (TEAC)	12	50
3.2h	15-crown-5	12	30
3.2i	sodium dodecyl sulfate (SDS)	12	15
3.2j	without PTC	24	12

Aqueous NaOH was used as a base in the above-described alkylation reaction that facilitated the synthesis of desired dialkylated fluorene in high yields. To ensure that dialkylation of fluorene proceeds smoothly, excess alkyl halide is used in these reactions. It is important that all the fluorene monomers get dialkylated before being exposed to

oxygen, since any monoalkylated fluorene remaining in the reaction can still form fluorenone in the presence of oxygen during device fabrication.[3.11] As discussed earlier, besides the role of base and PTC in the alkylation of fluorene, it is important to ensure that no oxygen is present in these reactions because the fluorene would react with this oxygen to generate undesired fluorenone. Since the conditions reported in Scheme 3.1 are easy and strikingly efficient, we expect this simple alkylation reaction to be of prime interest to the synthetic community and materials scientists to develop defect-free polyfluorene derivatives. Furthermore, we observed that the PTC has a prominent role in facilitating the dialkylation reaction, in addition to other favourable conditions required to achieve the dialkylated products. Table 3.2 represents a comparative reactivity study of the dialkylation of fluorene by 1-bromohexane in the presence of several PTCs at 70 °C.

TBAI showed the best performance (entry **3.2a**) both in terms of facilitating higher dialkylated product yields and lesser reaction time compared to all other PTCs examined here. These include tetrabutylammonium bromide (TBAB), tetrabutylammonium chloride (TBAC), tetrabutylammonium fluoride (TBAF), tetraethylammonium iodide (TEAI), tetraethylammonium bromide (TEAB), tetraethylammonium chloride (TEAC), 15-crown-5, sodium dodecyl sulfate (SDS), etc. As observed in Table 3.2, the product yield is best when performed in the presence of TBAI, followed by TBAB and TEAI (entries **3.2b** and **3.2e**) closely followed by TEAB (entry **3.2f**). A general trend observed in these reactions indicated that the iodide-containing PTC were most efficient (entries **3.2a** and **3.2e**) compared to bromide (entries **3.2b** and **3.2f**), chloride (entries **3.2c** and **3.2g**), and fluoride (entry **3.2d**) both in terms of shorter time durations and higher yields. 15-crown-5 and SDS showed little or no effect on the product yields (entries **3.2h** and **3.2i**). Alkylation performed in the absence of PTC gave very poor product yield in 24 h (entry **3.2j**), validating the use of appropriate PTC in these reactions. Since TBAI is one of the

cheapest and most easily available PTCs, its application benefits the overall economy of the alkylation reactions.

Table 3.3 Optimizing the Accurate Quantity of PTC Required for Obtaining Maximum Dialkylated Fluorene

Entry no.	TBAI quantity	Time (h)	Yield (%)
3.3a	0.01 g (2.5 mol %)	10	50
3.3b	0.02 g (5 mol %)	10	75
3.3c	0.03 g (7.5 mol %)	10	82
3.3d	0.046 g (10 mol %)	6	98
3.3e	0.1 g (25 mol %)	6	98
3.3f	0.5 g (>100 mol %)	6	98

After establishing that TBAI is the best PTC, we investigated its accurate quantity required for the best product yields. Table 3.3 depicts that 10 mol% of TBAI was sufficient for successful conversion of fluorene to dialkylated fluorene (entry **3.3d**). Adding greater than 10 mol% of TBAI did not enhance the yields of dialkylated products (entries **3.3e** and **3.3f**). However, decreasing the amount of TBAI below 10 mol% reduced the yield as well as prolonged the reaction time (entries **3.3a**–**c**). As part of our objective to bring simpler synthetic routes into the realm of "materials", the above-developed alkylation method was extended to other important substrates and reactions to authenticate this synthetic route for broader applications. Using the same conditions as above 2,7-dibromofluorene (entry **3.4a**) and 2-bromofluorene (entry **3.4b**) were dialkylated in outstanding yields of 99% and 98% with 1-bromohexane in shorter time duration than existing methods. Most notably, there was no fluorenone formation along with any of the final products, confirmed by TLC as well as the absence of 1720 cm^{-1} ketone peak in IR data.

Table 3.4: Alkylation of different substrates in water at 70°C with 1-Bromohexane

Entry no.	Substrate	Product	Time (h)	Yields %
3.4a	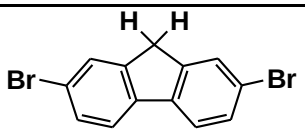	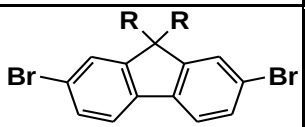	1	99
3.4b	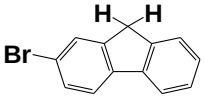	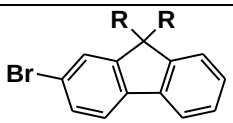	2	98
3.4c	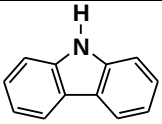	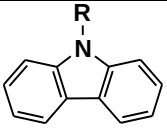	6	95
3.4d	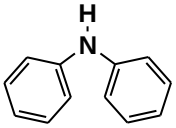	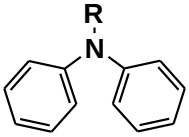	6	90
3.4e	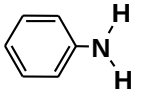	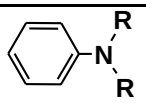	12	85

Furthermore, this alkylation method has been successfully extended to perform N-alkylation of carbazole, diphenylamine, and N,N-dialkylation of aniline. The high yields of 91 %, 75 %, and 72 % obtained for carbazole, diphenylamine, and aniline (Table **3.4**, entries **3.4c**–**e**) confirm that this facile and economical method is very efficient for the N-alkylation of primary and secondary amines (in addition to C-alkylation) that have been extensively applied in optoelectronic devices as emitting/transporting materials, sensors, and dopants.[3.12–3.14] The reactivity of fluorene, 2-bromofluorene, and 2, 7-dibromofluorene can be explained on the basis of pK_a values. As the pK_a of fluorene is 22.10, 2-bromofluorene= 20.56, and 2, 7-dibromofluorene= 17.80, of acids relative to a value of 18.59 for 9- phenylfluorene. [3.15] Remarkable change in acidity can be observed with the introduction of Br atoms on 2 and 7 positions of fluorene. Acidity of the 9-H's plays a vital role on alkylation reactions catalysed by bases which is reflected in the yield of these reactions.

3.3 Conclusion:

In summary, we have established a simple and economical methodology for the alkylation of fluorene (unsubstituted and substituted) and N-alkylation reactions in aqueous medium whose efficiency is much higher than that of currently applied methods. In view of the fact that these reactions are fundamental in organic synthesis and very critical for the development of defect free polymeric materials, this methodology offers advantages not just for fluorene alkylation reactions but also to a variety of N-alkylations. As a proof of concept, we utilized this reaction for the alkylation of primary and secondary aromatic amines, offering a wide variety of potential applications in peptide synthesis. We are presently making efforts to extend this reaction procedure for various other classes of substrates and chemoselective synthesis. Since our protocol proceeds under purely aqueous conditions, utilizes readily available, inexpensive, stable, and nontoxic chemicals and avoids use of metal catalyst, this method is very facile, economical, and environmentally benign and could be applied to wide-ranging alkylation reactions.

3.4 Experimental Section:

3.4.1 *Materials*:

Alkyl halides, fluorene, and tetrabutylammonium halides were used as received. Freshly distilled solvent was always used for workup and purification processes. Milli-Q grade water was used in all the experiments.

3.4.2 *General Procedure Followed for the Dialkylation of Fluorene (3.1c)*:

Fluorene (0.21g, 1.26 mmol), 50 % aq NaOH, and a catalytic amount of tetrabutylammonium iodide (0.046 g, 10 mol %) were added to a flask. The flask was degassed three times by applying freeze−thaw cycles. 2-Ethylhexyl bromide (1.70 g, 8.82

mmol) was added via syringe (degassed) and the mixture heated at 70 °C continuously for 4 h. The reaction mixture was cooled to room temperature and extracted with chloroform. The organic layer was washed with water and dried over anhydrous sodium sulfate. The solvent was removed under vacuum, and the crude was purified via column chromatography over a small pad of silica gel with 10% chloroform in hexane as the eluent to give the desired dialkylated product. The same procedure was adopted for all substrates (**3.1a**–**3.4b**).

(3.1a) 9,9-Dihexyl-9H-fluorene:[06] $C_{25}H_{34}$, (0.405 g, 96 %).

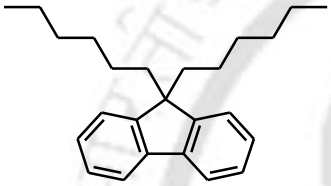

(3.1b) 9,9-Dioctyl-9H-fluorene:[3.10] $C_{29}H_{42}$, (0.48 g, 98 %).

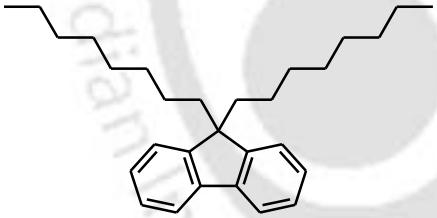

(3.1c) 9,9-Bis(2-ethylhexyl)-9H-fluorene: $C_{29}H_{42}$ (0.43 g, 88 %); ^{1}H NMR (400 MHz, $CDCl_3$): δ_{ppm}, 7.68 (d, 2H), 7.30 (m, 6H), 1.97 (m, 4H), 0.75 (m, 26H), 0.50 (m, 4H); ^{13}C NMR (100 MHz, $CDCl_3$): δ_{ppm}, 150.5, 141.5, 126.8, 126.5, 124.2, 119.7, 55.0, 44.7, 34.7, 34.7, 33.8, 28.2, 27.0, 22.8, 14.2, 10.4; exact mass 390.3287; HR MS 390.3253.

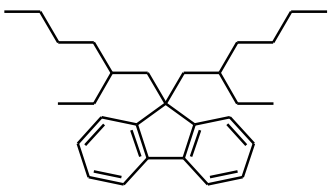

(3.1d) 9,9-Diundecyl-9H-fluorene: $C_{35}H_{54}$, (0.52 g, 88 %); ^{1}H NMR (400 MHz, $CDCl_3$): δ_{ppm}, 7.65(d, 2H), 7.28(m, 6H), 1.91(m, 4H), 1.38(m, 4H), 1.15(m, 22H), 0.99(s, 6H), 0.82(m, 6H), 0.56(m, 4H). ^{13}CNMR (100 MHz, $CDCl_3$): δ_{ppm}, 150.8, 141.2, 127.2, 126.8, 122.9, 119.8, 55.1, 40.6, 34.1, 33.1, 32.1, 30.3, 29.5, 29.0, 28.4, 23.9, 22.9, 14.3. Exact Mass: 474.4226, HR MS: 474.4257.

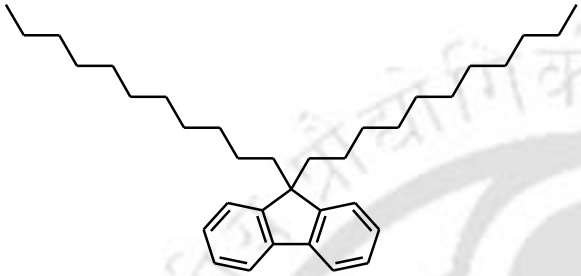

(3.1e) 9,9-Bis-(6-bromohexyl)-9H-fluorene: $C_{25}H_{32}Br_2$, (0.58 g, 95 %); ^{1}H NMR (400 MHz, $CDCl_3$): δ_{ppm}, 7.68(m, 2H), 7.28(m, 6H), 3.25(t, 4H), 1.95(m, 4H), 1.61(m, 4H), 1.15(m, 4H), 1.05(m, 4H), 0.60(m, 4H). ^{13}C NMR (100 MHz, $CDCl_3$): δ_{ppm}, 150.8, 141.2, 127.2, 126.9, 122.8, 119.8, 54.9, 40.3, 34.1, 32.7, 29.2, 27.8, 23.6. Exact Mass: 490.0871, HR MS: 490.0870.

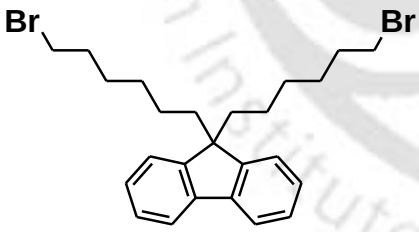

(3.1f) 9,9-Bis-(8-bromooctyl)-9H-fluorene: $C_{29}H_{40}Br_2$, (0.62 g, 90 %); ^{1}H NMR (400MHz, $CDCl_3$): δ_{ppm}, 7.69(m, 2H), 7.31(m, 6H), 3.33(t, 4H), 1.94(m, 4H), 1.74(m, 4H), 1.25(m, 4H), 1.05(m, 12H), 0.58(m, 4H). ^{13}C NMR (100 MHz, $CDCl_3$): δ_{ppm}, 150.6, 141.2, 127.1, 126.8, 122.8, 119.7, 55.0, 40.4, 34.1, 32.8, 29.94, 29.1, 28.6, 28.1, 23.7. Exact Mass: 546.1497, HR MS: 546.1489.

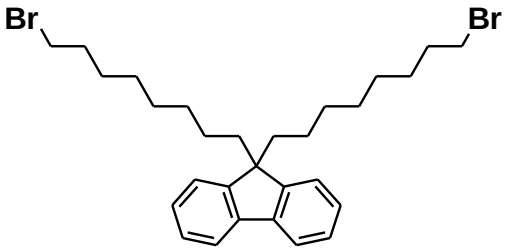

(3.1g) 9,9-Bis-(6-iodohexyl)-9H-fluorene: $C_{25}H_{32}I_2$, (0.66 g, 90 %); ^{1}H NMR (400 MHz, $CDCl_3$): δ_{ppm}, 7.69(d, 2H), 7.31(m, 6H), 3.04(t, 4H), 1.95(m, 4H), 1.60(m, 4H), 1.13(m, 4H), 1.04(m, 4H), 0.59(m, 4H). ^{13}C NMR (100 MHz, $CDCl_3$): δ_{ppm}, 147.5, 141.3, 127.1, 127.0, 124.4, 119.9, 47.5, 33.5, 32.9, 30.4, 29.0, 25.4, 7.8. Exact mass: 586.0593, HR MS: 586.0589.

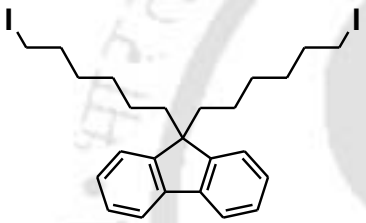

(3.1h) 9,9-Bis-(8-iodooctyl)-9H-fluorene: $C_{29}H_{40}I_2$, (0.71 g, 88 %); ^{1}H NMR (400 MHz, $CDCl_3$): δ_{ppm}, 7.69(d, 2H), 7.31(m, 6H), 3.26(t, 4H), 1.96(m, 4H), 1.62(m, 4H), 1.17(m, 4H), 1.05(m, 8H), 0.60(m, 4H). ^{13}C NMR (100 MHz, $CDCl_3$): δ_{ppm}, 150.7, 141.3, 127.2, 126.8, 123.0, 119.8, 55.1, 40.5, 34.3, 32.9, 30.1, 29.2, 28.8, 28, 23.8. Exact Mass: 642.1219, HR MS: 642.1216.

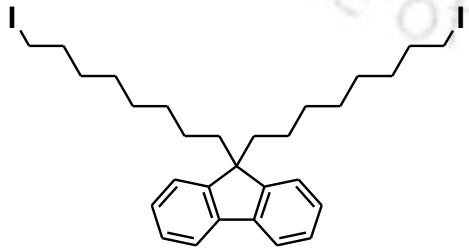

(3.1i) 9,9-Dihexyl-9H-fluorene: $C_{25}H_{34}$. Product same as **3.1a**. (0.36 g, 85 %).

(3.1j) 9,9-Dioctyl-9H-fluorene: $C_{29}H_{42}$. Product same as **3.1b**. (0.43 g, 87 %).

(3.4a) 2,7-dibromo-9,9-dihexylfluorene:[3.10] (0.31 g, 99 %).

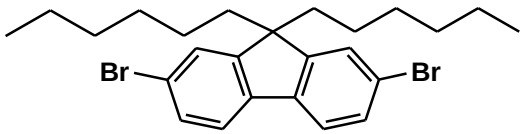

(3.4b) 2-bromo-9,9-dihexylfluorene:[3.8] (0.347 g, 98 %).

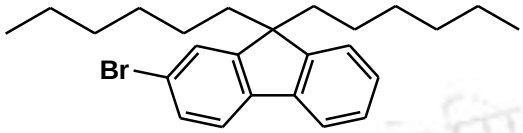

(3.4c) 9-Hexyl-9H-carbazole:[3.12(c)] (0.28 g, 91 %).

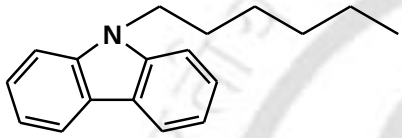

(3.4d) N-hexyl-diphenylamine: (0.235 g, 75 %); ^{1}H NMR (400 MHz, $CDCl_3$): δ_{ppm}, 7.26(t, 4H), 7.08(d, 4H), 6.92(t, 2H), 3.36(t, 2H), 1.68(m, 2h), 1.46(m, 2H), 1.09(m, 7H). ^{13}C NMR (100 MHz, $CDCl_3$): δ_{ppm}, 143.1, 128.9, 120.3, 117.3, 52.4, 25.1, 23.9, 19.9, 19.5, 13.5. Exact Mass: 253.1830, MS: 253.1800.

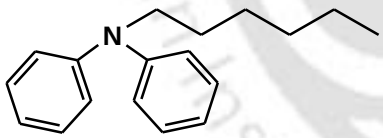

(3.4e) N,N-Di-n-hexylaniline:[3.177] (0.23 g, 72%);

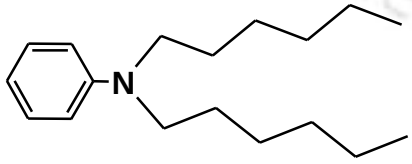

3.5. Reference:

3.1 Grell, M.; Knoll, W.; Lupo, D.; Meisel, A.; Miteva, T.; Neher, D.; Nothofer, H.-G.; Scherf, U.; Yasuda, A. *Adv. Mater.* **1999**, *11*, 671.

3.2 (a) Gaylord, B. S.; Heeger, A. J.; Bazan, G. C. *J. Am. Chem. Soc.* **2003**, *125*, 896.

(b) Wang, S.; Gaylord, B. S.; Bazan, G. C. *Adv. Mater*. **2004**, *16*, 2127.

3.3 (a) Weinfurtner, K.-H.; Fujikawa, H.; Tokito, S.; Taga, Y. *Appl. Phys. Lett*. **2000**, *76*, 2502.

(b) Uckert, F.; Tak, Y. H.; Mullen, K.; Bassler, H. *Adv. Mater*. **2000**, *12*, 905.

3.4 (a) Lee, J.-I.; Klaerner, G.; Miller, R. D. *Chem. Mater*. **1999,** *11*, 1083.

(b) List, E. J. W.; Guentner, R.; Scanducci de Freitas, P.; Scherf, U. *Adv. Mater*. **2002**, *14*, 374.

(c) Scherf, U.; List, E. J. W. *Adv. Mater*. **2002**, *14*, 477.

(d) Zojer, E.; Pogantsch, A.; Hennebicq, E.; Beljonne, D.; Bredas, J. L.; Scandiucci de Freitas, P.; Scherf, U.; List, E. J. W. *J. Chem. Phys*. **2002**, *117*, 6794.

3.5 (a) Murphy, W. S.; Hauser, C. R. *J. Org. Chem.* **1966**, *31*, 85.

(b) Gonzalez, J. J.; Garcia, N.; Gomez-Lor, B.; Echavarren, A. M. *J. Org. Chem*. **1997**, *62*, 1286.

3.6 (a) Pie, Q.; Yang, Y. *J. Am. Chem. Soc*. **1996**, *118*, 7416.

(b) Belfield, D. K.; Schafer, K. J.; Mourad, W.; Reinhardt, B. A. *J. Org. Chem*. **2000**, *65*, 4475.

(c) Fujiwara, S.-I.; Maeda, H.; Matsuya, T.; Shin-I., T.; Kambe, N.; Sonoda, N. *J. Org. Chem*. **2000**, *65*, 5022.

3.7 Fedorynski, M.; Wojciechowski, K.; Matacz, Z.; Makosza, M. *J. Org. Chem*. **1978**, *43*, 4682.

3.8 Xia, C.; Advincula, R. C. *Macromolecules* **2001**, *34*, 6922.

3.9 Leonetti, F.; Favia, A.; Rao, A.; Aliano, R.; Paluszcak, A.; Hartmann, R. W.; Carotti, A. *J. Med. Chem*. **2004**, *47*, 6792.

3.10 (a) Ranger, M.; Rondeau, D.; Leclerc, M. *Macromolecules* **1997**, *30*, 7686.

(b) Hagaman, E. W.; Lee, S. K. *Energy & Fuels* **1999**, *13*, 1006.

(c) Stigers, K. D.; Koutroulis, M. R.; Chung, D. M.; Nowick, J. S. *J. Org. Chem*. **2000**, *65*, 3858.

(d) Cho, S. Y.; Grimsdale, A. C.; Jones, D. J.; Watkins, S. E.; Holmes, A. B. *J. Am. Chem. Soc*. **2007**, *129*, 11910.

3.11 Gong, X.; Iyer, P. K.; Moses, D.; Xiao, S. S.; Bazan, G. C.; Heeger, A. J. *Adv. Funct. Mater*. **2003**, *4*, 325.

3.12 (a) Peng, Z.; Bao, Z.; Yu, L. *J. Am. Chem. Soc*. **1994**, *116*, 6003.

(b) Kuo, W.-J.; Hsiue, G.-H.; Jeng, R.-J. *Macromolecules* **2001**, *34*, 2373.

(c) Liu, S.; Jiang, X.; Ma, H.; Liu, M. S.; Jen, A. K. Y. *Macromolecules* **2000**, *33*, 3514.

(d) Huang, Q.; Evmenenko, G.; Dutta, P.; Marks, T. J. *J. Am. Chem. Soc*. **2003**, *125*, 14704.

3.13 (a) Cho, J.-S.; Kimoto, A.; Higuchi, M.; Yamamoto, K. *Macromol. Chem. Phys*. **2005**, *206*, 635.

(b) Chi, C.-C.; Chiang, C.-L.; Liu, S.-W.; Yueh, H.; Chen, C.-T.; Chen, C.-T. *J. Mater. Chem*. **2009**, *19*, 5561.

3.14 (a) Brunner, K.; Dijken, A. V.; Boerner, H.; Bastiaansen, J. J. A. M.; Kiggen, N. M. M.; Langeveld, B. M. W. *J. Am. Chem. Soc.* **2004**, *126*, 6035.

(b) Thomas, K. R. J.; Velusamy, M.; Lin, J. T.; Chuen, C.-H.; Tao, Y.-T. *Chem. Mater.* **2005**, *17*, 1860.

(c) You, Y.; Kim, S. H.; Jung, H. K.; Park, S. Y. *Macromolecules* **2006**, *39*, 349.

(d) Tao, Y.; Wang, Q.; Yang, C.; Wang, Q.; Zhang, Z.; Zou, T.; Qin, J.; Ma, D. *Angew. Chem., Int. Ed.* **2008**, *47*, 8104. K. BOWDEN* and A. F. COCKERI

3.15 Bowden, K.; Cockeri, A. F. *Chem. Comm.* **1967**, 989.

3.16 Liu, B.; Yu, W.-L.; Lai, Y.-H.; Huang, W. *Macromolecules* **2000**, *33*, 8945.

3.17 Mishra, A.; Nayak, P. K.; Ray, D.; Patankar, M. P.; Narasimhan, K. L.; Periasamy, N. *Tetrahedron Lett.* **2004**, *45*, 6265.

Chapter 4

Synthesis, characterization and OLED fabrication studies with polyfluorene copolymers.

Chapter 4

Synthesis, characterization and OLED fabrication studies with polyfluorene copolymers.

Abstract:

Alkylation of fluorene is achieved via direct C−H alkylation under aqueous conditions, wherein the formation of fluorenone is totally inhibited. 9,9-dialkylated polyfluorene copolymers having alkyl chains of varying lengths were synthesized by Suzuki coupling reaction of 9,9-dialkylated fluorene derivatives and benzene 1,4-diboronic acid using Pd(0) as catalyst. All the polymers were well characterized by FT-IR, ^{1}H NMR, ^{13}C NMR spectroscopy, GPC, TGA, DSC and elemental analysis. The thermal stability of the polymers was above 420 °C as obtained from TGA analysis. DSC indicated the polymers to be crystalline in nature as all of them exhibited a melt temperature on controlled heating. The improvement in other aspects like solubility in common organic solvents i.e. chloroform, dichloromethane, toluene, tetrahydrofuran, xylene, etc., good film-forming properties and colour tunability were observed. Optical and electrochemical band gaps were determined using UV-Visible spectroscopy and cyclic voltammetry. These polymers exhibit blue emission in solution with photoluminescence maximum ranging from 426-444 nm. We also studied the absorption, photoluminescence quantum efficiency (PLQE) that were in the range of (10-16.3%) in the film form and compared it with solution PL. Single layered polymer devices showed good transport properties, electroluminescence (EL) spectrum exhibits a small shift in blue peak and emission from the higher wavelength shoulder peak is of low intensity. Overall the copolymers of polyfluorene are expected to show enhanced stability, processability and brightness characteristics.

4.1 Introduction:

Polyfluorenes are well-known materials and applied extensively as emissive material for polymer light emitting diodes (PLED) due to their high luminescence efficiency, excellent thermal stability charge transport property, and good processability color tunability. Recently, high-efficiency and stable pure blue light emitting devices-LEDs have attracted much attention. Blue emission from polymer or organic materials are now much studied and one of the most important parameter required for full color displays.[4.1] In producing a full-color display it is important to have pure red, green, and blue emissive polymers or in other words a blue PLED alone may generate all colors while green or red cannot be converted to blue by the same method.[4.2] It can also be used as the energy donor in the doping or down conversion system to realize high efficiency emission of other colors.[4.3-4.4] Blue LEDs based on small organic molecules by vacuum evaporation procedure have been investigated in the past few years and promising results have been obtained.[4.5-4.6] Remarkable results were obtained by structural modifications, such as end or side-chain modification, electrode modification, blending, or host-dopant system. [4.7-4.12] However, high performance pure blue LEDs, which are fabricated through solution procedure, are still under intensive investigation, especially, based on polyfluorenes (PFs).

Though polyfluorenes have shown great promise as blue emitting material, it has a green shoulder to the primary blue peak that has tendency to grow with prolonged exposure to heat and atmospheric oxygen to generate undesired green emission. The low energy emission band has been mostly attributed to reordering of the polymer chains and subsequent aggregate or excimer formation.[4.13-4.14] Recently, it was proposed that the red-shifted emission band in polyfluorene as well as in poly-*p*-phenylenes was caused by an on-chain oxidative defect in the form of 9-fluorenone resulting from an electrical, photo-

initiated or thermal oxidation of the conjugated polymer.[4.15] There is good evidence that the emission from defect containing polyfluorene is caused by on-chain fluorescence from a charge transfer pp*-state associated with the fluorenone defect.[4.16-4.17] The intensity of the green band has also been demonstrated to increase with increasing concentration of fluorenone containing polymers. This suggests that there is a dependence on the interaction between polymer chains/segments containing polyfluorenone defects. The functionalization of fluorene at the methylene bridge has been done to control the formation of undesirable fluorenone so as to reduce the green emission. This way it is possible to modify its charge injection and charge mobility of the polymer and improve the thermal properties as well as increase the solubility of the PF in common organic solvents. In most of the cases the modifications do not fully stabilize the blue emission but are able to limit interchain interactions without reducing charge mobility.

In the present chapter incorporation of long chain alkyl groups at 9-position of fluorene molecule by modifying the alkylation process for stabilized blue emission is presented.[4.18] Similarly PF containing bulky pendant groups terminated on the top of the alkyl chain was introduced to improve charge injection and to reduce inter chain interaction. In both the cases improvement of the thermal properties of the polymers as well as the EL quantum efficiency was observed. Attachment of a hole-transporting dimethyl pyrazole, diphenylamine, and carbazole resulted in a stable blue emission with improved charge injection.

4.2 Result and discussion:

4.2.1 *Synthesis*:

The fluorene ring system can be readily functionalized on the 2, 7, and at 9-positions. The tuning of electronic character of the π-conjugated central fluorene ring system was done by varying the substituents at the 9-position. In addition, bulky aromatic groups

terminated at the top of the alkyl chains were incorporated to enhance transport property of the polymer. Details of the synthetic methodology and characterization data for the series of fluorene derivatives are presented in Schemes 4.1.

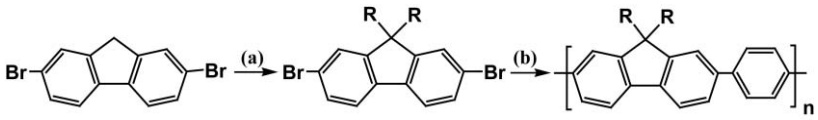

Scheme 4.1: Synthesis protocol followed to obtain the desired monomers & polymers. Where, (**a**) Aq. NaOH, Alkylbromide, Catalyst, 80 °C, 4-8 h. (**b**) Benzene 1-4,diboronic acid, Pd(0), K_2CO_3, in 2:1 THF/water as solvent, 80 °C for 36 h. R may be hexyl, octyl, ehylhexyl or undecyl alkyl chain.

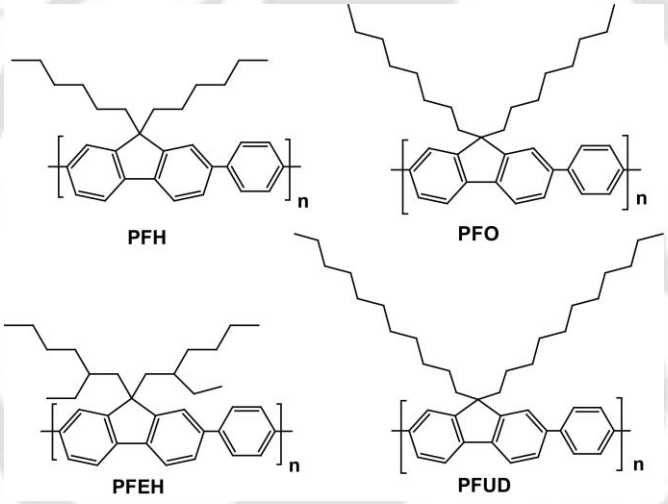

Figure: 4.1 Structure of the PF copolymers containing only long alkyl chain as pendant group.

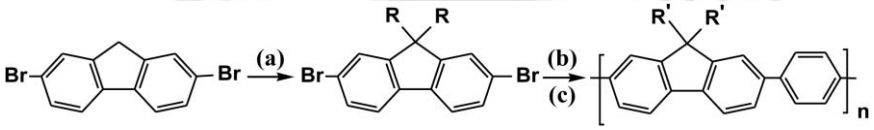

Scheme 4.2: Synthesis protocol followed to obtain the below monomers & polymers, PFPH, PFSH, PF1N, PFDMP, PFCARB, and PFDPA. Where, **(a)** Aq. NaOH, 1,6-dibromohexane, Catalyst, 80 °C, 4 h. **(b)** Benzene 1-4,diboronic acid, Pd(0), K_2CO_3, in 2:1 THF/water as solvent, 80 °C for 36 h. **(c)** NaH in dry THF at 70 °C for 12 h.

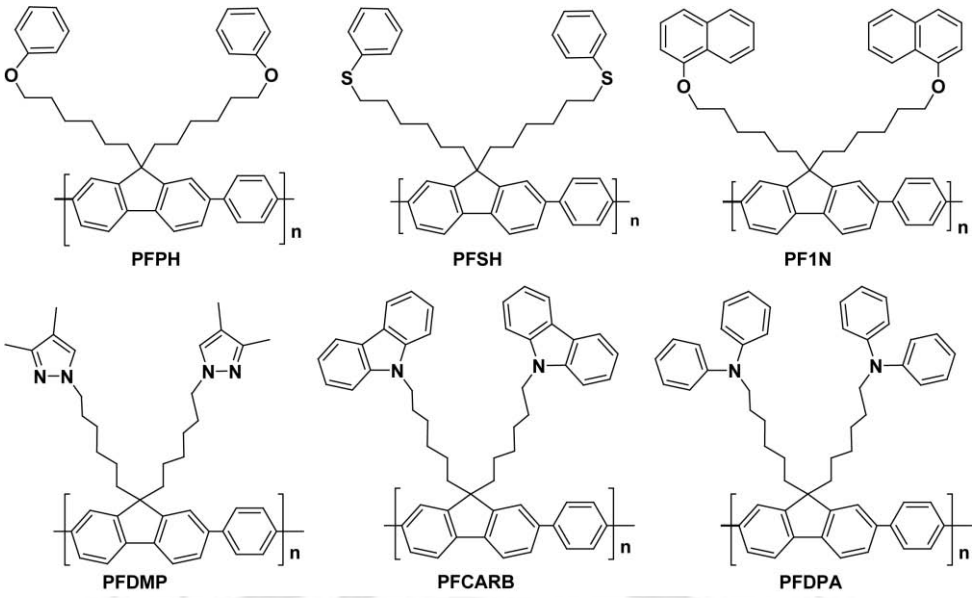

Figure 4.2 Structure of polymers synthesized by following Scheme 4.2.

Scheme-4.1 depicts the synthesis of desired PF polymer in high yield. In the first step of the synthetic route Scheme 4.1 fluorene was brominated with molecular bromine in CCl_4 at liquid nitrogen temperature followed by alkylation with various alkyl halides (1-bromo-hexane, 1-bromo-octane, 1-ethylhexyl-bromide, 1-bromo-undecane, and 1,6-dibromo-hexane) in 50% aqueous NaOH medium using tetrabutyl ammonium iodide as catalyst at 80-90 $^{\circ}$C.[4.18] The 2,7-dibromo-9,9-bis(6-bromohexyl)-9H-fluorene, was further substituted at the terminal position with phenol, 1-naphthol, thiophenol, dimethyl pyrazole, carbazole, and diphenyl amine in the presence of K_2CO_3 or sodium hydride to give 94 % yield. Suzuki coupling[4.19] of these monomers with 1, 4-phenylboronic acid resulted in the formation of desired copolymer as yellow-brown solid in 60-80% yield. Polymers were characterized by ^{1}H and ^{13}C NMR spectroscopic technique. Molecular weight of these polymers was determined by GPC in THF-PS as internal standard. Mw and polydispersity units are given in Table 4.1. Since all PF were soluble in several organic solvents such as chloroform, toluene, benzene, THF, DMSO and DMF, they

could be easy characterized and processed, which is an important criteria for materials for optoelectronic industry.

4.2.2 *Thermal Properties of the Polymers*:

The thermal stability of the polymers was studied by TGA performed under N_2 atmosphere at a heating rate of 10 °C/min (Figure 4.3)(table 4.1). Polyfluorene (PF) derivatives with pendent alkyl chains and of varying lengths were found to be thermally stable up to 400 °C. Whereas PF with bulky groups terminated at the top of the alkyl chain of the fluorene units were stable up to 420 °C. These bulky substituted PF derivatives were also having higher molecular weight as compaired to PF derivatives without pendent bulky groups. Which shows the improvement on the thermal stability of the PF polymers after incorporation of bulky groups on the top of the alkyl chain and it is similar for polymers already reported in literature.[4.20] This is due to higher molecular weight and defect free structures generated by carefully executed synthesis.

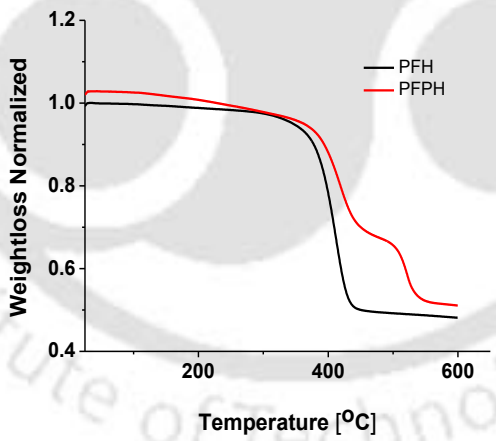

Figure 4.3. Thermo-gravimetric analysis (TGA) plots of PFH and PFPH performed at a heating rate of 10 °C min^{-1}

The DSC studies of the polymers were carried out under nitrogen atmosphere at 10 °C /min. In its second heating cycle, the endothermic peak was observed due to crystallization ~106 °C (table 4.1). The PF backbone contains some phenylene moieties

because of which planarity should be less compared to homo-polymers of fluorene. But still it is stiffer to rotate and show similar values of glass transition and crystallization.[4.21]

Table 4.1. Structural and Thermal Properties of the polymers

	Mw	**PDI**	**Tg (DSC)**	**TGA [°C]**
PFH	15623	2.3	105	373
PFO	18639	2.01	104	390
PFEH	31088	1.8	105	400
PFUD	17128	1.7	105	385
PFPH	30982	1.8	104	420
PFSH	17779	1.6	104	410
PF1N	18913	1.8	105	400
PFDMP	8509	1.12	105	400
PFCARB	9697	1.2	104	405
PFDPA	26691	2	106	412

4.2.3 *Optical and electrochemical characteristics*:

PF is soluble in THF, toluene, DMF, $CHCl_3$, and other common organic solvents. The absorption (figure 4.4.1 & figure 4.4.2) and PL (figure 4.5.1 & figure 4.5.2) spectra of polyfluorenes in thin film were recorded by preparing thin films on glass substrates. The absorption maximum of PF in dilute solution has a relatively sharp peak at 355-365 nm. The absorption peak is broader in case of thin film compared to the spectrum in solution state. In PF, the side groups that render the polymer soluble are well separated from the side groups on the adjacent fluorene unit. Therefore, the steric interaction between side groups and polymer backbone is negligible in PF.

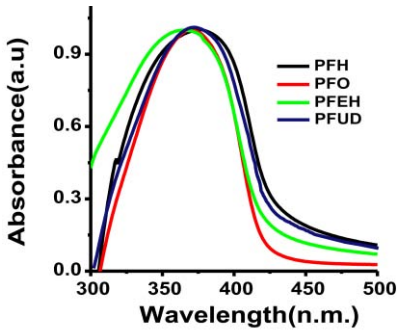

Figure 4.4.1 Absorbance spectra of PF varying the length of alkyl chain in thin film.

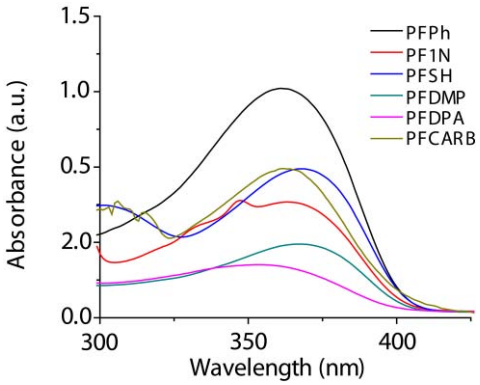

Figure 4.4.2 Absorbance spectra of PF having bulky groups into the top of the alkyl chain at C-9 position of the fluorene units.

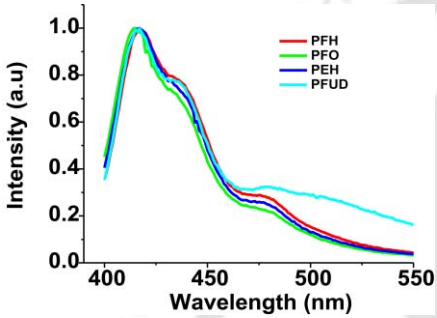

Figure 4.5.1 Fluorescence spectra of PF varying the length of alkyl chain in thin film.

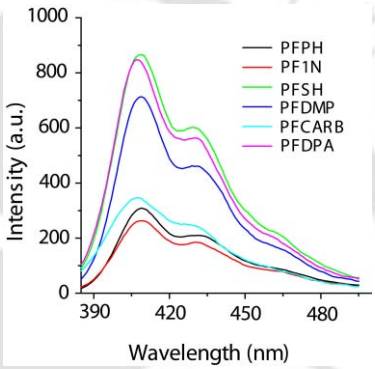

Figure 4.5.1 PL spectra of PF having bulky groups into the top of the alkyl chain at C-9 position of the fluorene units.

These fluorene copolymers with fluorene and phenylene units at the backbone exhibits a UV-vis at 354-378 nm and PL maxima at 414-420 nm for the thin film [4.22]. It is apparent that the phenylene group develops a poor coplanarity with the fluorene unit and rather reduces the planarity of the fluorene unit. The solubility is improved and the excimeric emission is reduced compared to those of PPP type polymers indicating that chromophore stacking is unlikely with this molecular configuration. The PL spectrum is not modified by attaching hexyl, octyl, undecyl or ethylhexyl groups on the fluorene units

and does not show any change with the introduction of bulky groups on the top of the alkyl chain in the copolymer showing a PL maximum in thin film at 407-416 nm.[4.23]

4.2.4 *Electrochemical Studies*:

The redox behavior of the polymers was investigated by cyclic voltammetry (CV) with a standard three-electrode electrochemical cell in a 0.10 M tetrabutylammonium perchlorate solution in acetonitrile at room temperature under nitrogen atmosphere with a scanning rate of 20 mV/s. (Figure 4.6.**)** The polymer film on a glassy carbon disc was taken as a working electrode and a platinum wire as a quasi- reference electrode. In the figure-4.6 only three representative spectra's of PF has been shown for clarity; total band gap calculation is mentioned in Table-4.2. The polymer exhibits redox behavior electrochemically. From cyclic voltammetry study the π-π* band gap was found for the polymers to be 3.0-3.4 eV which were almost equal to the optical band gap determined from the onset of optical absorption; ~3.4 eV. The calculated band gap was found to be almost equal to the band gap of polyfluorene homo polymers; revealing that the phenylene units fail to extend or reduce the conjugation in the fluorene units.

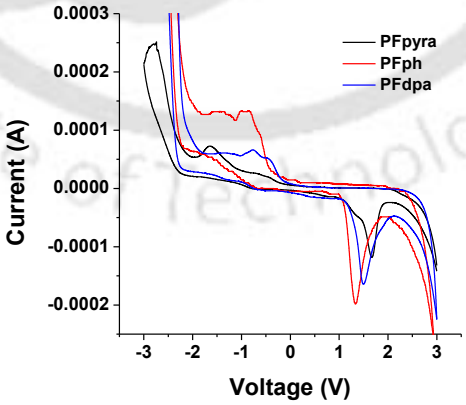

Figure 4.6. Some representative cyclic voltammogram of polyfluorene polymers.

Table 4.2 Band gap characteristics of the polymers as determined from **CV** data and absorption onset

Polymer	PFH	PFO	PFEH	PFUD	PFPH	PFSH	PF1N	PFDMP	PFCARB	PFDPA
HOMO	6.01	6.18	6.20	6.08	6.21	6.19	6.15	6.04	6.17	6.11
LUMO	3.00	3.04	3.06	2.89	3.05	3.09	3.01	2.93	2.94	2.95
Band gap/eV	3.01	3.14	3.14	3.19	3.16	3.1	3.14	3.11	3.23	3.16

4.2.5 *Fabrication of Device*:

Single layer devices were fabricated using these new materials by sandwiching a thin film of PF (~800 Å thick, spin-cast from a solution in chloroform) between an ITO-coated glass as anode and a vacuum evaporated calcium film as cathode. The derivatives of PF were dissolved in toluene/chloroform mixture and spin casted onto indium tinoxide patterned glass substrates with 3, 4-polyethylenedioxythiophene: polystyrenesulfonante (PEDOT: PSS).

The overall spectral features were not significantly affected by changes in the device thickness within the range of 80–140 nm. For double-layer devices, a 70 nm thick layer of PF was spin casted onto the PEDOT layers and thermally treated to 120 $^{\circ}$C. The current–voltage–luminance (I/V) and electroluminescence (EL) spectra were measured in a dry nitrogen atmosphere. All LEDs were fabricated and tested under inert atmosphere in a glove box. I-V curve of a characteristic device of PF series is shown [Figure 4.7(a-d)] where turn on voltage of the device is high since there is an imbalance in charge injection and transportation due to large injection barriers and different charge carrier mobility.

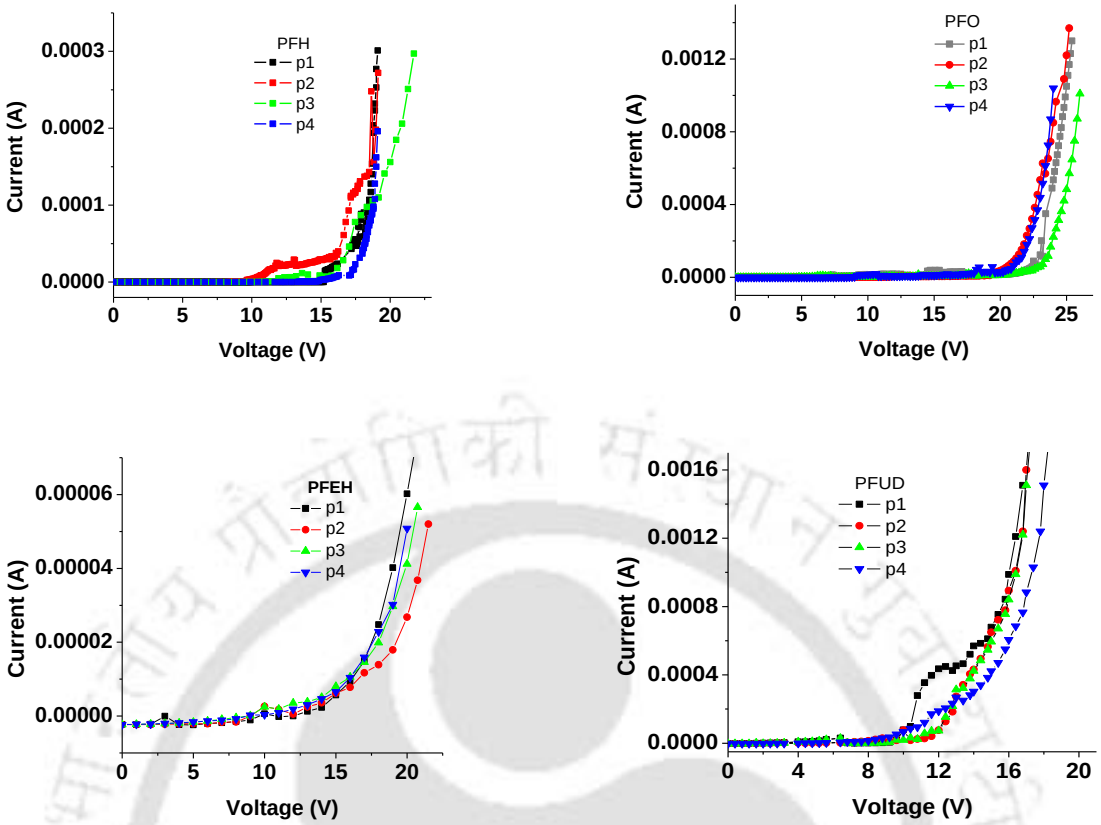

Figure 4.7(a-b) I/V curve of Polyfluorene; long chain alkyl group substituted at 9-position of fluorene molecule.

On introduction of BCP as electron transporting material (ETL) the threshold voltage decreases (Figure 4.8) to a reasonable amount. Additionally, we have not observed any EL at higher wavelength which confirms that by modification of the synthetic root the monomers give us defect free polymeric materials for pure blue emission. (Figure 4.9.)

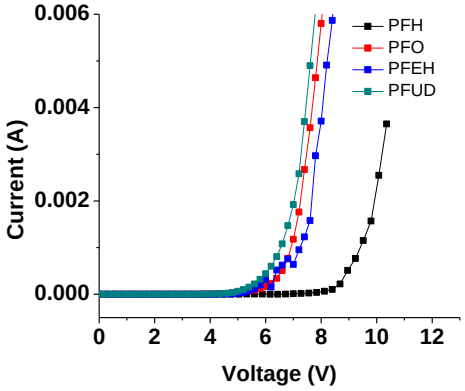

(a)

Figure 4.8. I/V curve of Polyfluorene derivatives containing only alkul chains at 9-positions of fluorene units with BCP as ETL

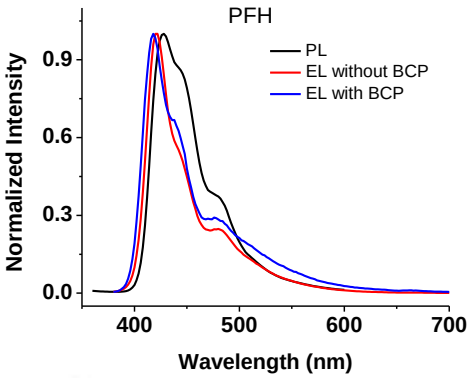

(b)

Figure 4.9. Comparison of PL and EL spectra of Hexyl chain substituted PF with or without BCP as ETL.

In Figure 4.9, we show the PL and EL spectra for single-layer and double-layer devices to compare the effects of the ETL. The EL spectra and the photoluminescence spectra show peaks at 417-23 nm and with a weak shoulder at 437-44 nm; these peaks attributed to arising from vibrational structure between the energy levels. In addition, a broad peak between 477 and 480 nm is observed for all. This peak is typically assigned to emission from an aggregated species, excimer, or exciplex.[4.24] For double-layer devices substantial improvements in turn-on voltage, and device efficiency were observed.

The physicochemical properties of PF did not shown any major improvement on changing the length of the side chain at the C-9 position of the fluorene units.

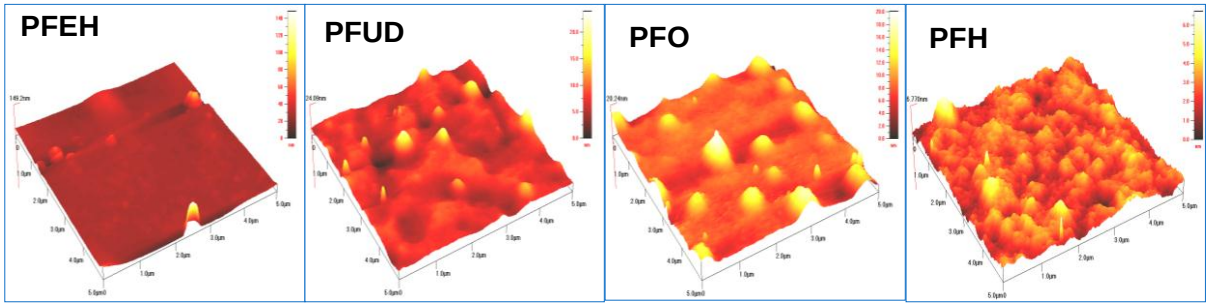

Figure 4.10 AFM images of some of the polymer thin films on glass substrate.

But with the increasing length of alkyl chain, PFO film shows lower roughness (1.37 nm) compared to highest roughness (5.49 nm) observed in PFO films with shorter alkyl chains. Figure 4.10 represents the AFM image of some of the PF thin films. Branched chain alkyl substituted PFs (ethyl hexyl derivative) shows fine grain and dense morphology with lowest roughness. While with decreasing alkyl chain length decrease in the film quality along with increase in the overall roughness is observed.

When bulky groups are incorporated into the top of the alkyl chain at C-9 position of the fluorene units, it not only provides large steric hindrance and reduces inter-chain interaction but also enhances thermal stability and morphological features without substantially changing the electronic properties of the polymer backbone. Insertion of this type of groups not only increases the mobility of charge carriers in the polymer unit but also prevents the aggregation. Single layered device have been fabricated with all these materials. UV-vis, PL, and EL spectra of the device showed a great improvement in colour purity. In figure 4.11 it is clearly seen that all three peaks are sharp and EL spectra doesn't have any green emission. Device performance can be further improved by making multilayered devices. In single layered devices due to the imbalance in charge injection, overall performance is less which can be improved by introducing ETL layer just above the emissive layer.

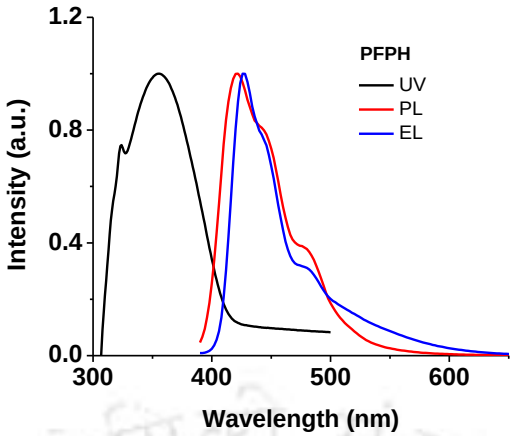

Figure 4.11. Absorbance, PL, and EL spectra of PF having bulky groups into the top of the alkyl chain at C-9 position of the fluorene units.

Also LED performance is controlled by various factors such as the qualities of the emitting and charge transporting materials, thickness of the polymer layers, operation voltages and quantum yields. A balanced charge recombination takes place in multi-layered LEDs at a given layer depending on the device structures and bias potentials.

The presence of the bulky aromatic systems as a pendent group on the polymer backbone can be used as an electron sink to increase the transport properties of the conjugated polymers. Other than the use of these type of polymers in OLEDs, they can be successfully used as probes for chemical and biological sensors. These bulky aromatic systems are of considerable interest due to their presence as binding sites for metals in several biological systems, especially as mimics of histidine-imidazole system to bind various metal ions specifically.

4.3 Conclusion:

A strategy was developed in which the alkylation reaction provided access to a number of fluorene analogues from common substrates. The synthetic methodology facilitated facile functionalization at 9 position of the fluorene ring. Thus, efficient synthesis of different defect free polyfluorenes of various molecular structures was accomplished, providing

derivatives of varying electronic character. The thermal stability of the polymers was above 420 °C as obtained from TGA analysis. DSC indicated the polymers to be crystalline in nature as all of them exhibited a melt temperature on controlled heating. The improvement in other aspects like solubility, good film-forming properties and colour tunability were observed. Optical and electrochemical band gaps were determined using UV-Visible spectroscopy and cyclic voltammetry. These polymers exhibit blue emission in solution with photoluminescence maximum ranging from 407-416 nm with good colour purity. PLEDs made with neat polymers exhibit high turn-on voltage. Further improvement in the devices is possible by blending these materials with hole injection and hole/electron transport materials.

4.4 Experimental section:

4.4.1 *General synthetic Procedure*:

Synthesis of monomer: 2,7-dibromo-9H-fluorene (1gm, 3.10 mmol), haloalkane (bromo-hexane) (2.03gm, 12.4 mmol), 50% aq NaOH and catalytic amount of TBAI (10 mol %) was taken in a flask. The flask was degassed thrice by applying freeze thaw cycles and heated at 70 ^{o}C continuously for 4 hrs. The reaction mixture was cooled to room temperature, and extracted with chloroform. The organic layer was washed with water and dried over anhydrous sodium sulphate. The solvent was removed under vacuum and the crude was purified by column chromatography over silica gel with 10% chloroform in hexane as the eluent to give the product (0.405g). Yield=96%

4.4.2 *Synthesis of polymer*:

A mixture of 2,7-dibromo-9,9-dihexyl-9H-fluorene (0.5 g, 1.02 mmol), 1,4-phenylenediboronic acid(0.172 g, 1.04 mmol), potassium carbonate (0.70 g, 5.10 mmol), THF (10 mL)/water (5 mL), and Pd(0) (3 % mol) were carefully degassed and stirred at 60 ^{o}C for 36 hrs. After the solution was cooled to room temperature, it was precipitated in

methanol to remove monomers. The filtrate was concentrated, precipitated into methanol, and the obtained solid was then washed with a lot of acetone. The resultant polymer was obtained as brown power. Yield=75.6 %.

PFH: Reported in literature

PFO: Reported in literature

PFEH: Reported in literature.[4.13(d)]

PFUD: *^{1}H NMR (400 MHz, $CDCl_3$): $\delta_{ppm,}$* 7.20(m), 6.28(t) 2.90(t), 2.17(m), 1.49(m), 1.23(d), 1.12(m), 0.75(s). *^{13}C NMR (100 MHz, $CDCl_3$): $\delta_{ppm,}$* 130.2, 128.9, 127.8, 125.7, 121.6, 45.4, 40.6, 33.6, 29.7, 29.2, 28.6, 25.1, 24.5, 23.9. *Elemental analysis calculated*: C, 89.72; H, 10.28; *found*: C, 88.97; H, 10.08.

PFPH: Reported in different journal.[4.25]

PFSH: *^{1}H NMR (400 MHz, $CDCl_3$): $\delta_{ppm,}$* 7.81(m), 7.64(s), 7.57(s), 7.20(m), 2.80(t), 2.07(m), 1.49(m), 1.23(d), 1.12(s), 0.75(s). *^{13}C NMR (75.5 MHz, $CDCl_3$): $\delta_{ppm,}$* 151.7, 140.6, 137.2, 128.9, 127.8, 125.7, 121.6, 55.4, 40.6, 33.6, 29.7, 29.2, 28.6, 23.9. *Elemental analysis calculated*: C, 82.64; H, 7.10; *found*: C, 81.97; H, 6.98.

PF1N: *^{1}H NMR (400 MHz, $CDCl_3$): $\delta_{ppm,}$* 8.19(d), 7.76(d), 7.45(m), 7.34(m), 7.06(s), 6.79(d), 3.98(t), 1.99(m), 1.87(m), 1.64(t) 1.42(m). *^{13}C NMR (100 MHz, $CDCl_3$): $\delta_{ppm,}$* 151.7, 147.1, 140.1, 138.5, 127.8, 126.2, 121.5, 120.4, 104.8, 55.4, 48.7, 40.7, 30.5, 29.9, 26.6, 24.0, 13.6, 11.1. *Elemental analysis calculated*: C, 88.40; H, 6.98; *found*: C, 88.10; H, 7.23.

PFDMP: *^{1}H NMR (400 MHz, $CDCl_3$): $\delta_{ppm,}$* 7.77(m), 7.65(d), 7.60(s), 5.67(s), 3.77(t), 2.13(s), 2.06(s), 1.75(m), 1.58(m), 1.09(m), 0.72(s). *^{13}C NMR (75.5 MHz, $CDCl_3$): $\delta_{ppm,}$* 151.7, 147.1, 140.1, 138.5, 127.8, 126.2, 121.5, 120.4, 104.8, 55.4, 48.7, 40.7, 30.5, 29.9,

26.6, 24.0, 13.6, 11.1. *Elemental analysis calculated*: C, 82.51; H, 8.11; N, 9.39; *found*: C, 80.99; H, 9.1; N, 9.41.

PFCARB: *^{1}H NMR (400 MHz, $CDCl_3$): $\delta_{ppm,}$* 7.94(s), 7.65(m), 7.27(s), 7.17(s), 7.06(s), 4.03(m), 1.94(m), 1.80(s), 1.57(m), 1.055(m), 0.64(s). *^{13}C NMR (75.5 MHz, $CDCl_3$): $\delta_{ppm,}$* 157.2, 151.9, 139.9, 132.4, 129.8, 127.8, 126.4, 121.6, 120.5, 114.6, 68.1, 40.6, 30.0, 29.4, 25.9, 24.1, 20.7. *Elemental analysis calculated*: C, 89.39; H, 6.82; N, 3.79; *found*: C, 90.21; H, 7.22; N, 3.8.

PFDPA: *^{1}H NMR (400 MHz, $CDCl_3$): $\delta_{ppm,}$* 7.81(d), 7.63(d), 7.45(s), 7.17(m), 6.86(s), 3.54(m), 2.05(m), 1.48(m), 1.12(m), 0.75(m). *^{13}C NMR (75.5 MHz, $CDCl_3$): $\delta_{ppm,}$* 151.2, 148.2, 140.5, 132.0, 129.1, 127.8, 126.3, 121.2, 52.3, 40.6, 30.0, 27.6, 26.9, 25.8, 24.1. *Elemental analysis calculated*: C, 88.90; H, 7.33; N, 3.77; *found*: C, 88.18; H, 8.1; N, 3.00.

4.4.4 *Fabrication of devices*:

Indium tin oxide (ITO) coated glass substrates were first treated by oxygen plasma and poly(3,4-ethylenedioxythiophene):poly(styrene sulfonate) (PEDOT:PSS) was coated on these substrates followed by vacuum drying at 120 °C for 1 h. Then the solution of polymer in toluene was spin coated on the substrates followed by vacuum drying at 100 °C for 1 h. Subsequently Ca (215Å) and Al (1250Å) were deposited by vapor deposition to form the cathode. For double-layer devices, an 80 nm thick layer of BCP was spin casted onto the polymer layers and thermally treated followed by vapor deposition of Ca and Al to form the cathode. The current/voltage curve and EL spectra were measured in inert atmosphere (nitrogen atmosphere).

4.5 References:

4.1 Kim, D. Y.; Cho, H. N.; Kim, C. Y. *Prog. Polym. Sci.* **2000**, *25*, 1089.

4.2 (a) Rothberg, L. J.; Lovinger, A. J. *J. Mater. Res.* **1996**, *11*, 3174.

(b) Virgili, T.; Lidzey, D. G.; Bradley, D. D. C. *Adv. Mater.* **2000**, *12(1)*, 58.

4.3 Jiang, C. Y.; Yang, W.; Peng, J. B.; Xiao, S.; Cao, Y. *Adv. Mater.*, **2004**, *16*, 537.

4.4 Krummacher, B. C.; Choong, V.-E.; Mathai, M. K.; Choulis, S. A.; So, F.; Jermann, F.; Fiedler, T.; Zachau, M. *Appl. Phys. Lett.* **2006**, *88*, 113506.

4.5 Lee, M. T.; Liao, C. H.; Tsai, C. H.; Chen, C. H. *Adv. Mater.* **2005**, *17*, 2493.

4.6 Cheng, G.; Zhang, Y.; Zhao, Y.; Liu, S.; Tang, S.; Ma, Y. *Appl. Phys. Lett.* **2005**, *87*, 151905.

4.7 Hung, M. C.; Liao, J. L.; Chen, S. A.; Chen, S. H.; Su, A. C. *J. Am. Chem. Soc.* **2005**, *127*, 14576.

4.8 Su, H. J.; Wu, F. I.; Tseng, Y. H.; Shu, C. F. *Adv. Funct. Mater.* **2005**, *15*, 1209.

4.9 Jiang, X. Z.; Liu, S.; Ma, H.; Jen, A. K. Y. *Appl. Phys. Lett.* **2000**, *76*, 1813.

4.10 Sainova, D.; Miteva, T.; Nothofer, H. G.; Scherf, U.; Glowacki, I.; Ulanski, J.; Fujikawa, H.; Neher, D. *Appl. Phys. Lett.* **2000,** *76*, 1810.

4.11 Kulkarni, A. P.; Jenekhe, S. A. *Macromolecules* **2003,** *36*, 5285.

4.12 Liu, J.; Min, C. C.; Zhou, Q. G.; Cheng, Y. X.; Wang, L. X.; Ma, D. G.; Jing, X. B.; Wang, F. S. *Appl. Phys. Lett.* **2006,** *88*, 83505.

4.13 (a) List, E. J. W.; Guntner, R.; Scandiucci de Freitas, P.; Scherf, U. *Adv. Mater.* **2002,** *14*, 374.

(b) Scherf, U.; List, E. J. W. *Adv. Mater.* **2002**, *14*, 477.

(c) Lemmer, U.; Heun, S.; Mahrt, R. F.; Scherf, U.; Hopmeier, M.; Siegner, U.; Goebel, E. O.; Muellen, K.; Baessler, H. *Chem. Phys. Lett.* **1995**, *240*, 373.

4.14 (a) Pannozo, S.; Vial, J.-C.; Kervalla, Y.; Ste´phan, O. *J. Appl. Phys.* **2002**, *92*, 3495.

(b) Herz, L. M.; Phillips, R. T. *Phys. Rev. B*, **2000**, *61*, 13691.

(c) Zeng, G.; Yu, W. L.; Chua, S. J.; Huang, W. *Macromolecules* **2002**, *35*, 6907.

4.15 Romaner, L.; Heimel, G.; Wiesenhofer, H.; Scandiucci de Freitas, P.; Scherf, U.; Bredas, J.-L.; Zojer, E.; List, E. J. W. *Chem. Mater.* **2004**, *16*, 4667.

4.16 Romaner, L.; Pogantsch, A.; Scandiucci de Freitas, P.; Scherf, U.; Gaal, M.; Zojer, E.; List, E. J. W. *Adv. Funct. Mater*. **2004,** *13*, 597.

4.17 Zojer, E.; Pogantsch, A.; Hennebicq, E.; Beljonne, D.; Bredas, J. L.; Scandiucci de Freitas, P.; Scherf, U.; List, E. J. W. *J. Chem. Phys.* **2002,** *117*, 6794.

4.18 Saikia, G.; Iyer, P. K. *J. Org. Chem*. **2010**, *75*, 2714.

4.19 (a) Miyaura, N.; Yanagi, T.; Suzuki, A. *Synth. Commun.* **1981**, *11*, 513.

(b) Inbasekaran, M.; Wu, W.; Woo, E. P. US Patent 5,777,070, July 7, **1998**.

4.20 Zhu, R.; Lai, W.-Y.; Wang, H.-Y.; Yu, N.; Wei, W.; Peng, B.; Huang, W.; Hou, L.-T.; Peng, J.-B.; Cao Y. *Appl. Phys. Lett.* **2007**, *90*, 141909.

4.21 Fukuda, M.; Sawada, K.; Yoshino, K. *J. Polym. Sci., Part A: Polm. Chem*. **1997**, *31*, 2465.

4.22 (a) Cho, H. N.; Kim, D. Y.; Kim, J. K.; Kim, C. Y. *Synth. Met*. **1997**, *91*, 293.

(b) Ranger, M.; Rondeau, D.; Leclerc, M. *Macromolecules* **1997**, *30*, 7686.

4.23 (a) Kreyenschmidt, M.; Klaerner, G.; Fuhrer, T.; Ashenhurst, J.; Karg, S.; Chen, W. D.; Lee, V. Y.; Scott, J. C.; Miller, R. D. *Macromolecules* **1998**, *31*, 1099.

(b) Yu, W.-L.; Pei, J.; Cao, Y.; Huang, W.; Heeger, A. J. *Chem. Commun.* **1999**, 1837.

4.24 (a) Conwell, E. M. *Synth. Met.* **1997**, *85*, 995.

(b) Jenekhe, S. A.; Osaheni, J. A. *Science* **1994,** *265*, 765.

(c) Yan, M.; Rothberg, L. J.; Kwock, E. W.; Milles, T. M. *Phys. Rev. Lett.* **1995**, *75*, 1992.

4.25 Herz, L. M.; Phillips, R. T. *Phys. Rev. B* **2000,** *61*, 13691.

4.26 Dwivedi, A. K.; Saikia, G.; Iyer, P. K. *J. Mater. Chem.* **DOI**: 10.1039/COJMO3054F

Chapter 5

Tuning the Optical Characteristics of Poly(p-phenylene vinylene) by in Situ Au Nanoparticle Generation

Chapter – 5

Tuning the Optical Characteristics of Poly(p-phenylene vinylene) by in Situ Au Nanoparticle Generation

Abstract:

A composite of 1,4-dihexyloxy-poly(p-phenylenevinylene) (**DHPPV**) and gold nanoparticles (AuNPs) was prepared by an efficient and simple in situ method. The formation of **DHPPV-AuNP** composites was confirmed through high-resolution transmission electron microscopy (TEM); UV-vis absorption spectra showed a large blue shift in the polymer absorption peak, which was greater than 60 nm in solution, accompanied by a remarkable change in the intensity, whereas the photoluminescence (PL) spectra in the solution showed only a marginal decrease in intensity in the presence of AuNPs. Solid-state UV-vis spectra of DHPPV-AuNP also showed a decrease in the intensity of the shoulder peak in the region of 400-450 nm. Interesting features were observed in the solid-state PL spectra, where the efficient energy transfer from AuNP to DHPPV results in the complete disappearance of the 585 nm peak with a dominant peak appearing at 635 nm. TEM analysis confirmed that AuNPs were embedded in the DHPPV matrix systematically, thus presenting a simple tool to assemble hybrid nanowires comprising π-conjugated organic/polymeric systems and inorganic nanoparticles with likely applications in nanosized optoelectronic devices. The optical properties of DHPPV-AuNP could be further tuned by treating the composite with octadecane thiol or sodium sulfide, resulting in a further blue shift of 65 nm.

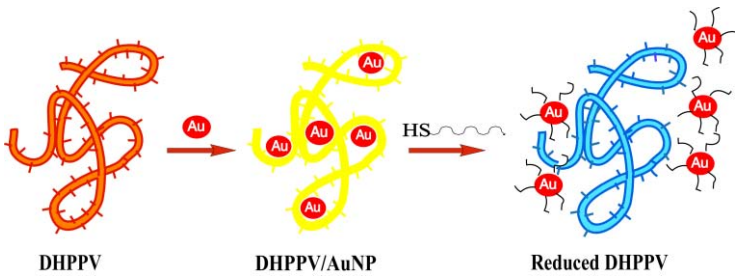

5.1 Introduction:

The discovery that polyacetylene could conduct electricity on doping generated considerable scientific interest, leading to the exploration of conjugated materials for several diversified applications such as organic light-emitting diodes, field effect transistors, photovoltaic cells, and sensors.[5.1] Poly(p-phenylenevinylene) (PPV) was the first reported example of a polymer that could emit light upon passing electric current.[5.2] This major breakthrough expanded the interest in conjugated polymeric materials that offered an alternative display technology having numerous advantages over the existing inorganic-display-based technology. These advantages include the ease in processing, high mechanical flexibility, color tunability, and potential preparation of large-area displays. The polymers can be designed on a molecular level, and synthesis of high-purity materials can be achieved by utilizing well-established chemical transformations. Thus, by varying the polymer backbone and functional groups, tuning of the HOMO-LUMO band gap can also be performed.[5.3] Another method of improving the properties of polymers is the physical doping/blending by inorganic metals and/or their complexes, nanoparticles (NPs), or organic dyes with the polymer and casting them onto substrates as thin films.[5.4-5.6] Alternatively, fabricating a multilayer device with these materials by spin-casting or evaporating over the polymer layer has also shown improvements in device performance. This has helped to enhance the carrier injection, lower the turn-on voltage, and improve brightness, leading to overall improvement of organic device efficiency. Herein, we report that in situ synthesis of Au nanoparticles (AuNPs) in the presence of a PPV derivative, DHPPV, dissolved in chloroform solution has a remarkable effect on the optical properties of the polymer.[5.4-5.8] Due to the higher solubility of alkoxy-substituted PPV derivatives, we chose 1,4-dihexyloxy-poly(p-phenylenevinylene) DHPPV for our studies. AuNPs were chosen as dopants in our experiments as they are used extensively in

nanodevices, for plating connection pads and for making electrical contacts.[5.7-5.10] Moreover, gold does not corrode, and the synthesis of AuNPs can be achieved by a straightforward reduction method from commercially available $HAuCl_4$.[5.11] Reports also suggest that gold layers modify the work function of an indium tin oxide (ITO) anode in organic light-emitting diodes (OLEDs), providing remarkable improvement in injection efficiency and fabricating brighter devices with greater overall efficiency.[5.12-5.14] In a recent report on PPV-AuNP hybrids, it was observed that a blue shift in the absorption spectra of PPV resulted when AuNPs were added to a solution of PPV.[5.7] Considerable enhancement of PL intensity was reported for the MEH-PPV/Au single NP compared to that of the MEH-PPV as single NP.[5.15-5.17] The enhanced PL of the MEH-PPV/AuNP complex might have originated from the energy-transfer effect in the SPR coupling between the MEH-PPV NP and AuNPs and/or from a local EM field enhancement of nanogaps between AuNPs in the background of a light-emitting MEH-PPV NP. Additional significant aspects that are desirable for device fabrication using polymer composites include uniform dispersity of AuNPs, the film-forming ability of the hybrid material, and systematic concentration dependent color tuning of the polymer, which has not been studied. We present here a simple way to disperse AuNPs at different concentrations in an appropriate organic solvent having PPV (Figure 5.1.) dissolved in it, by in situ preparation of the NPs in the presence of the polymer. This permits us to make a homogeneous composite with highly stabilized AuNPs that are dispersed uniformly in the PPV matrix.

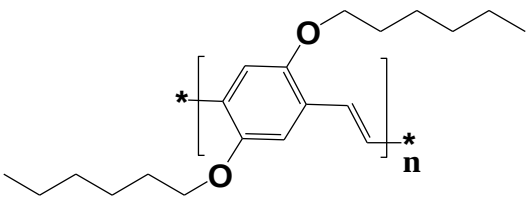

Figure 5.1 Structure of the **DHPPV** Polymer.

5.2 Results and Discussion:

In a typical experiment to prepare DHPPV-AuNP composites, it was observed that the initial orange-red solution of the pristine DHPPV changes its color to yellow-green with increasing concentration of $HAuCl_4$, as seen under an illuminated UV lamp. Additionally, the initial UV-vis absorption peak of 488 nm corresponding to DHPPV started disappearing and was significantly modified with the formation of a new blue shifted peak at 425 nm (Figure 5.2) up to the addition of 90 μL of $HAuCl_4$. No further blue shift of the 425 nm absorption peak was observed upon increasing the quantity of $HAuCl_4$. It is interesting to note that the shift in the UV-vis absorption peak could be as much as 63 nm upon addition of $HAuCl_4$. It is plausible that AuNPs that would have possibly formed in the medium and their presence in the DHPPV matrix leads to decreased delocalization of the π-electrons along the conjugated backbone and a decrease in interchain polymer-polymer interactions, which causes a large blue shift in the absorption spectrum of the polymer in the composite.[5.8] On the other hand, the PL spectrum did not show any notable shift of peak position except the reduction of intensity with increasing concentration of AuNP (in chloroform solution) (Figure 5.3).[5.4] However, a small broadening in the PL spectrum was observed. This was attributed to a larger structural disorder induced in the polymer matrix by the colloidal NPs.[5.7,5.8] Figure 5.4 shows absorption spectra of the DHPPV film and DHPPV-Au nanocomposite film recorded at room temperature. The spectrum of the DHPPV-Au nanocomposite film showed a ~20 nm blue shift (456 nm) compared to that of the DHPPV film (456 and 485 nm). There was also a reduction in the intensity of the shoulder peak. The absorption bandwidths of the DHPPV and DHPPV-Au nanocomposite films were broader than those of their respective absorption bandwidths in the solution state due to the presence of aggregate formation in the solution state of DHPPV.[5.15] These peaks were also found to be slightly blue shifted in a pristine film

reported as the solid-phase dilution in the DHPPV matrix and have been observed in similar PPV composites with silica and alumina.[5.23–5.25]

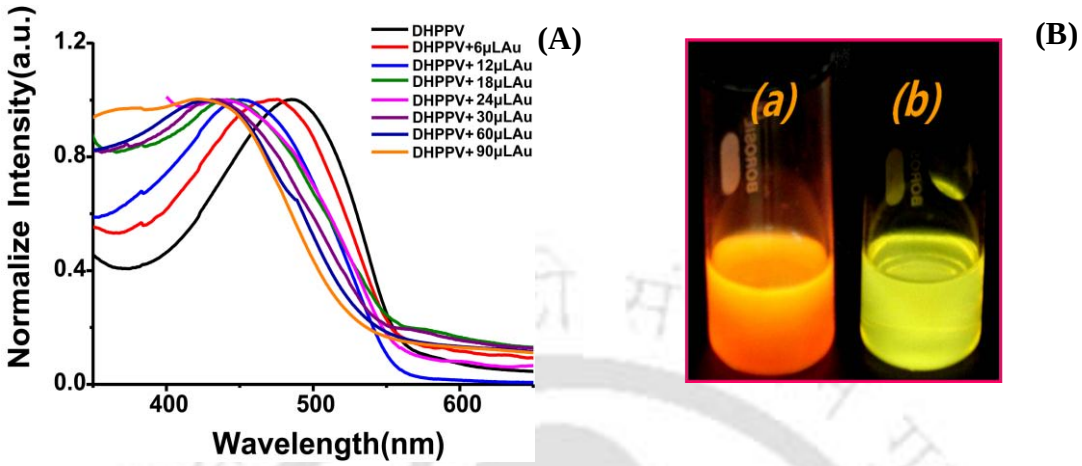

Figure 5.2 (A) UV-vis spectra of DHPPV and its nanocomposites at varying quantity of $HAuCl_4$ in Chloroform. (B) Photographs of (a) DHPPV and (b) DHPPV-AuNP composite under UV light.

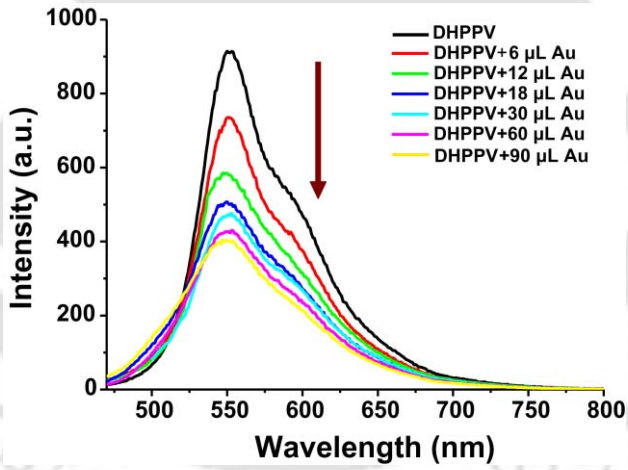

Figure 5.3 PL spectra of DHPPV and its nanocomposites at varying quantity of $HAuCl_4$ in chloroform.

The PL of the DHPPV-AuNP film was also remarkably different from the PL in the solution state (Figure 5.5). The PL spectrum of the pure DHPPV film consisted of two peaks at 590 nm with a strong shoulder at 630 nm. It is clearly observed that in the presence of AuNPs, the PL peak of DHPPV centered at 590 nm completely disappeared,

whereas the intensity of the shoulder peak present at 630 nm was enhanced significantly with broadening. However, there is an overall narrowing of the DHPPV-AuNP peak in comparison to that of the DHPPV films. It is known that the PL of PPV-type polymers in solution exhibits only intrachain motion of excitons, whereas in the film form, the energy relaxations via exciton migration between different polymer chains are dominant due to less interchain distance.[5.15]

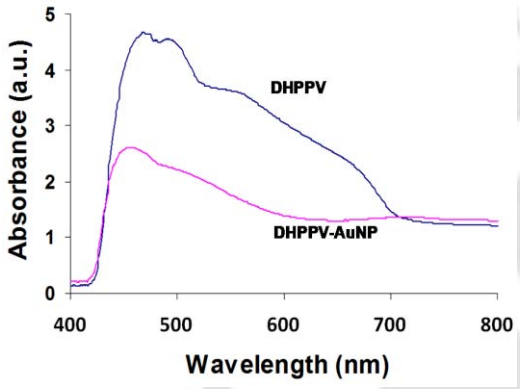

Figure 5.4 Solid state UV-vis spectra of pure DHPPV and its composite with AuNP.

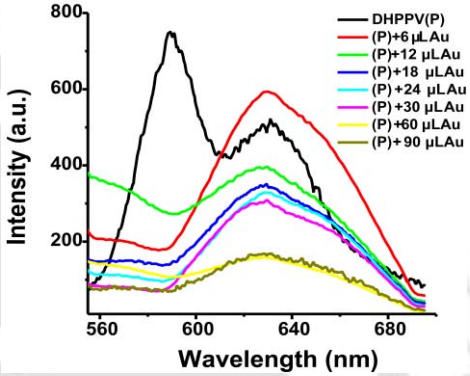

Figure 5.5 Solid state PL spectra of DHPPV and its nanocomposite with varying quantities of $HAuCl_4$.

Hence, in the DHPPV films, the PL spectra display the features of those segments of the polymer chains that are longest. This explains the disappearance of the 590 nm peak and the dominance of the red-shifted peak at 630 nm. The surface of the AuNP being capped by an organic material ensures its solubility and modifies the surface electronically. The absorption and emission energy of π-conjugated systems can thus be tuned by inserting AuNPs. This ability to tune the electronic structure of the DHPPV by AuNPs makes them very attractive optical materials and composites. Overall, these results demonstrate that maximum optical tuning of DHPPV can be achieved by in situ synthesis of AuNP dissolved in an organic solvent and are in agreement with literature that reports on the PPV photophysics being dominated by singlet, intrachain excitons and not by aggregated

or eximeric excited states.[5.15–5.18] TEM was used to characterize the AuNP-embedded DHPPV composites. (Figure 5.6) A small amount of the composite was placed on a carbon-coated copper grid (300 mesh), and it was allowed to dry under reduced pressure at room temperature. Figure 5.6 shows that spherical AuNPs (with an average diameter of 8.4 nm) were aligned in a definite array along the PPV matrix seen in the form of nanowires.

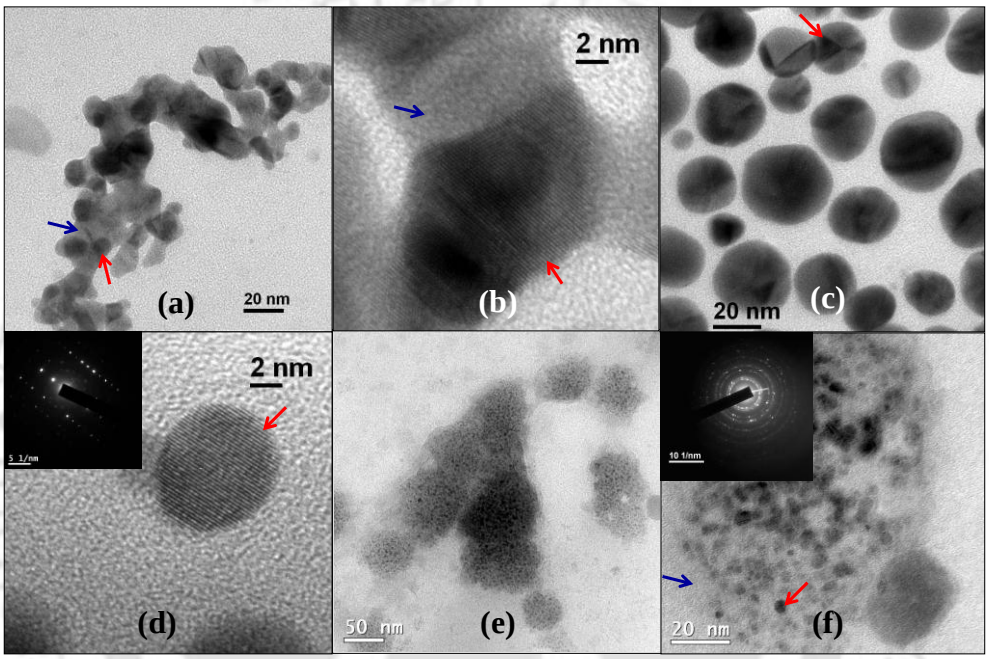

Figure 5.6 TEM images of PPV and Au-nanocomposites in chloroform. (a) & (b) are the TEM image of DHPPV at lowest Au concentration (6 µL), (c) & (d) at moderate concentration of Au (18 µL) and (e) & (f) at higher Au concentration (90 µL). (Red and blue arrows are used to indicate the crystalline gold nano particles and amorphous polymer respectively).

The DHPPV-AuNP hybrids are seen sharing a relationship as the nanowire core (with thickness of <30 nm) and NP shell (with an average diameter of <10 nm) and were clearly visualized by TEM (Figure 5.6a), indicating the encapsulation and formation of a desired polymer-NPs hybrid. Thus, a clear illustration of the presence of AuNPs within the network structure of DHPPV nanowires is confirmed. Because DHPPV coats the

AuNPs systematically, their encapsulation reduces the nonradiative contribution of surface states and would increase the overall quantum efficiency of the composite.[5.14] Importantly, upon increasing the quantity of $HAuCl_4$, we still are able to generate AuNPs in the range of 2-5 nm. (Figure 5.6e, f) Additionally, the amount of AuNP formation also increases with increasing quantity of $HAuCl_4$, yet remaining encapsulated within the DHPPV matrix (Figure 5.6b, c) and causing a maximum blue shift, as seen in the UV-vis spectra. This observation of maximum blue shift also implies that the increased number of AuNPs within the DHPPV matrix reduces the π-electron delocalization in the polymer chain. Such systematic doping is very unlikely to be achieved by mixing of previously synthesized AuNPs with DHPPV solution. In addition, the small size (2-7 nm) of the AuNP is also achieved while preparing the composite material, which showed exceptionally high stability (for months) in solution as well as in the solid state. DLS-based particle size analyses of the DHPPVAuNP composite indicated the average diameter of 8.4 nm and a standard deviation of (1.2 nm. Figure 5.7 clearly confirms that particles of 5 nm size are highly distributed in this composite compared to those of other sizes, agreeing well with the TEM results. During all PL and absorption spectral measurements, the samples were maintained under a dark environment to avoid photodegradation. It has been reported that the rate of photooxidation in PPV was drastically reduced by doping with SiO_2-AuNPs.[5.16] Contrary to the UV-vis spectra, the solutionstate PL spectra did not show any particular features, except the reduction in intensity. Thus, the UV-vis and PL spectra of the DHPPV-AuNP composite in solution and films display very

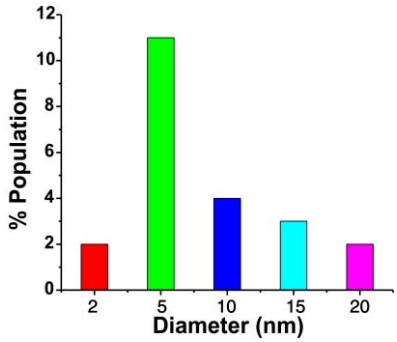

Figure 5.7 Dynamic light scattering profile of the **DHPPV-AuNPs** (6 μL $HAuCl_4$).

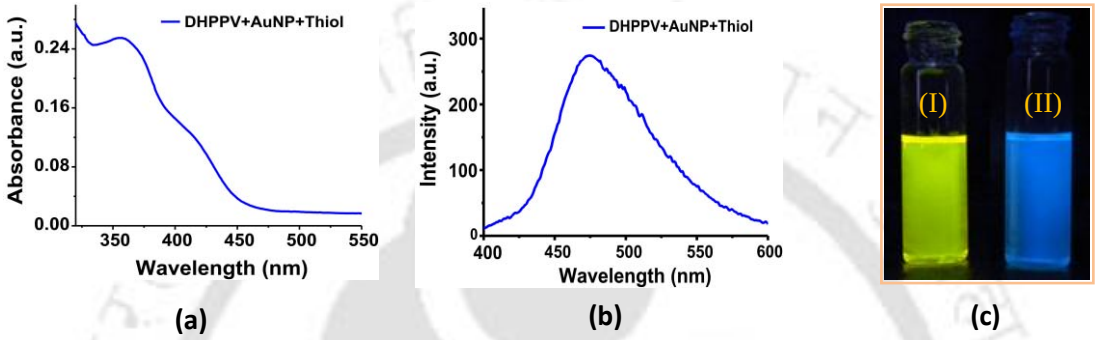

Figure 5.8 (a). UV-vis spectra of DHPPV/Au nanocomposite after treating with octadecanethiol in chloroform. **(b).** PL spectra of DHPPV /Au nanocomposite after treating with octadecanethiol in chloroform. **(c).** Colour of the neat DHPPV /Au nanocomposite (I) and thiol treated DHPPV /**Au** nanocomposite (II) in chloroform under UV light.

different characteristics. A significant blue shift (63 nm) was seen in the UV-vis spectra of DHPPV upon doping with AuNPs in solution, whereas the films of the composite showed a minor blue shift and reduction in the intensity. The PL spectra of the DHPPV-AuNP composites in solution showed reduction in the intensity compared to that of DHPPV, whereas the PL spectra of the DHPPV-AuNP composite film showed significant broadening of the 630 nm peak and disappearance of the 590 nm peak possibly due to the surface plasmon effect and efficient energy transfer from the AuNP to the DHPPV.[5.16,5.17,5.27] The peak emission wavelength, associated with the polymer energy gap between the highest occupied orbital (HOMO) and the lowest unoccupied orbital (LUMO), can thus be tailored by doping with AuNPs.

In our attempt to ascertain the stability of DHPPV-AuNP, we treated these composites with thiol/sulfur-containing compounds such as aqueous sodium sulfide and octadecane thiol, which are known to form stable composites with AuNPs [5.28,5.29] These thiol compounds were not able to destabilize the DHPPV-AuNP composites upon stirring at room temperature indefinitely. However, when DHPPV-AuNP was stirred and heated at 60 °C for 12 h in the presence of octadecane thiol (0.2 g), optical changes were observed in the composites, especially the polymer backbone. Figure 5.8a-c represents the UV-vis and PL spectra and the photographs of the DHPPVAuNP composite and octadecane-thiol-treated DHPPV-AuNP composite as seen under UV light. The UV-vis spectrum showed that a new peak with absorption maxima at 360 nm appeared, whereas the earlier peaks corresponding to pristine DHPPV as well as its composite with AuNP had disappeared. Figure 5.8b shows the photoluminescence peak of the thiol-treated DHPPVAuNP composite at 475 nm when excited at 370 nm, whereas the intense PL peak observed earlier upon excitation at 495 nm was not present. Moreover, ^{1}H NMR of this sample showed the disappearance of the vinyl peak of DHPPV, confirming that there is a modification in the backbone of the polymer in the form of a conjugation break, resulting in this large blue shift of the absorption spectrum. The color of the reaction mixture changed from fluorescent yellow [Figure 5.8c (I)] to light blue, as observed under UV light [Figure 5.8c (II)]. These results confirm that it is possible to reduce the vinylene portion of the PPV backbone (within the polymer matrix) upon treating the DHPPV-AuNP composite material with species like aqueous sodium sulfide, long-chain thiols (dodecane thiol and octadecane thiol), and so forth. The AuNP may have acted as the catalyst in the reduction of the DHPPV backbone in the presence of the above thiol. This result is the first example representing the formation and stabilization of the DHPPV-AuNP composites in the presence of thiol-containing compounds. Even under harsh

conditions such as applying heat or extensive stirring, the composites do not break; however, reduction of the vinylene portion of the polymer backbone occurs. Thus, desired tuning of HOMO-LUMO energy levels of PPV-type polymers is possible via in situ generation of AuNPs in addition to the formation of highly stable nanocomposites.

5.3 Conclusion:

A simple and efficient method to prepare DHPPV-AuNP is demonstrated. The main advantages of this method are the generation of uniform AuNPs even while using a mixture of polar and nonpolar solvents. Additionally, the hybrid materials can be processed as films over desired substrates for optoelectronic applications. Tuning of the optical properties is an added benefit. Due to the high stability of these hybrid materials, it was possible to characterize them easily by absorption, photoluminescence, and TEM measurements in solution as well as in the film form. On the basis of experimental results, the relatively large blue shift observed in the absorption characteristic of the polymer-AuNP composite material was explained as a consequence of the interactions of the AuNP with the DHPPV backbone in the polymer matrix. The small size of AuNP is achieved during synthesis, which is very important for OLED/OPV application, as the typical thickness of the emitting layer required is less than 100 nm. If the size is bigger, the film uniformity will be affected, which will eventually lead to poor device performance. The optical properties of DHPPV can be further tuned by treating the nanocomposite with thiol derivatives, which results in breaking of the conjugation of the polymer backbone but not destabilize the DHPPV-AuNP composites. These results open the possibility to investigate and to explore the tuning of energy levels in PPV-type materials and derivatives using the NP in situ synthesis or doping routes of desired shapes and sizes.

5.4 Experimental Section:

5.4.1 *Materials*:

Alkyl halides and hydrogen tetrachloroaurate ($HAuCl_4$, 17% Au in HCl) were purchased from Sigma-Aldrich. Sodium borohydride ($NaBH_4$, 95%) was purchased from Merck, India. All chemicals/reagents were used as received. Freshly dried and distilled solvents were always used for performing all reactions, including polymerization. Milli-Q grade water was used in all of the experiments.

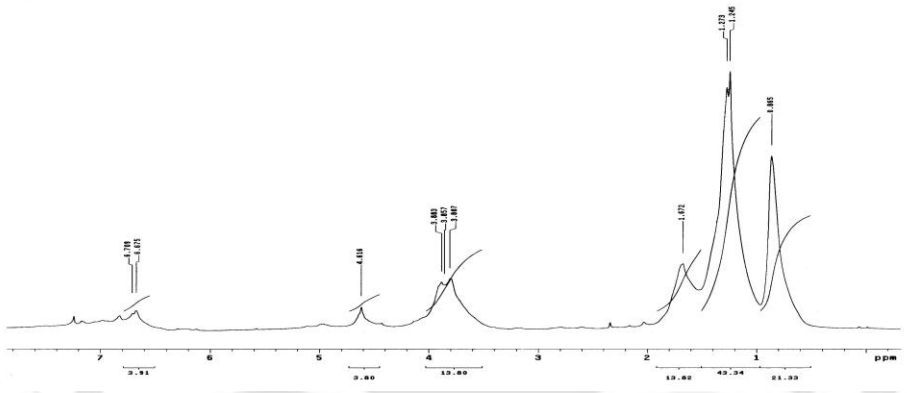

Figure 5.9: **^{1}HNMR** Spectra of DHPPV in $CDCl_3$**.**

5.4.2 *Polymer Synthesis and Characterization*:

Poly(2,5-dihexyloxy)- 1,4-phenylenevinylene was synthesized by following a previously established literature (Figure 5.1) procedure.[5.18-5.20] 1,4- Bis-chloromethyl-2,5-bis-hexyloxy benzene (0.5 g, 1.3 mmol) was treated with potassium-tert-butoxide (0.6 g, 5.4 mmol) in anhydrous tetrahydrofuran (THF) under a nitrogen atmosphere at room temperature for 24 h to give an orange-red powder (0.29 g), with 70% yield, upon adding to methanol solution and filtration. The polymer was well-characterized by FTIR, ^{1}H NMR, and ^{13}C NMR spectroscopy. The molecular weight of the polymer was determined by GPC (gel permeation chromatography) and found to be 34410, PDI-2.10 with reference to polystyrene standards and THF as the eluent. The polymer was found to be

readily soluble in a range of solvents, such as chloroform, dichloromethane, tetrahydrofuran, xylenes, toluene, chlorobenzene, and so forth.

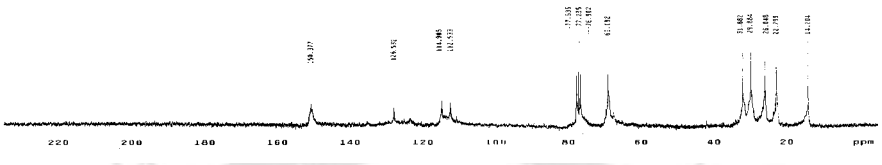

Figure 5.10: **^{13}CNMR** Spectra of DHPPV in $CDCl_3$

5.4.3 *Synthesis of DHPPV-Stabilized Gold Nanoparticle*:

AuNPs were prepared by the known method of $NaBH_4$ reduction of $HAuCl_4$.[5.21,5.22] For the in situ preparation of the polymer/Au composite, $HAuCl_4$ (6-90 μL) (Table 1) was taken in a glass bottle containing 3 mL of 0.02% DHPPV in chloroform and stirred for 10 min; 3 mL of DHPPV solution, 0.02% (w/v) in chloroform, was taken in a 10 mL round-bottom flask, and the mixture was stirred under ice-cold conditions, followed by the addition of 6 μL of 17.3 mM $HAuCl_4$. Freshly prepared 20.0 mM sodium borohydride solution (in water) (25 μL) was slowly added to the reaction mixture under vigorous stirring conditions. Finally, the stopper was tightly closed, and the stirring was continued for 17 h under the same conditions. The reaction mixture was then washed with water, and the organic part was separated and filtered through 0.2 μm filter paper. The separated organic part was observed to be yellowish-green from its original color of orange-red with increasing volume of $HAuCl_4$.

5.4.4 *Analytical Measurements*:

UV-visible spectra of the liquid samples as well as solid films were recorded using Perkin-Elmer lambda-25 spectrophotometer in the range of 200-1100 nm. For the PL measurements, a Varian Cary Eclipse fluorescence spectrophotometer was used. The excitation wavelengths of these samples were in the range of 480-434 nm. Transmission electron microscopy (TEM) of the composite solutions, placed on carbon-coated copper grids, was performed using JEOL-2100 equipment operating at a maximum acceleration voltage at 200 kV. The TEM samples were prepared by drop casting the liquid samples onto a copper grid of 300 mesh followed by evaporation of the solvent at room temperature. Scanning electron micrograph (SEM) images were obtained by means of a LEO-1430 VP electron microscope and ZEISS Sigma VP field emission scanning electron micrograph (FESEM) on samples glued on an aluminium stub and gold sputtered. FT-IR analysis was carried out on air-dried samples with a Perkin-Elmer Spectrum One FT-IR Spectrometer from 4000 to 450 cm^{-1}. Particle size analysis was done by the dynamic light scattering (DLS) method. A 20 mL portion (in chloroform) of the DHPPV-AuNP in chloroform solution was taken in a cell for which the particle size distribution was measured using a HORIBA LB-550 instrument.

5.5 References:

5.1. Chiang, C. K.; Fincher, C. R.; Park, Y. W.; Heeger, A. J.; Shirakawa, H.; Louis, E. J.; Gau, S. C.; MacDiarmid, A. G. *Phys. Rev. Lett.* **1977**, *39*, 1098.

5.2. Burroughes, J. H.; Bradley, D. D. C.; Brown, A. R. *Nature* **1990**, *347*, 539.

5.3. Shim, H. K.; Jang, M. S.; Ahn, T.; Hwang, D. H.; Zyung, T. *Macromolecules* **1999**, *32*, 3279.

5.4. Huynh, W. U.; Dittmer, J. J.; Alivisatos, P. *Science* **2002**, *295*, 2425.

5.5. Wu, C.; Szymanski, C.; McNeill, J. *Langmuir* **2006**, *22*, 2956.

5.6. Chen, X. C.; Green, P. F. *Langmuir* **2010**, *26*, 3659.

5.7. Cury, L. A.; Ladeira, L. O.; Righi, A. *Synth. Met.* **2003**, *139*, 283.

5.8. Szymanski, C.; Wu, C.; Hooper, J.; Salazar, M. A.; Perdomo, A.; Dukes, A.; McNeill, J. *J. Phys. Chem. B* **2005**, *109*, 8543.

5.9. Sun, Y.; Rogers, J. A. *Adv. Mater.* **2007**, *19*, 1897.

5.10. Ho, P. K. H.; Thomas, D. S.; Friend, R. H.; Tessler, N. *Science* **1999**, *285*, 233.

5.11. Brust, M.; Walker, M.; Bethell, D.; Schiffrin, D. J.; Whyman, R. *J. Chem. Soc., Chem. Commun.* **1994**, 801.

5.12. Hutter, E.; Fendler, J. H. *Adv. Mater.* **2004**, *16*, 1685.

5.13. Fang, Y.; Seong, N.-H.; Dlott, D. D. *Science* **2008**, *321*, 388.

5.14. Park, J. H.; Lim, Y. T.; Park, O. O.; Kim, J. K.; Yu, J.-W.; Kim, Y. C. *Chem. Mater.* **2004**, *16*, 688.

5.15. Chiavarone, L.; DiTerlizzi, M.; Scarmacio, G.; Babudri, F.; Farino, G. M.; Naso, F. *Appl. Phys. Lett*. **1999**, *75*, 2053.

5.16. Kim, M. S.; Park, D. H.; Cho, E. H.; Kim, K. H.; Park, Q.-H.; Song, H.; Kim, D.-C.; Kim, J.; Joo, J. *ACS Nano* **2009**, *3*, 1329.

5.17. Grey, J. K.; Kim, D. Y.; Norris, B. C.; Miller, W. L.; Barbara, P. F. *J. Phys. Chem. B* **2006**, *110*, 25568.

5.18. Klimov, V. I.; McBranch, D. W.; Barashkov, N. N.; Ferraris, J. P. *Chem. Phys. Lett.* **1997**, *277*, 109.

5.19. Gilch, H. G.; Wheelwright, W. L. *J. Polym. Sci., Part A: Polym. Chem*. **1966**, *4*, 1337.

5.20. Wudl, F.; Allemand, P. M.; Srdanov, G.; Ni, Z.; McBranch, D. *Materials for Nonlinear Optics: Chemical Perspectives*; American Chemical Society: Washington, DC, 1991; p 983.

5.21. Bing, C.; Mei, E. O.; Kimihiro, S.; Dorothy, F. T. J.; Mountziaris, H. M. *Langmuir* **2009**, *25*, 10604.

5.22. Murugadoss, A.; Chattopadhyay, A. *J. Phys. Chem. C* **2008**, *112*, 11265.

5.23. Lemmer, U.; Mahrt, R. F.; Wada, Y.; Greiner, A.; Bassler, H.; Gobel, E. O. *Appl. Phys. Lett.* **1993**, *62*, 2827.

5.24. Nguyen, T.-Q.; Wu, J.; Liu, J.; Doan, V.; Schwartz, B. J.; Tolbert, S. H. *Science* **2000**, *288*, 652.

5.25. Qi, D.; Kwong, K.; Rademacher, K.; Wolf, M. O.; Young, J. F. *Nano Lett.* **2003**, *3*, 1265.

5.26. Lim, Y. T.; Lee, T.-W.; Lee, H.-C.; Park, O. O. *Synth. Met.* **2002**, *128*, 133.

5.27. Lim, Y. T.; Park, O. O.; Jung, H.-T. *J. Colloid Interface Sci*. **2003**, *263*, 449.

5.28. Lee, K.-H.; Chen, S.-J.; Jeng, J.-Y.; Cheng, Y.-C.; Shiea, J.-T.; Chang, H.-T. *J. Colloid Interface Sci.* **2007**, *307*, 340.

5.29. Casero, E.; Darder, M.; Pariente, F.; Lorenzo, E.; Martin-Benito, J.; Vázquez, L. *Nano Lett.* **2002**, *2*, 577.

Chapter 6

Polyfluorene containing pendant benzimidazole as a non-invasive probe for the detection of Fe3+ and inorganic phosphates in human saliva

Chapter 6

Polyfluorene containing pendant benzimidazole as a non-invasive probe for the detection of Fe^{3+} and inorganic phosphates in human saliva

Abstract:

A neutral polyfluorene derivative, poly(9,9-bis(6'-benzimidazole)hexyl) fluorene-*alt*-1,4-phenylene (**PBP**), is synthesized and well characterized by ^{1}H NMR, ^{13}C NMR and GPC. PBP exhibits exemplary activity as noninvasive fluorescence sensor and accomplishes in-situ monitoring of important biological targets like Fe^{3+} and inorganic phosphates in saliva. On binding Fe^{3+} the fluorescence of PBP is quenched by 97% in label free conditions. The fluorescence of PBP is regained on adding inorganic phosphate with a fluorescence enhancement of 106% due to the displacement of Fe^{3+} from the PBP. This PBP assay is further used to detect and estimate inorganic phosphate in fresh saliva samples which is also able to enhance the fluorescence by >94%. This ability of PBP to accomplish in-situ monitoring and estimation of indispensable biological targets like Fe^{3+} and inorganic phosphates rapidly, at very low concentration with very high selectivity corroborates the extension of this assay system for safe clinical applications.

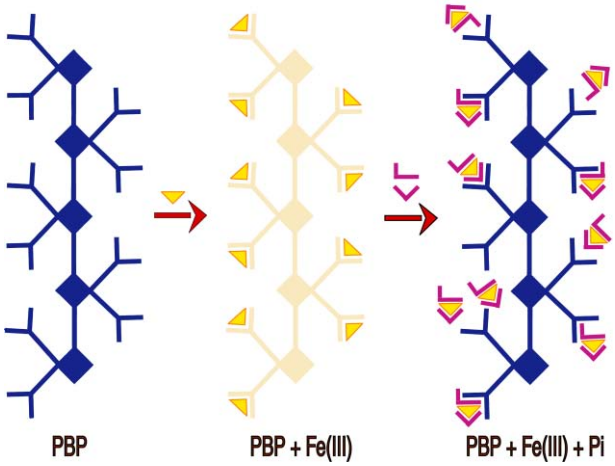

6.1 Introduction:

The increasing need for accurate detection of inorganic phosphate (P_i) remains an imperative frontier in clinical analysis.[6.1] In cells starved of glucose, the P_i quantity is found to be very high because intracellular glycolysis depends on the level of P_i.[6.2] As a consequence of the vital role of P_i in physiological system and medical diagnostics, few approaches such as ELISA[6.3] column chromatography[6.4] spectrometric assay,[6.5] potentiometric assay[6.6] and the conventional malachite green assay method[6.7] have been developed in the past. Although some of these techniques are still in use, they are less sensitive and have focussed on measuring the P_i content present in blood. Since all these assays are invasive, require labelling and need longer duration, it is essential to develop rapid, sensitive and consistent method for the determination of P_i. In this regard, saliva monitoring offers a simple and non-invasive approach for rapidly evaluating it as a diagnostic fluid in real time.[6.8] Yet, neutral systems based on conjugated polymers (CPs) that are highly efficient, selective and sensitive to small alteration have not been developed for P_i detection non-invasively. Furthermore, saliva has lesser proteins compared to blood and the amount of P_i in saliva is three orders of magnitude more than blood serum. Due to these potential advantages and the ability to monitor systemic health and disease states easily, the development of saliva based diagnostic assays that would be non-invasive, cheap, painless and patient friendly is extremely crucial and necessary.

Similarly, iron is the highly abundant and vital metal in physiological system and has a central role in metabolism, for oxygen transport and oxidative phosphorylation. Iron deficiency causes anaemia and formation of haemoglobin ceases, whereas iron overload damages cells and tissues.[6.9] Hence, newer approaches for the selective detection of Fe^{3+} have appeared recently.[6.10] Because of their unique signal amplification properties, CPs have been widely investigated as optical transducers in highly sensitive chemical and

biological sensors.[6.11] Polyfluorenes and its derivatives are imperative class of CPs that have been extensively studied for blue LED's and photovoltaics due to their extraordinary optical, electrical and thermal properties.[6.12] These properties can be altered and tuned as desired by preparing copolymers, composites and controlling the side chain length as well as incorporating different functional groups onto them.[6.13] This has helped to achieve higher device performance and widened their applications in diverse interdisciplinary fields such as medical diagnostics, chemical and biological probing and energy conversion by harnessing the unique molecular wire effect and fluorescence amplifying capabilities.[6.14] CP based fluorescent chemosensors for detecting physiologically and environmentally relevant alkali, alkaline earth metal ions, as well as heavy and transition metal ions has attracted considerable attention in recent years.[6.15] Yet neutral CP sensors for detecting analytes in biological fluids such as saliva, serum etc. have not been developed. Hence, designing neutral CPs possessing biocompatible characteristics and functional groups capable of selectively binding vital biological analytes remains a fascinating challenge. In this article, we report the synthesis of poly(9,9-bis(6'-benzimidazole)hexyl) fluorene-*alt*-1,4-phenylene (PBP), a novel polyfluorene derivative, that performs selective recognition of Fe^{3+} and P_i in aqueous medium and saliva.

6.2. Results and Discussion.

Scheme-6.1 depicts the synthesis of desired PBP polymer in high yield. In the first step of the synthetic route, 2-phenyl benzimidazole was N-alkylated with 2,7-dibromo-9,9-bis(6-bromohexyl)-9H-fluorene, M1, in the presence of sodium hydride to give M2 in 94 % yield. Suzuki coupling of M2 with 1,4-phenylboronic acid resulted in the formation of desired copolymer, PBP, as yellow-brown solid in 80% yield. PBP was well characterized by ^{1}H and ^{13}C NMR and was found to have MW of 13964, PDI-2.01 (GPC in THF-PS as internal standard). Since PBP was soluble in several organic solvents including a

combination of solvents such as THF/water, DMSO/water and DMF/water, the detection of several important analytes that are present in diagnostic assays such as saliva, serum etc. could be conveniently carried out.

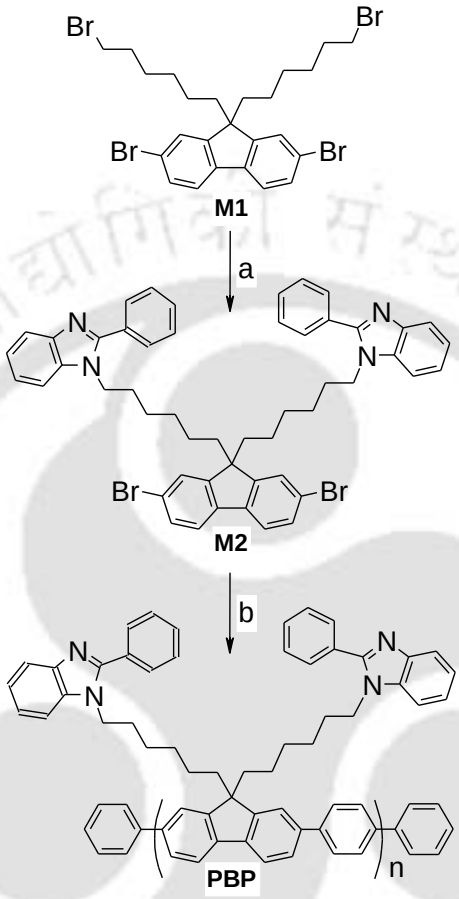

Scheme 6.1 Synthetic procedure for M2 and **PBP**. a = 2-Phenyl benzimidazole, sodium hydride, dry THF, Reflux, 24 hrs, 94%. b = 1,4-phenylboronic acid, $Pd(PPh_3)_4$, K_2CO_3 in THF/water mixture, Reflux, 36 hrs, 80%.

The optical properties of CPs are modified when they associate with analytes, resulting in spectral changes that can be monitored by the shift in wavelength or quenching of the fluorescence intensity.[6.16] Since PBP possesses benzimidazole groups which are known to bind metal ions, we studied its interaction with a series of metal salts such as Na^+, K^+, Mg^{2+}, Al^{3+}, Ca^{2+}, Cr^{3+}, Mn^{2+}, Mn^{3+}, Fe^{2+}, Fe^{3+}, Co^{2+}, Ni^{2+}, Cu^{2+}, Zn^{2+}, Cd^{2+} and Hg^{2+} having concentrations 3.2×10^{-6} M in water and monitored the changes by fluorescence spectroscopy. Metal salts like Zn^{2+} and Al^{3+} caused fluorescence quenching of PBP at

(a)

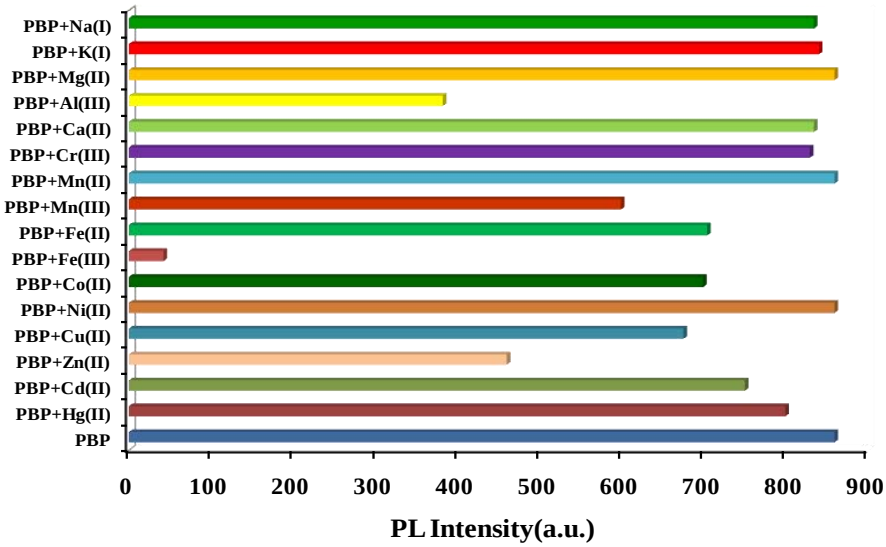

(b)

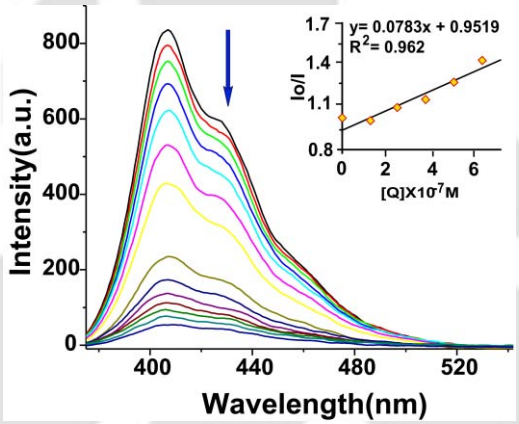

Figure 6.1(a) Bar diagram depicting effect of various metals on the fluorescence intensity of PBP in THF:Water (4:1) **(b)** PL spectra of PBP (1.6 X 10^{-6} M) in THF:Water (4:1) with increasing concentration of Fe^{3+} shows >97% quenching. Inset: Stern-Volmer quenching trend of PBP upon addition of Fe^{3+}.

very high concentrations whereas all other metal salts had negligible or virtually no effect on PBP (Figure 6.1a). Performing titration with aqueous solution of Fe^{3+} metal salts (chloride and perchlorate) induced large quenching in the fluorescence of PBP (Figure 6.1b), with >97 % reduction in fluorescence intensity, clearly implying strong and selective association of PBP and Fe^{3+}. Such remarkable quenching of the polymer PBP by Fe^{3+} occurs due to several factors such as transfer of electron, competent energy

migration and exciton delocalization along the PBP simultaneously.[6.17] The quenching behaviour of PBP was studied using the Fe^{3+} titration data. Figure 6.1b (Inset) shows Stern-Volmer plot (SV), (Io/I vs. [Q]) where Io is the fluorescence intensity of PBP, and I is the fluorescence intensity of PBP after addition of a given concentration of quencher [Q] where [Q] = Fe^{3+}. The KSV value was found to be 7.8 x 10^5 M^{-1}.

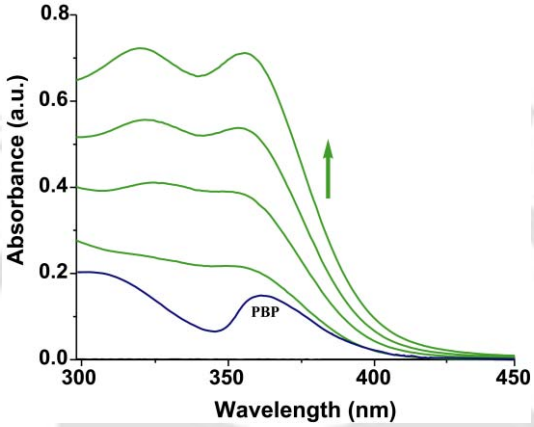

Figure 6.2 UV-vis titration of PBP in THF: Water (4:1) with increasing concentration of Fe^{3+}.

The absorption maxima (360 nm) of PBP showed ~7 nm shift on titration with Fe^{3+} (Figure 6.2) confirming the static quenching mechanism.[6.18] Further, lifetime values of PBP were not modified on titration with Fe^{3+}, signifying the static quenching mechanism.

Figure 6.1(b) indicates that maximum quenching of PBP (~97 %) occurs at total concentration as low as 3.38 x 10^{-6} M of Fe^{3+}. This significant capability of PBP to detect aqueous solution of Fe^{3+} irrespective of various salts widens its utility in probing Fe^{3+} in biological systems with a extensive range of possible applications that comprise iron metabolism, and anaemia etc. Recently, there has been growing interest in using Fe^{3+} compounds as binders of phosphate[6.19] in blood serum, whole blood and dietary phosphates, instead of traditional binders like salts of calcium, aluminium[6.20] and lanthanum,[6.21] that have numerous drawbacks like toxicity, intolerance to patients, expensive and unidentified side effects.[6.22] Yet, non-invasive techniques utilizing Fe^{3+} and

CP based phosphate binders, that are safe and simple for patients, remains undeveloped and merits investigation. Employing the PBP-Fe^{3+} assay system, we examined the binding of P_i at pH-7.4 by fluorescence spectroscopy. Since HPO_4^{2-}: $H_2PO_4^{1-}$ exists in 61:39 ratio at pH 7.4 we have used the term "inorganic phosphates or only P_i" in this chapter.

Figure 3a depicts the rapid fluorescence dequenching up to 106 % on titration of aqueous P_i with PBP-Fe^{3+} assay (pH-7.4 in water). It is clearly observed that the largest spectral enhancement occurs at concentration of 5.3 X 10^{-7} M of P_i, which gradually leveled off at a concentration of 6.6 X 10^{-6} M. To determine the effect of other anions on the dequenching of PBP-Fe^{3+} spectra, similar titration experiments were carried out with several anions such as bromide, chloride, nitrate, thiosulfate, carbonate, iodide, nitrite, cyanate, sulfate, and disulphite anions.

(a) (b)

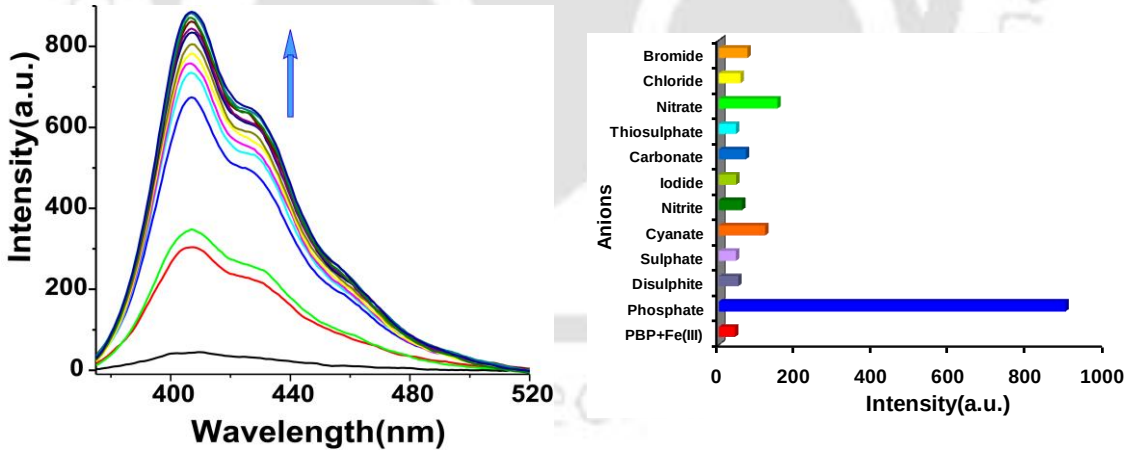

Figure 6.3(a). PL spectra of PBP-Fe^{3+} with increasing concentration of P_i (pH-7.4 in water) shows 106 % dequenching. (b). Bar diagram depicting effect of various anions on the fluorescence intensity of PBP-Fe^{3+}.

As observed in Figure 6.3b, the fluorescence of PBP-Fe^{3+} assay is barely dequenched on addition of these anions. The >100 % dequenching of PBP-Fe^{3+} assay on adding aqueous

P_i to the quenched PBP-Fe^{3+} assay indicates that the Fe^{3+} attached to PBP has been displaced that leads to recovery of the fluorescence. The mechanism for the remarkable fluorescence dequenching is proved by examining the changes in the UV-Vis spectra of the PBP polymer on adding Fe^{3+} and the spectral changes occurring thereafter in the presence of P_i. As shown in figure 6.2 (green), it is clearly observed that there is a 7 nm shift in absorption and significant spectral enhancement on addition of Fe^{3+} to PBP. However, on addition of P_i to the cuvette containing the PBP-Fe^{3+} complex, the PBP-Fe^{3+} spectra is modified (red, Figure 6.4) to an extent of having similarity with that of the original PBP spectra. (blue, Figure 6.4) This clearly suggests that the addition of P_i to a solution of PBP-Fe^{3+} results in the displacement of Fe^{3+} from the polymer PBP.

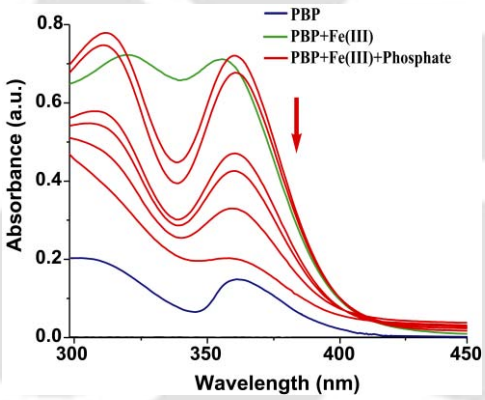

Figure 6.4 UV-vis spectra of **PBP**-Fe^{3+} with increasing concentration of P_i (pH-7.4 in water).

The interaction of PBP-Fe^{3+} with few representative inorganic and organic phosphates was also performed and is represented in Figure 6.5. The fluorescence dequenching of PBP-Fe^{3+} by pyrophosphate (PyPi) and polyphosphate (PolyPi) was 93% and 90%, whereas, adenosine diphosphate (ADP), adenosine triphosphate (ATP), glucose-6-phosphate (G6P), triethyl phosphate (TEP) and o-phospho-L-serine (oPLS) cause no changes to the fluorescence spectra of PBP-Fe^{3+}. The above dequencing results are clear indications that PBP based assay can be selectively used for the detection of P_i in aqueous

medium. The outstanding "superdequenching" of PBP-Fe^{3+} assay on adding P_i presents an exceptional, exceedingly sensitive and homogenous assay exclusively for P_i detection.

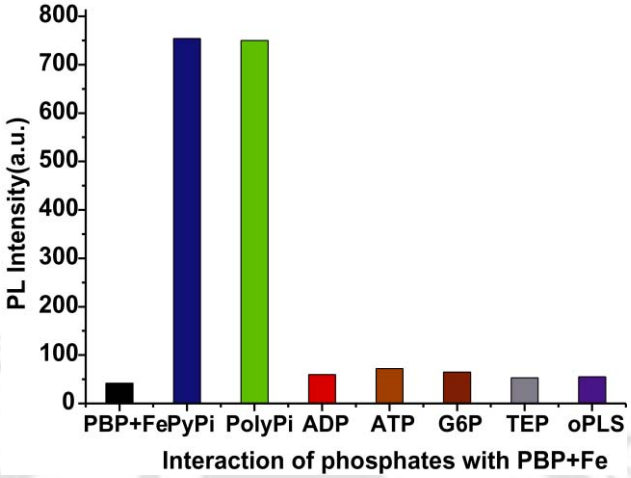

Figure 6.5 Bar diagram depicting effect of organic/inorganic phosphates on the fluorescence intensity of PBP-Fe^{3+}.

Given that PBP-Fe^{3+} assay is capable to detect P_i at such low concentrations, we employed this platform for fluorometric detection and estimation of P_i in saliva. Fresh saliva sample was used in the study and was always obtained after cleaning the mouth with water. In a typical collection procedure, saliva was allowed to accumulate in the base of mouth for ~3 minutes and collected in a sample vial. This was repeated till approximately 5 mL was obtained and which was used immediately for analysis. Since the procedure adopted for obtaining saliva is totally non-invasive and painless to a patient and fresh samples are available whenever desired, this method provides a safe and alternative investigative fluid to serum for diagnostic application. This freshly obtained whole saliva was directly used in the titration experiments with **PBP**-Fe^{3+} assay. On increasing the quantity of saliva (2 µL aliquot) in the cuvette, maximum fluorescence dequenching taking place was 94% (Figure 6.6). Importantly the spectral characteristics observed on adding saliva to the **PBP**- Fe^{3+} was identical to that observed with P_i indicating that the fluorescent enhancement occurring is due to the P_i present in saliva.

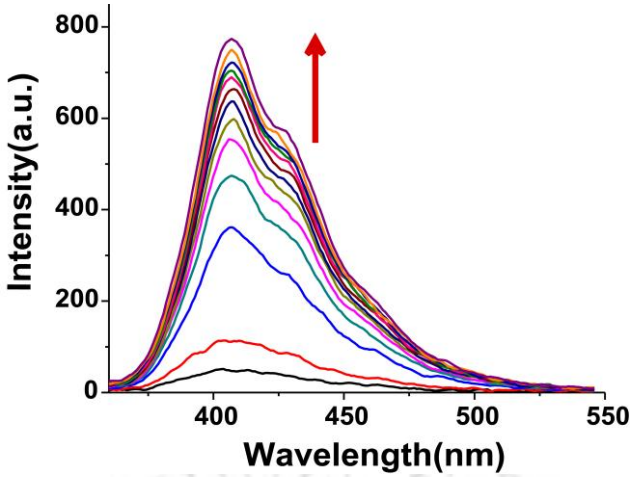

Figure 6.6 Enhancement in PL spectra of **PBP**+Fe^{3+} on addition of 2 µL aliquots of saliva.

With the above spectral studies, we have also performed the estimation of P_i in saliva using this fluorometric titration method since the **PBP** based assay shows remarkable dequenching in the presence of P_i detection at very low concentration. From the spectral changes depicted in figure 6.6, the minimum quantity of P_i that could be estimated accurately in saliva (4 µL) is found to be 1.44 mmol/L that was in agreement with the standard titration plots (Figure 6.3a) values, implying that extremely low quantities of P_i could be estimated using this assay. The maximum fluorescence enhancement observed was 94% implying the presence of 8.64 mmol/L (± 0.09) of P_i in saliva, analyzed by performing four sets of titration experiments. With the help of the above assay, the analysis of P_i in saliva can be performed within 30 minutes and has the advantage of being very precise and uncomplicated. The results obtained by PBP-Fe^{3+} assay for P_i detection in saliva has several advantages over serum based clinically permitted method,[6.23] such as higher order of sensitivity, non-invasive, rapid, label-free and direct sampling of fresh saliva as and when required. Furthermore, since the absorbance (280 nm) and fluorescence (340 nm) peaks of saliva[6.24] do not overlap or interfere with the PBP-Fe^{3+} assay system, PBP based assays can be applied for the detection of vital saliva components.

Experiments with this neutral polymer PBP suggests that detection of biologically essential and indispensable cations and anions such as Fe^{3+} and P_i can be performed accurately by the above assay. PBP exhibits very high fluorescence quenching and dequenching in the presence of Fe^{3+} and P_i without requiring labelling and in a patient friendly method using saliva as a detection fluid. The most important obstacle to use saliva as a diagnostic fluid has been the fact that several vital analytes are generally present in lower quantities in saliva than in serum. However, this is not the case with P_i, which is usually present in much higher quantities in saliva than in serum. Yet, there are no available methods for the detection of P_i from whole saliva. From practical point, since this PBP based assay detects P_i in saliva (non-invasively) with exceedingly high selectivity and sensitivity than currently used clinical methods from serum, it can have immediate use in diagnostic application, forensic science and dental monitoring. These studies also demonstrate that it is possible to identify many more vital disease-associated salivary biomarkers with emerging technology platforms such as the fluorimetric estimation method in combination with neutral CPs.

6.3 Conclusion:

In conclusion, we have described for the first time the use of a neutral fluorescent polymer PBP as a rapid, sensitive and practical technique for the detection of P_i in saliva. Systems such as PBP with such robust fluorescence "superquenching and dequenching" activity are unexplored, providing unique platform for a plethora of safe diagnostic applications. Additionally as a compelling reason, saliva as a diagnostic fluid has several advantages over serum, most prominently, the non-invasive collecting techniques dramatically reduces anxiety and discomfort among patients and procurement of samples repeatedly over time for accurate monitoring. In general, application of neutral CP based assays for saliva monitoring can revolutionize healthcare and diagnostic procedure that

presently rely mainly on painful and unsafe venepuncture techniques. Through these studies we have thus demonstrated that it is possible to identify and estimate vital disease-associated salivary biomarkers by using emerging technology platforms such as neutral CP materials along with patient friendly and simple to perform methods.

6.4 Experimental

6.4.1 *Reagents and materials*:

All chemicals and solvents were purchased from Aldrich Chemicals (India), Merck (India) or Ranbaxy (India) and were used as received. THF distilled over sodium benzophenone and Milli-Q water is used.

6.4.2 *Instrumentation*:

Compounds were characterized by FTIR, ^{1}H-NMR and ^{13}C-NMR spectroscopy. Molecular weight was determined by using gel permeation chromatography (Waters) and found to have MW of 13964 PDI 2.01 (GPC-PS as standard in THF). ^{1}H NMR and ^{13}C NMR analysis were recorded in a Varian – AS400 (Oxford) 400 MHz instrument and the chemical shifts were recorded in parts per million (ppm) on the scale using tetramethylsilane (TMS) as a reference. FTIR analysis was carried out on air-dried samples with a Perkin Elmer-Spectrum One FTIR Spectrometer from 4000 to 450 cm^{-1}. UV-visible spectra were recorded, by dissolving a calculated amount of the sample in an appropriate solvent, on a Hitachi UV–visible U–2001 Spectrophotometer or on a Perkin Elmer Lambda UV–visible Spectrophotometer. Photoluminescence spectra were recorded using Varian Spectrometer by excitation of the polymer at 370 nm.

6.4.3 *Synthesis and characterization of monomer (M2) and polymer (PBP)*:

Synthesis of Monomer: Monomer M1 was prepared by previously reported method. M2: A mixture of 2,7-Dibromo-9,9-bis(6-bromohexyl)-9H-fluorene (1.0 g, 1.54 mmol) (M1),

2-Phenyl-1H-benzoimidazole (1.21 g, 6.19 mmol) and Sodium hydride (0.15 g, 6.19 mmol) was stirred in dry THF for 24 hours under nitrogen atmosphere. Reaction progress was monitored by TLC (1:9 EtOAc: Hexane). After completion of the reaction, the base was removed by filtering through a celite pad. The compound was purified by recrystallization from EtOH to obtain pure compound (1.21 g, Yield= 94%), confirmed by FTIR, NMR and Mass spectroscopy.

^{1}H NMR (400MHz, $CDCl_3$) δ (ppm): 7.81 (d), 7.61 (d), 7.45(m), 7.26.93 (t), 4.09(t), 1.78 (m), 1.60 (t), 0.95 (q), 0.46 (q). ^{13}C NMR (100MHz, $CDCl_3$) δ (ppm): 153.7, 152.0, 142.8, 139.1, 135.4, 130.5, 129.8, 129.3, 128.8, 126.0, 122.8, 122.5, 121.7, 121.4, 119.8, 110.2, 55.4, 44.5, 40.0, 29.6, 29.1, 26.2, 23.4. FTIR (KBr pellete): 3417, 2928, 1643, 1520, 1450, 1394, 1155, 1060, 812, 743, 698 cm^{-1}. MS for $C_{37}H_{40}Br_2O_2$: calculated- 675.80; found- 675.3.

6.4.4 *Synthesis of the polymer, PBP*:

A mixture of M2 (0.50 g, 0.57 mmol), 1,4-phenylenediboronic acid (0.11 g, 0.64 mmol), potassium carbonate (0.20 g, 1.10 mmol), THF (10 mL)/water (5 mL), and Pd(0) (0.033 g 0.028 mmol) were carefully degassed and stirred at 70 °C for 24 hrs. After 24 h iodobenzene (0.02 g, 0.11 mmol) was added and allowed to continue at 70 °C for 12 hours followed by addition of 0.05g phenylboronic acid. The solution was cooled to room temperature; and was precipitated in methanol to remove monomers. The filtrate was concentrated, precipitated into methanol again, and the obtained solid was then washed with 200 mL of acetone. The resultant polymer PBP was obtained as powder, 0.36 g, Yield=80 %.

^{1}H NMR (400MHz, $CDCl_3$) δ (ppm): 7.71(d), 7.51(d), 7.38(m), 7.26(s), 4.04(m), 1.93(m), 1.59(m), 0.98(m), 0.65(d). ^{13}C NMR (100MHz, $CDCl_3$) δ (ppm): 153.8, 143.2,

140.5, 135.7, 130.8, 129.8, 129.1, 128.8, 127.7, 122.8, 122.5, 121.4, 120.12, 110.2, 55.4, 44.7, 40.5, 29.7, 29.4, 26.4, 23.7.

UV titration of polymer with metal: Stock solution of PBP (5×10-5 M) in THF/water and stock solution of Fe(III) (2×10^{-4} M) in Milli-Q water was prepared. 30µl of PBP solution was diluted to 3 ml THF and this was titrated with Fe(III) metal solution upto 1:2 concentration. PBP absorption maximum (λ_{max}) was found 370 nm.

6.4.5 ***UV titration of polymer+metal with phosphate*:**

Stock solution of P_i was prepared (2×10^{-4} M) in Milli-Q water. The stock solution was diluted upto ten times and titrated against PBP+Fe(III) as above.

6.4.6 ***PL titration of PBP with metal*:**

PBP stock solution of 5×10^{-5} M in THF/water and metal 2×10^{-4} M solution in Milli-Q water was prepared. Concentration of PBP in cuvette was adjusted to be 1.6×10^{-6} M.. The fluorescence response with various metals was performed in aqueous solution till PBP and metal ratio in cuvette reached 1:2 at excitation wavelength of 370 nm. This was found to be highly sensitive towards Fe(III), as in the concentration ratio reached 1:2, 97% quenching was observed.

6.4.7 ***PL titration of PBP+Fe(III) assay with anions*:**

A solution of PBP (5.0×10^{-5} M) was prepared in THF/water and metal (2×10^{-4} M) solution in Milli-Q water. The solutions of NaOH were prepared in Milli-Q water and was used to adjust the pH-7.4. A solution of PBP was placed in a quartz cell and the fluorescence spectrum was recorded. First Fe^{3+} was added to quench the fluorescence, and titration was performed with various anions up to 1:2 ratio of PBP+Fe(III) and anions to dequench the fluorescence. The fluorescence intensity changes were recorded at room temperature each time (excitation wavelength: 370 nm).

6.4.8 ***PL titration of PBP+Fe(III) assay with phosphates*:**

A solution of PBP (5.0×10^{-5} M) was prepared in THF/water. The solution of inorganic phosphates were prepared in Milli-Q water. A solution of PBP was placed in a quartz cell (10.0 mm width) and the fluorescence spectrum was recorded. After the addition of solution of Fe(III) (3.2×10^{-6} M) to quench the fluorescence of PBP, the solution of phosphate (6.24×10^{-6} M) was introduced in portions and the fluorescence intensity changes were recorded at room temperature each time (excitation wavelength: 370 nm).

6.4.9 ***PL titration of PBP+Fe(III) assay with pyrophosphate*:**

Same procedure as described in section 6.4.8.

6.4.10 ***Fluorescence response of PBP+Fe(III) with Human saliva*:**

Fresh saliva was always used for analysis after rinsing the mouth with Milli-Q water. In a typical collection procedure, saliva was allowed to accumulate in the base of mouth for 3 minutes and collected in a sample vial. This was repeated till approximately 5 mL was obtained and was used immediately for analysis. Saliva was added in 2 μL aliquots to the cuvette and changes were recorded in the PL spectra.

6.5 References:

6.1 Dwivedi, A. K.; Saikia, G.; Iyer, P. K. *J. Mater. Chem.* **DOI**: 10.1039/COJMO3054F

6.2 Mason, P. W.; Carbone, D. P.; Cushman, R. A.; Waggoner, A. S.; J. Biol. Chem. **1981**, *256,* 1861.

6.3 Tan, W.; Sabet, L.; Li, Y.; Yu, T.; Klokkevold, P. R.; Wong, D. T.; Ho, C.-M. *Biosens. Bioelectron.* **2008**, *24*, 266.

6.4 Barrett, G. R. *J. Biol. Chem.* **1959**, *234*, 466.

6.5 Webb, M. R. *Proc. Natl. Acad. Sci. USA* **1992**, *89*, 4884.

6.6 Katsu, T.; Kayamoto, T. *Anal. Chim. Acta*. **1992**, *265*, 1.

6.7 Zhou, X.; Arthur, G. *J. Lipid Res.* **1992**, *33*, 1233.

6.8 (a) Tobey, S. L.; Anslyn, E. V. *Org. Lett.* **2003**, *5*, 2029.

(b) Christodoulides, N.; Mohanty, S.; Miller, C. S.; Langub, M. C.; Floriano, P. N.; Dharshan, P.; Ali, M. F.; Bernard, B.; Romanovicz, D.; Anslyn, E. V.; Fox, P. C.; McDevitt, J. T. *Lab. Chip*, **2005**, *5*, 261.

6.9 (a) Neilands, J. B. S. *Bonding* **1984**, *58*, 1.

(b) Winkelmann, G.; Helm, van der D.; Neilands, J. B. Iron Transport in Microbes, Plants, and Animals; VCH, D-6940: Weinheim, Germany, 1987.

(c) Brugnara, C. Clin. Chem. 2003, 49, 1573.

6.10 (a) Bricks, J. L.; Kovalchuk, A.; Trieflinger, C.; Notz, M.; Büschel, M.; Tolmachev, A. I.; Daub, J.; Rurack, K. *J. Am. Chem. Soc.* **2005**, *127*, 13522.

(b) Xiang, Y.; Tong, A. *Org. Lett.* **2006**, *8*, 1549.

(c) Qin, C.; Cheng, Y.; Wang, L.; Jing, X.; Wang, F. *Macromolecules* **2008**, *41*, 7798.

6.11 (a) Swager, T. M. *Acc. Chem. Res.* **1998**, *31*, 201-207.

(b) Chen, L.; McBranch, D. W.; Wang, H.-L.; Helgeson, R.; Wudl, F.; Whitten, D. G. *Proc. Natl. Acad. Sci. USA*. **1999**, *96*, 12287.

6.12 (a) Fukada, M.; Sawaka, K.; Yoshino, K. *Jpn. J. Appl. Phys.* **1989**, *28*, 1433.

(b) Yang, P. Y. *J. Am. Chem. Soc*. **1996**, *118*, 7416.

6.13 (a) Sainova, D.; Miteva, T.; Nothofer, H. G.; Scherf, U.; Glowacki, I.; Ulanski, J.; Fujikawa, H.; Neher, D. *Appl. Phys. Lett*. **2000**, *76*, 1810.

(b) Jiang, X. Z.; Liu, S.; Ma, H.; Jen, A. K. Y. *Appl. Phys. Lett.* **2000**, *76*, 1813.

(c) Hung, M. C.; Liao, J. L.; Chen, S. A.; Chen, S. H.; Su, A. C. *J. Am. Chem. Soc*. **2005**, *127*, 14576.

6.14 (a) Leclerc, M. *Adv. Mater*. **1999**, *11*, 1491.

(b) Stork, M.; Gaylord, B. S.; Heeger, A. J.; Bazan, G. C. *Adv. Mater*. **2002**, *14*, 361.

(c) Wang, S.; Liu, B.; Gaylord, B. S.; Bazan, G. C. *Adv. Funct. Mater*. **2003**, *13*, 463.

6.15 (a) de Silva, A. P.; Gunaratne, H. Q. N.; Gunnlaugsson, T.; Huxley, A. J. M.; McCoy, C. P.; Rademacher, J. T.; Rice, T. E. *Chem. Rev*. **1997**, *97*, 1515.

(b) Kimura, E.; Koike, T. *Chem. Soc. Rev*. **1998**, *27*, 179.

(c) Gokel, G. W.; Leevy, W. M.; Weber M. E. *Chem. Rev*. **2004**, *104*, 2723.

6.16 Rininsland, F.; Xia, W.; Wittenburg, S.; Shi, X.; Stankewicz, C.; Achyuthan, K.; McBranch, D. W.; Whitten, D. G. *Proc. Natl. Acad. Sci. USA* **2004**, *101*, 15295.

6.17 (a) Bredas, J.-L.; Cornil, J.; Beljonne, D.; Dos Santos, D. A.; Shuai, Z. *Acc. Chem. Res.* **1999**, *32*, 267.

(b) Nguyen, T.-Q.; Wu, J.; Doan, V.; Schwartz, B. J.; Tolbert, S. H. *Science*, **2000**, *288*, 652.

6.18 (a) Zhou, Q.; Swager, T. M. *J. Am. Chem. Soc*., **1995**, *117*, 7017.

(b) Lakowicz, J. R. Principles of fluorescence spectroscopy, (Kluwer Academic/Plenum Publishers, New York 1999).

6.19 Hsu, C. H.; Patel, S. R.; Young, E. W. *J. Am. Soc. Nephrol*. **1999**, *10*, 1274.

6.20 Wills, M. R.; Savory, J. *Lancet*, **1983**, *2*, 29.

6.21 Autisser, V.; Damment, S. J. P.; Henderson, R. A. *J. Pharm. Sci*. **2007**, *96*, 2818.

6.22 (a) Clarkson, E. M.; Durrant, C.; Phillips, M. E.; Gower, P. E.; Jewkes, R. F.; de Wardener, H. E. *Clin. Sci.* **1970**, *39*, 693.

(b) Clarkson, E. M.; Eastwood, J. B.; Koutsaimanis, K. G.; De Wardener H. E. *Kidney Int*. **1973**, *3*, 258.

6.23 Kanbay, M.; Goldsmith, D.; Akcay, A.; Covic, A. *Blood Purif*. **2009**, *27*, 220.

6.24 Soukos, N. S.; Crowley, K.; Bamberg, M. P.; Gillies, R.; Doukas, A. G.; Evans, R.; Kollias, N. *Forensic Sci. Int*. **2000**, *114*, 133.

Chapter 7

A dual sensing neutral conjugated polymer fluorescent probe for detection of Copper(II) and Fluoride ions in water

Chapter 7

A dual sensing neutral conjugated polymer fluorescent probe for detection of Copper(II) and Fluoride ions in water

Abstract:

A neutral poly-*p*-phenylene (**PPP**) polymer derivative, poly(1,4-Bis-(8-imidazole-octyloxy)-benzene) (**PPI**), was prepared by a straightforward and economical method of oxidative polymerization at room temperature in two high yielding steps. All the newly synthesized monomers and polymers were characterized by FTIR, ^{1}H NMR, ^{13}C NMR and mass spectroscopic techniques. The molecular weight of the polymer was determined by GPC. This neutral polymer PPI, showed very high fluorescence intensity, selectively to bind Cu^{2+} ions in solution state (in THF/water) that could be easily monitored by the efficient fluorescence quenching of the PPI by over 98%. The fluorescence intensity of the PPI could be reverted back when fluoride is added to the solution of PPI-Cu^{2+} in the cuvette indicating selective and highly sensitive interaction with fluoride anion resulting in the displacement of the bound Cu^{2+} to the PPI. The quenching mechanism is explained by carefully examining the UV/Vis changes on addition of the Cu^{2+} and fluoride. Fluorescence dequenching occurs up to 81% on addition of fluoride ion to the PPI-Cu^{+2} assay and is found to be highly selective for fluoride ion.

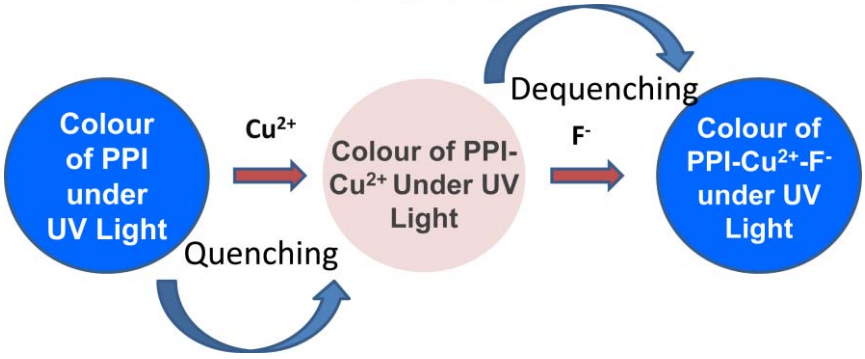

7.1 Introduction:

We report here the extremely sensitive dual sensing ability of PPI, a novel polyphenylene derivative, to accomplish selective recognition of Cu(II) and fluorides in competitive environment. Photoluminescence is the most common[7.1] and highly sensitive optical transduction method, and analyte binding events that produce a reduction, enhancement, or wavelength shift in the emission can be used to produce a functional sensor.[7.2] Conjugated polymers with receptors affixed to the backbone put forward a feasible approach to selectivity via changes in absorption and emission spectra.[7.3] The development of optical sensing approaches for the detection of environmentally and biologically important species, such as transition and heavy metal ions, has been an important goal in the field of chemical sensors for several decades. A fluorescence-based one is a very appealing motif for future practical applications due to its intrinsic sensitivity, its straightforward application to fiber optical-based detection, and it being capable of affording high spatial resolution via microscopic imaging.[7.4] A fluorescent probe molecule would involve the covalent linking of a receptor domain to a fluorescent fragment (i.e., the signaling unit). The two components are intramolecularly connected together such that the binding of the target analyte causes significant changes to the photophysical properties of the fluorescent fragment. [7.5]

Copper is a significant metal pollutant due to its widespread use, but it is also an essential second most abundant trace element in human health and other biological systems. Copper toxicity is rather less for humans compared to other heavy metal ions. Fluorescent sensing of Cu^{2+} could be utilized to clarify the physiological role of the metal in vivo as well as to monitor its concentration in the metal-contaminated sources. Although several copper based fluorescent sensors have been designed in the past few years[7.6] there is still a

need to develop a highly selective fluorescent sensing method that allows real-time monitoring of the metal ion.

The design of fluoride sensors is an area of active investigation because of the possible toxicity of this anion,[7.7] which is present in drinking water, toothpaste, and osteoporosis drugs. The development of fluoride-selective optical sensors is of practical importance and would offer an attractive low cost/ disposable alternative to the widely used solid-state LaF_3 ion selective electrode, especially for mass production (e.g., via screen printing) of planar sensor arrays and single-use devices. Highly selective fluoride sensors are useful for the determination of fluoride levels in potable water. Organo boron sensor compounds are not much useful for F^- ion detection in aqueous medium because of the higher affinity of F^- ions towards water. Hence, these classes of sensors have that limitation and remain far away from practical validation. The polymeric sensory system demonstrated in this chapter exhibits extraordinary optical selectivity and sensitivity for fluoride in water/organic mix medium over a wide range of other anions, including anions with far more positive free energies of hydration (e.g. perchlorate, thiocyanate, nitrate, etc.).[7.8] Enzymatic and metal ion catalyzed degradations of these species liberate fluoride ion, which could be detected quickly using a suitable fluoride sensing probe.[7.9-7.10] To date, very few optical sensors have been developed for fluoride ions based on fluorescence or absorbance/reflectance measurements since they suffer from low selectivity and a high detection limit.[7.11] For example, fluoride optical sensors based on physical immobilization of dyes (e.g., zirconium-calcein blue and alizarine) at the distal end of bifurcated optical fiber showed a high fluoride detection limit, long response times, and poor fluoride selectivity over common anions such as sulfate, phosphate, and acetate. Studies of a new sensing system comprising aluminum(III)-octaethylporphyrin

ionophore are also reported in order to gain more insight into the nature of the fluoride interaction.[7.12]

Fluoride has one of the most negative Gibbs free energies of hydration among common anions;[7.13] thus partitioning of fluoride into an organic polymer phase is thermodynamically unfavorable. Therefore, to devise a bulk optode for fluoride, a highly selective ion carrier in the organic phase is needed to counterbalance the hydrophilicity of this anion.[7.14] Recently it was found that polymer membranes doped with Ga(III) and Zr(IV) porphyrins exhibit an enhanced potentiometric selectivity for fluoride due to the ability of these species to interact selectively with fluoride ion via a preferred axial ligation reaction.[7.15]

7.2 Experimental:

7.2.1 *Reagents and materials*:

Tetrahydrofuran (THF) was dried over and distilled from Na metal under an atmosphere of dry nitrogen. 1,8-dibromooctane, Hydroquinone and Tetrabutyl salts were purchased from Aldrich. All the metal salts and anions, purchased from Meark India and Ranbaxy, India, were of analytical reagent grade and used without further purification. Milli-Q water was used for all experiments.

7.2.2 *Synthesis of monomer*:

A general method adopted for the synthesis of oligomers and polymers is outlined in Scheme 7.1. Synthesis of 1,4-Bis-(8-bromo-octyloxy)-benzene was carried out using a previously established procedure from the literature.[7.16] In a 250mL round-bottomed flask, KOH (10.16 g, 181 mmol) and dry dimethyl sulfoxide (DMSO, 48 mL) was stirred under N_2 atmosphere for 3 h at room temperature. To the mixture was added hydroquinone (2g, 18.17 mmol) and 1,8-dibromooctane (19.62 g, 72.6 mmol) and stirred

for additional 25 h. The brown solution thus obtained was poured into water (400 mL). The aqueous layer was extracted with hexane (400 mL) and the organic layer was separated, washed with water, dried over anhydrous Na_2SO_4, and concentrated to obtain yellow-brown liquid. Excess 1,8-dibromooctane was distilled out under reduced pressure and the crude on further purification by silica gel column chromatography (ethyl acetate/hexane, 0.5:9.5) yielded 1,4-Bis-(8-bromo-octyloxy)-benzene as white solid flakes. 7.25 g, Yield: 82%;

^1H NMR (400 MHz, $CDCl_3$): δ_{ppm}, 6.89(s), 3.89(t), 3.41(t) 1.89(m), 1.76(m), 1.44(m), 1.35(m). *^{13}C NMR (100 MHz, $CDCl_3$)*: δ_{ppm}, 153.3, 115.5, 68.7, 42.1, 34.1, 32.9, 29.5, 29.2, 28.8, 28.2, 26.1. m.p., 82 ^oC. GC-MS: m/z 491.11(M+1) (calculated 490.108).

7.2.3 *Synthesis of PPB*:

Polymers were prepared by methods reported earlier.[7.17] The synthesis of poly(1,4-Bis-(8-bromo-octyloxy)-benzene) proceeded as follows. In a 100 mL three-necked round-bottom flask equipped with a nitrogen inlet, anhydrous ferric chloride (1.48 g, 9.18 mmol) was dissolved in 20 mL of nitrobenzene. 1,4-Bis-(8-bromo-octyloxy)-benzene (2.0 g, 4.08 mmol) dissolved in 15 mL nitrobenzene was added to the flask using a syringe. The reaction mixture was stirred at room temperature for 36 h, followed by precipitation from ethanol. This was stirred for 1 h, centrifuged and washed repeatedly with ethanol. The resulting polymer was dried under reduced pressure to obtain 1.39 g (70%) as light brown powder.

^1H NMR (400 MHz, $CDCl_3$):δ_{ppm}, 7.09(s), 3.92(m), 3.37(m) 1.82(m), 1.68(m), 1.37(m), 1.2(m). *^{13}C NMR (100 MHz, $CDCl_3$)*: δ_{ppm}, 150.2, 115.1, 67.8, 40.1, 33.6, 33.1, 28.9, 28.0, 27.8, 27.2, 26.3. Mw, 35219, PDI, 1.9 (GPC, in THF, polystyrene calibration).

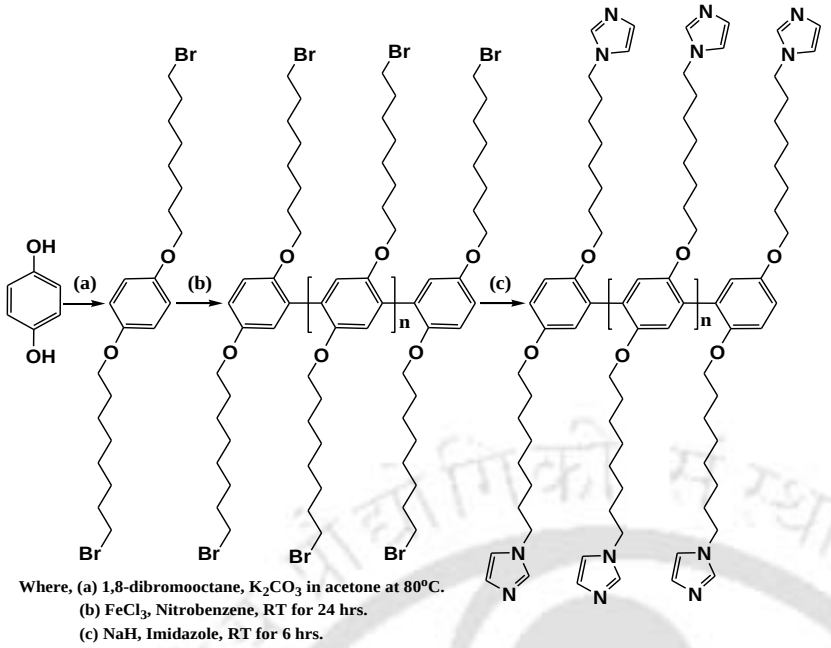

Scheme 7.1 Structure of **PPI**

7.2.4 *Synthesis of PPI*:

PPB (0.20 g. 0.41 mmol), imidazole (0.11g, 1.6 mmol) were dissolved in dry THF (2 mL) and sodium hydride (4 equivalent) as a catalyst. After stirring at RT for 12 h, the mixture was poured into a 50mL of cold MeOH. The obtained solid was dissolved in THF, and reprecipitated in methanol (100 mL), yellow precipitant was collected and washed with acetone, and dried in a vacuum desiccator (150 mg, 78 %).

^1H NMR ($CDCl_3$): δ_{ppm}, 7.45(s), 7.3(s), 7.1(m), 6.8(m), 4.2(m), 3.8(m), 1.7(m), 1.57(m), 1.22(m), 0.84(m). *^{13}C NMR (100 MHz, $CDCl_3$)*: δ_{ppm}, 150.2, 137.1, 129.2, 118.9, 117.3, 69.5, 47.0, 39.5, 37.5, 24.6, 19.8, 14.2, 11.9. *Elemental analysis calculated for PPI*: C, 72.38; H, 8.68; N, 12.06; found: C, 72.17; H, 8.97; N, 12.02.

7.2.5 *Optical Measurements*:

The absorption and fluorescence titrations of the polymer in THF and metal ions in water solution were run by directly adding small aliquots (typically 5μL) of the metal stock

solutions to 3 mL of the THF solution containing $6.0x10^{-6}$ M^{-1} PPI in a quartz sample cuvette (1 cm x 1 cm). After being mixed thoroughly the absorption or fluorescence spectra were then recorded at room temperature.

7.2.6 *Elemental analysis*:

Elemental analysis was performed in a Perkin Elmer Series II 2400 elemental analyser.

7.3 Result and Discussion:

To achieve high affinity binding by N-based moieties, we incorporated the imidazole moiety into our PPP polymer as a pendent group. The synthetic route of the polymer and corresponding monomers are illustrated in Scheme 7.1. PPI was obtained by a post functional method (Scheme 7.1). The imidazole moieties were introduced to the side chain of polymer directly by substituting terminal Br atoms of the alkyl chains in the polymer. The desired PPI polymer could be purified simply by precipitation. Overall, PPI synthesis consists of three steps without the use of costly metal catalysts/ phase-transfer catalysts, while still using simple synthetic steps, and mild reaction conditions. The structure of the polymer is determined by ^{1}H NMR, ^{13}C NMR, elemental analysis and FTIR spectroscopic technique.

Generally, PPP derivatives exhibited strong blue luminescence (Figure 7.1) in diluted solutions with the maximum emission wavelength ~401 nm. The absorption and emission maxima for PPI in solution state did not show any change in position and intensity with other PPP derivatives. Its optical behaviour, studied in the presence of a set of metal ions indicated that only Cu^{2+} ions endorse a notable response in its fluorescence spectra and could be quenched efficiently by trace copper ions while the other metal ions have negligible responses (Figure 7.2). The imidazole moieties could efficiently transfer the

energy from the conjugated backbone to the copper ions, leading to the quenching of the strong luminescence of the polymer.[7.18]

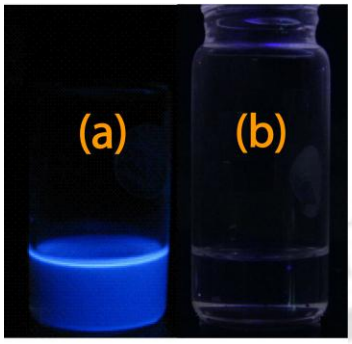

Figure 7.1(**a**) Colour of the PPI solution in THF under UV light. (**b**) Colour of the **PPI**-Cu^{2+} solution in THF under UV light.

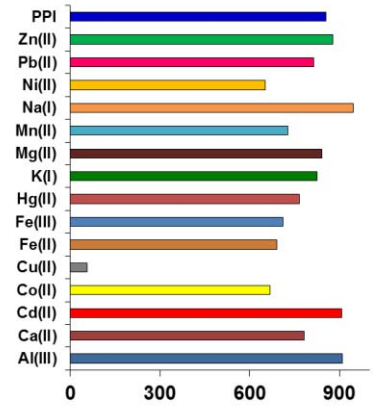

Figure 7.2 Bar diagram depicting effect of various metals on the fluorescence intensity of **PPI**.

The decrease in fluorescence intensity was investigated by adding successive aliquots of aqueous stock solutions of Cu^{2+} ions to the solution of PPI in THF (Figure 7.3). PL quenching of PPP decreases completely at (9.98×10^{-6} M^{-1}). Efficiency of quenching was studied by plotting Stern-Volmer plot (KSV), (Io/I vs. [Q]) where Io is the fluorescence intensity of PPI, and I is the fluorescence intensity of PPI after addition of a given concentration of quencher [Q] where [Q] = Cu^{2+} ion concentration. The KSV value calculated from the plot was found to be 5.8×10^{5} M^{-1}. The absorption maxima peak (Figure 7.4) of PPP showed 4 nm blue shift on titrating with Cu^{2+} confirming the static quenching mechanism. [7.18]

PL titration of PPI in THF was done with 14 different metal ions. Except with Cu^{2+} the intensity of PPI was indistinctly affected upon the addition of metal ions like Zn^{2+}, Fe^{2+}, Fe^{3+}, Mn^{2+}, Ca^{2+}, Hg^{2+}, Ni^{2+} and Pb^{2+}. Alkali metal ions have no effect on polymer PL intensity which is due to the poor coordination ability of the imidazole receptor with these ions.

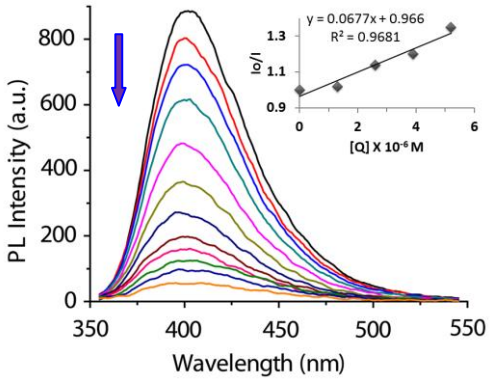

Figure 7.3 PL spectra of PPI in THF with increasing concentration of Cu^{+2}. *Inset: The Stern-Volmer plot of PPI upon addition of Cu^{+2} in aqueous medium.*

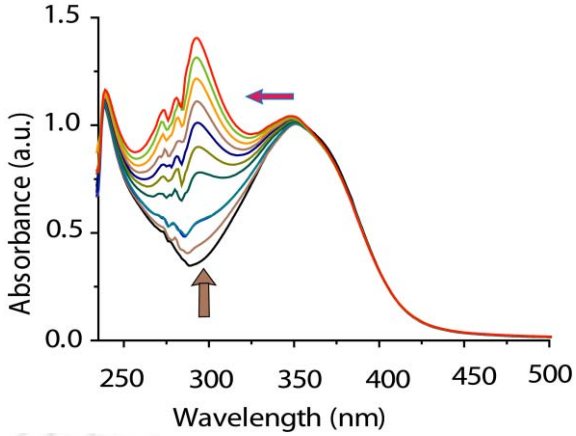

Figure 7.4 UV-vis titration spectrum of **PPI** in THF with Cu^{2+} solution in water.

Titration of copper ions with PPI was also monitored by UV-vis spectroscopy. All studies were done under exactly the same conditions as that of fluorescence. PPI showed slight blue shift of the main peak in absorption maxima (maximum 4 nm) after complexation with Cu^{2+}. Additionally, a new peak was seen developing at 275 nm on continuous addition of metal ions which became more intense than the original peak. The shift of absorption maxima in UV-vis titrations was consistent with the fact that the static quenching results from complexation of the analyte to the receptor sites of the polymer, PPI. A significant increase of absorption intensity at higher quencher concentration was observed which may be due to the charge transfer or aggregate formation.

The various metal salts have different affinity for imidazole moiety which showed different interaction between imidazole groups metal ions as well as with the conjugated polymer backbones that lead to the difference in electronic properties of the polymer. If the binding site is other than imidazole (pyrazole) or substituted imidazole, different sensing behaviour can be observed accordingly.[7.19]

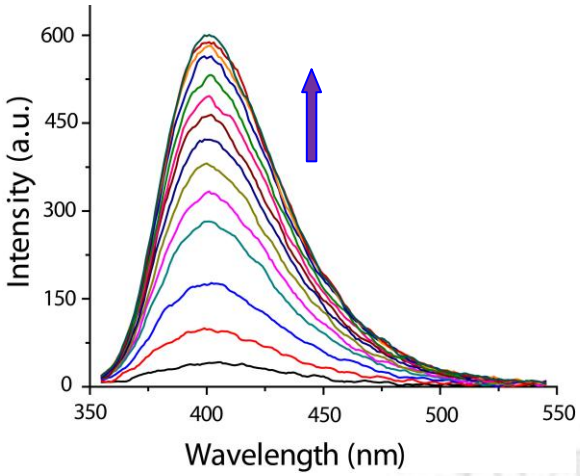

Figure 7.5 PL spectra of PPI-Cu^{+2} with increasing concentration of F^- ions.

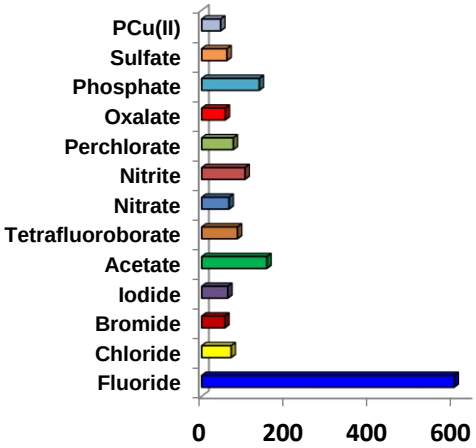

Figure 7.6 Bar diagram depicting effect of anions on the fluorescence intensity of PPI+Cu^{+2}.

Quenched fluorescence intensity of PPI-Cu^{2+} was dequenched significantly on addition of fluoride ions. The fluorescence intensity increases rapidly when the concentration of fluoride ion increases. The PL intensity could recover upto 81% of the original intensity of the pure polymer (Figure 7.5). Titration was performed with various anionic groups (Figure 7.6). Except with acetate and nitrate with other anions had no effect on the enhancement of fluorescence intensity.[7.20]

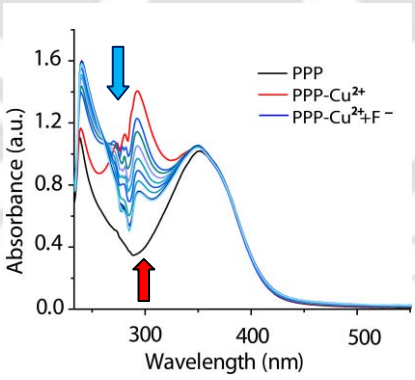

Figure 7.7 UV-vis titration spectrum of PPI in THF with Cu^{2+} solution in water.

Titration of PPI-Cu^{2+} assay with fluoride ion was performed in presence of various other anions, but no other anion can efficiently bind with copper ion to get back the fluorescence completely. We did not observe any remarkable change during titration of

PPI-Cu^{2+} with F^- in presence of other anions. As mentioned earlier, the addition of fluoride ion to the quenched fluorescence of PPI-Cu^{2+}, turned on the fluorescence even at a very low concentration. The intensity increased rapidly when the concentration of fluoride ion increased. The fluorescent intensity could be recovered to about 81% of the original intensity of PPI. F^- ion has high affinity towards water due to the high hydration enthalpy and sensing of this anions in presence of water is very difficult and sometimes misleading. To see the possible influence of the water added during titration as Cu^{2+} and F^- solution, a controlled PL titration was conducted by adding only water of 5 µL aliquots (up to 50 µL) to the PPI solution in THF of the cuvette. Same experiment was repeated for PPI-Cu^{2+} complex and for PPI-Cu^{2+}-F^- using same amounts of water but no obvious disturbance was observed even though the amount of added water was as large as 100 µL.

The mechanism of PL quenching/dequenching was investigated by UV-vis spectroscopy. (Figure 7.7) It is clearly observed that there is a 4 nm shift in absorption and significant spectral enhancement on addition of Cu^{2+} to PPI. However, on addition of F^- to the cuvette containing the PPI-Cu^{2+} complex, the PPI-Cu^{2+} spectra is modified (red, Figure 7.7) to an extent of having similarity with that of the original PPI spectra. (blue, Figure 7.7) This clearly suggests that the addition of F^- to a solution of PPI-Cu^{2+} results in the displacement of Cu^{2+} from the polymer PPI.

7.4 Conclusion:

In summary, a novel PPP derivative, poly(1,4-Bis-(8-imidazole-octyloxy)-benzene) was designed, synthesized and utilized for detection of indispensable dual biological targets like Cu^{2+} and fluoride ions in aqueous medium. Since PPI based assays are highly stable over a wide *pH* range, this easy approach of mixing and detecting various chemical and biological specimens, corroborate this system for clinical and diagnostic validation. Additionally their ability to transport electronic excited states and inherent film forming properties promises numerous interdisciplinary applications like healthcare, security, environmental monitoring and optoelectronic devices.

7.5 References:

7.1 Hirschfeld, T.; Callis, J. B.; Kowalski, B. R. *Science* **1984**, *226*, 312.

7.2 Bissell, R. A.; de Silva, A. P.; Gunaratne, H. Q. N.; Lynch, P. L. M.; Maguire, G. E. M.; McCoy, C. P.; Sandanayake, K. R. A. S. Sensors. In Topics in Current Chemistry; *Springer-Verlag: Berlin Heidelberg*, **1993**, *168*, 224.

7.3 (a) Borman, S. *Anal. Chem*. **1987**, *59*, 1161.

(b) Janata, A. J. Principles of Chemical Sensors; *Plenum Press: New York*, 1989.

(c) Swager, T. M. *Acc. Chem. Res.* **1998**, *31*, 201-207

7.4 (a) Czarnik, A. W.; ACS Symposium Series 538; *American Chemical Society: Washington*, DC, **1992**.

(b) Handbook of Fluorescent Probes and Research Chemicals, 9th ed.; *Haugland, R. P. Ed.*; Molecular Probes: Eugene, OR, **2002**.

7.5 (a) de Silva, A. P.; Nimal Gunaratne, H. Q.; Gunnlaugsson, T.; Huxley, A. J. M.; McCoy, C. P.; Rademacher, J. T.; Rice, T. E. *Chem. Rev*. **1997**, *97*, 1515.

(b) Valeur, B.; Leray, I. *Coord. Chem. Rev*. **2000**, *205*, 3.

(c) Prodi, L.; Bolletta, F.; Montalti, M. Zaccheroni, N. *Coord. Chem. Rev.* **2000**, *205*, 59.

(d) Yang, R. H.; Chan, W. H.; Lee, A. W. M.; Xia, P. F.; Zhang, H. K.; Li, K. A. *J. Am. Chem. Soc*. **2003**, *125*, 2884.

(e) Ono, A.; Togashi, H. *Angew. Chem., Int. Ed*. **2004**, *43*, 4300.

(f) Huang, H. M.; Wang, K. M.; Tan. W. H.; An. A. L.; Huang, S. S.; Zhai, Q.; Zhou, L. J.; Jin, Y. *Angew. Chem., Int. Ed*. **2004**, *43*, 5635.

(g) Arunkmar, E.; Ajayaghosh, A.; Daub, J. *J. Am. Chem. Soc*. **2005**, *122*, 3156.

7.6 (a) Kramer, R. *Angew. Chem., Int. Ed*. **1998**, *37*, 772.

(b) Grandini, P.; Mancin, F.; Tecilla, P.; Scrimin, P.; Tonellato, U. *Angew. Chem., Int. Ed*. **1999**, *38*, 3061.

(c) Rurack, K.; Kollmannsberger, M.; Resch-Genger, U.; Daub, J. *J. Am. Chem. Soc*. **2000**, *122*, 968.

(d) Mayr, T.; Klimant, I.; Wolfbeis O. S.; Werner, T. *Anal. Chim. Acta* **2002**, *462*, 1.

(e) Zheng, Y. J.; Orbulescu, J.; Ji, X. J.; Andreopoulos, F. M.; Pham, S. M.; Leblanc, R. M. *J. Am. Chem. Soc*. **2003**, *125*, 2680.

7.7 Fluorides. Environmental Health Criteria 227, IPCS International Programme on Chemical Safety, *World Health Organization*, 2002.

7.8 Ibrahim H. A.; Meyerhoff, M. E. *Anal. Chem*. **2005**, *77*, 6719.

7.9 Landis, W. G.; DeFrank, J. J. *Adv. Appl. Biotechnol. Ser*. **1990**, *4*, 183.

7.10 Wagner-Jauregg, T.; Hackley, B. E. Jr.; Lies, T. A.; Owens, O. O.; Proper, R. *J. Am. Chem. Soc*. **1955**, *77*, 922.

7.11 (a) Russell, D. A.; Narayanaswamy, R. *Analyst* **1989**, *114*, 381.

(b) Narayanaswamy, R.; Russell, D. A.; Sevilla, F. *Talanta* **1988**, *35*, 83.

7.12 Wang, L.; Meyerhoff, M. E. *Anal. Chim. Acta.*, **2008,** *611*, 97.

7.13 Zhan, C.-G.; Dixon, D. A. *J. Phys. Chem. A* **2004**, *108*, 2020.

7.14 Morf, W. E. The Principles of Ion-Selective Electrodes and Membrane Transport; *Elsevier: New York*, 1981.

7.15 (a) Steinle, E. D.; Schaller, U.; Meyerhoff, M. E. *Anal. Sci*. **1998**, *14*, 79.

(b) Malinowska, E.; Niedziolka, J.; Meyerhoff, M. E. *Anal. Chim. Acta* **2001**, *432*, 67.

(c) Malinowska, E.; Gorski, L.; Meyerhoff, M. E. *Anal. Chim. Acta*. **2002**, *468*, 133.

(d) Gorski, L.; Meyerhoff, M. E.; Malinowska, E. *Talanta* **2004**, *63*, 101.

7.16 (a) Paul, G. S.; Sarmah, P. J.; Iyer, P. K.; Agarwal, P. *Macromol. Chem. Phys*. **2008**, *209*, 417.

(b) Jinyun, Z.; Caimao, Z.; Song, W.; Lei, Z.; Xi, Y.; Rui, Z. Jingui, Q. *Polymer* **2002**, *43*, 1761.

(c) van Breemen, A. J. J. M.; Herwig, P. T.; Chlon, C. H. T.; Sweelssen, J.; Schoo, H. F. M.; Benito, E. M.; de Leeuw, D. M.; Tanase, C.; Wildeman, J.; Blom, P. W. M. *Adv. Funct. Mater*. **2005**, *15*, 872.

7.17 (a) Saikia, G.; Singh, R.; Sarmah, P. J.; Akhtar, Md. W.; Sinha, J.; Katiyar, M.; Iyer, P. K. *Macromol. Chem. Phys*. **2009**, *210*, 2153.

(b) de Halleux, V. M.; Geerts, Y. H. *React. Funct. Polym*. **2000**, *43*, 145.

7.18 (a) Lakowicz, J. R. Principles of fluorescence spectroscopy, Kluwer Academic/Plenum Publishers, New York 1999.

(b) Zhou, Q.; Swager, T. M. *J. Am. Chem. Soc*. **1995**, *117*, 7017.

7.19 Lam, J. W. Y.; Tang, B. Z. *Acc. Chem. Res*. **2005**, *38*, 745.

7.20 (a) Zeng, Q.; Cai, P.; Li, Z.; Qin, J.; Tang, B. Z. *Chem. Commun*. **2008**, 1094.

(b) Li, Z.; Lou, X.; Yu, H.; Li, Z.; Qin J. *Macromolecules* **2008**, *41*, 7433.

1. A remarkable superquenching and superdequenching sensor for the selective and noninvasive detection of inorganic phosphates in saliva. **G. Saikia**, P. K. Iyer, *Macromolecules*, DOI: 10.1021/ma1026675, Publication Date (Web): April 18, **2011**.
2. Aqueous polyfluorene probe for the detection and estimation of Fe^{+3} and phosphate in blood serum. A. K. Dwivedi, **G. Saikia**, P. K. Iyer, *Journal of Materials Chemistry*, **2011**, *21*, 2502-2507. **Paper featured on inside cover of the Journal**.
3. Tuning the optical characteristics of poly(p-phenylenevinylene) by in-situ Au-nanoparticle generation. **G. Saikia**, A. Murugadoss, P. J. Sarmah, A. Chattopadhyay, P. K. Iyer, *Journal of Physical Chemistry B*, **2010**, *114*, 14821–14826.
4. Facile C-H alkylation in water: enabling defect-free materials for optoelectronic devices. **G. Saikia**, P. K. Iyer, *Journal of Organic Chemistry* **2010**, *75*, 2714–2717.
5. Synthesis and characterization of soluble poly(p-phenylene) derivatives for PLED applications. **G. Saikia**, R. Singh, P. J. Sarmah, Md. W. Akhtar, J. Sinha, M. Katiyar, P. K. Iyer *Macromolecular Chemistry and Physics* **2009**, *210*, 2153–2159.
6. Removal of iron from groundwater by ash: a systematic study of a traditional method. B. Das, P. Hazarika, **G. Saikia**, H. Kalita, D. C. Goswami, H. B. Das, S. N. Dube, R. K. Dutta *Journal of Hazardous Materials*, **2007**, *141*, 834-841.
7. Fluoride contamination in groundwater of central Assam, India, R. K. Dutta, **G. Saikia**, B. Das, C. Bezbaruah, H. B. Das and S. N. Dube, *Asian Journal of Water, Environment & Pollution*, **2006**, *3*, 93-100.
8. Poly-p-phenylene containing imidazole as a pendent group: A new assay for Cu^{2+}/Fluoride Ion dual sensor in aqueous condition. G. Saikia and P. K. Iyer, (manuscript under communication)

Patents: Indian patent: IN 2008 KO02228

A process for the production of 9, 9-dialkyl substituted fluorene monomer and obtaining the polyfluorene polymers (PFO) thereof. P. K. Iyer, P. J. Sarmah, G. Saikia, P. Thapa, Department of Chemistry, Indian Institute of Technology Guwahati, Guwahati-781039, Assam, India.